DOD-NAVY-ONR N00014-91-J-1092

TROPICAL CYCLONE MOTION AND RECURVATURE IN TCM-90

by Michael E. Fitzpatrick

P.I.–William M. Gray

Colorado State University

DEPARTMENT OF ATMOSPHERIC SCIENCE

PAPER NO. 508

TROPICAL CYCLONE MOTION AND RECURVATURE IN TCM-90

By
Michael E. Fitzpatrick

Department of Atmospheric Science
Colorado State University
Fort Collins, CO 80523

September, 1992

Atmospheric Science Paper No. 508

ABSTRACT

Rawinsonde and satellite data collected during the Tropical Cyclone Motion (TCM-90) experiment, which was conducted during the summer of 1990 in the Western North Pacific, is used to examine tropical cyclone steering motion and recurvature. TCM-90 composite results are compared with those found in a previous composite study using twenty-one years (1957-77) of Western North Pacific rawinsonde data during the same August–September period and also for August–September months during this same 21-year period.

Both data sets indicate that the composite deep-layer-mean (850-300 mb) winds 5-7° from the cyclone center provide an important component of the steering flow for tropical cyclones. However, despite the rawinsonde data enhancements of the TCM-90 experiment, data limitations prevented an accurate observation of steering flow conditions at individual time periods or for the average of only 5-10 time periods when composited together.

Examination of environmental wind fields surrounding a recurving cyclone (Typhoon Flo, Sept. 1990), and those for non-recurving TCM-90 storms verify significant differences in the upper tropospheric zonal wind fields north and northwest of the tropical cyclone one to two days prior to the beginning of the initial right turn of recurvature. Typhoon Flo actually began to recurve when 200 mb positive zonal winds had penetrated to within 6 degrees radius of the cyclones' center from the northwest. Tropical cyclones which did not recurve had negative zonal winds at this radius and azimuth. This special area to the north and northwest of the cyclone has been termed the "window of forecast opportunity".

Basic statistical analyses of the typical spread of individual wind values at specific octants and 2 degree radial belts were made for all TCM-90 rawinsonde and satellite wind data composites. The typical standard deviation about the mean of composited zonal and meridional winds in individual octants and radial belts was 5-6 m/s at lower levels and 6-7 m/s at upper levels. Zonal wind differences in excess of this threshold would be required for confidence in distinguishing between individual cases of recurvature and non-recurvature.

TABLE OF CONTENTS

LIST OF SYMBOLS, ACRONYMS AND DEFINITIONS

Best Track = A subjectively smoothed path (versus a precise but very erratic fix-to-fix path) used to represent the estimated best known movement of a tropical cyclone.

BMRC = (Australian) Bureau of Meteorology Research Centre

CSU = Colorado State University

GMS = (Japanese) Geostationary Meteorological Satellite

IOP = Intensive Observing Period

HRD = Hurricane Research Division

JTWC = Joint Typhoon Warning Center, Guam

mb = millibar

NAT = Natural Coordinate system-with respect to N-S-E-W geographical reference.

NCAR = National Center for Atmospheric Research

NOAA = National Oceanic and Atmospheric Administration

OCT = Octant

ODW = Omega dropwindsonde

n mi = nautical mile

NR = Non-recurving cyclones

R = Recurving cyclones

R point = The location where a recurving cyclone first begins to deviate from its previous west-northwest course.

Rawinsonde = Instrument used to measure the vertical profile of atmospheric temperature, relative humidity, pressure and winds. It is carried aloft by balloon and data are transmitted over radio frequencies to the receiving location.

Recurvature = The turning of a tropical cyclone from an initial path toward the west and poleward to east and poleward.

ROT = Coordinate system oriented with respect to the cyclone direction of motion.

S.D. = Standard Deviation

SPECTRUM = SPecial Experiment Concerning Typhoon Recurvature and Unusual Motion.

TATEX = Taiwan Area Typhoon EXperiment.

TC = Tropical Cyclone

TS = Tropical Storm

TCM-90 = Tropical Cyclone Motion 1990 field experiment

WMO = World Meteorological Organization

WNP = Western North Pacific

Chapter 1

INTRODUCTION

1.1 Tropical Cyclone Motion

Forecasting the movement of tropical cyclones is one of the most challenging problems in tropical meteorology. Although many attempts at objectively predicting cyclone motion have been made using statistical and dynamical methods, forecasts for specific tropical cyclones remain highly uncertain. The determination of whether a cyclone will move on a westerly course or recurve to the north or northeast typically results in large forecast errors. This is shown in the typical position error statistics (Fig. 1.1) published by the Joint Typhoon Warning Center (JTWC, 1990). Using the 1989 tropical cyclone season, a typical mean forecast position error for a 24 hour forecast is about 120 n mi. The largest forecast errors are generally associated with an incorrect assessment of the recurvature situation. Errors of 1850 km (1000 n mi) or more at the 72 hour forecast point may occur in these cases (Elsberry, 1988). These errors can have a devastating impact if the storm is approaching a heavily populated coastline. If a landfall forecast is made but the cyclone recurves, millions of dollars are lost on unnecessary evacuation and preparations. On the other hand, if the cyclone is predicted to recurve away from the coast, but does not, the loss of lives and property can be tremendous. It is estimated that the cost of preparing a 450 km stretch of U.S. Gulf Coast for a hurricane to be about 50 million dollars (Sheets, 1990).

Position errors can usually be attributed to (1) poor initial storm motion estimates or (2) poor steering flow wind observations and forecasts. Individual tropical cyclones often behave somewhat erratically. There are several obvious reasons why cyclones can move erratically over a short period of time. (1) Apparent changes in motion are due to

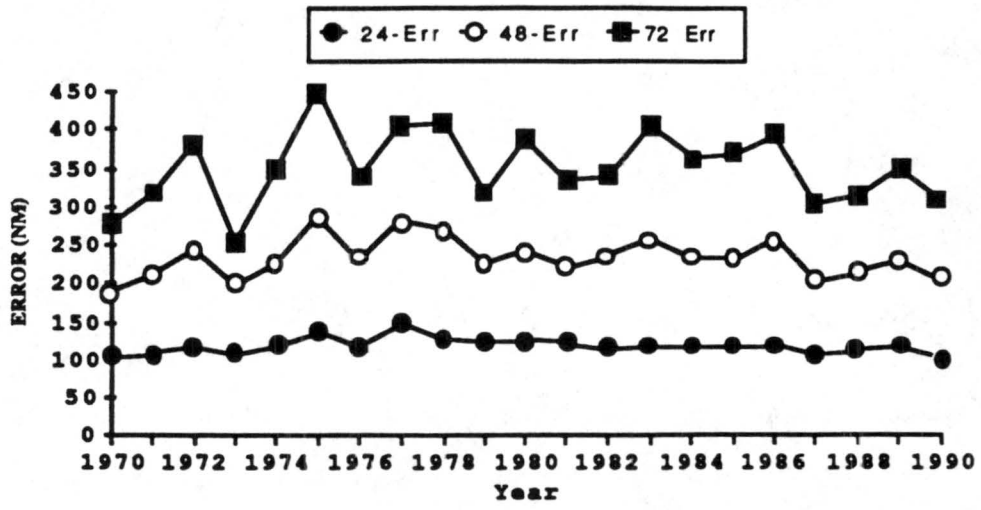

Figure 1.1: The forecast errors for the positions of Northwest Pacific storms from 1970-1990. From the 1990 Annual Tropical Cyclone Report.

measurement errors. Various position-fixing techniques such as by satellite, aircraft, or radar have characteristic reliabilities. The accuracy of an individual measurement depends upon the instrument system used in determining position and on the stage of development of the storm. (2) Actual changes in the tropical cyclone's motion can occur due to internal or external influences. A subjective after-the-fact estimate of storm track is available and is called the "best track". These position estimates weigh the relative merits of cyclone center fixes and determine the most likely position of a storm at six-hour intervals. The best track positions are assumed to be the storm position data with the least amount of overall position scatter. Figure 1.2 shows the very large variation in storm motion that can occur during a season. In particular, note that Typhoon Orchid had three periods where the direction of movement varied through 360 degrees in a short period of time.

1.2 TCM-90 Project

Many researchers have examined the relationship of tropical cyclone movement to surrounding flow. But surrounding cyclone data sources are always very limited. However, during August and September 1990, four separate but concurrent field experiments were conducted over the Western North Pacific (WNP) to study the motion of tropical

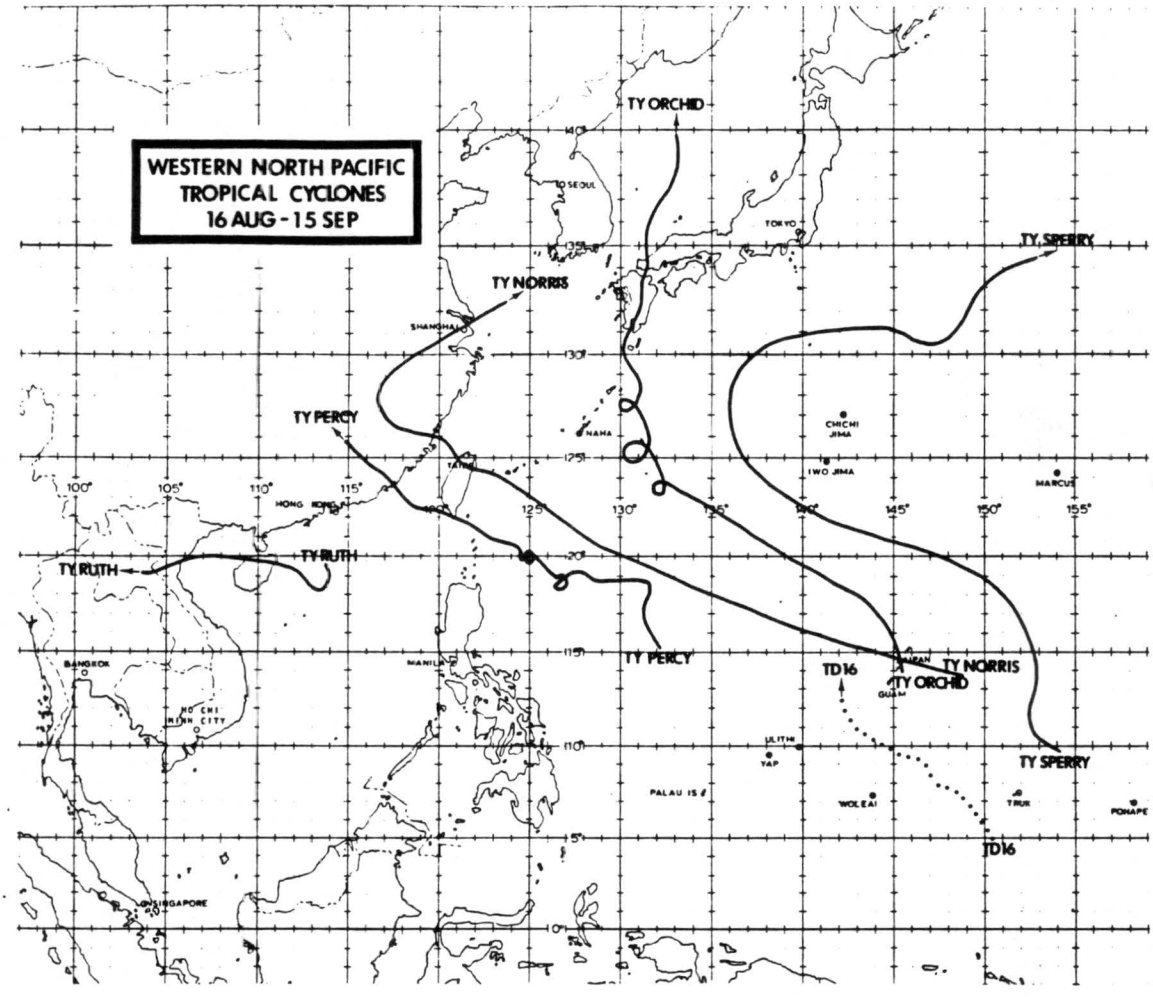

Figure 1.2: 1980 Best track positions of Northwest Pacific storms. From the 1980 Annual Tropical Cyclone Report.

cyclones. These included the Tropical Cyclone Motion Experiment of the US Navy (TCM-90), TYPHOON-90, a combined atmospheric-oceanographic experiment conducted by the USSR, the SPECTRUM (Special Experiment Concerning Typhoon Recurvature and Unusual Motion) project of the Typhoon Committee of the Economic and Social Commission for Asia and the Pacific (ESCAP), which is part of the World Meteorological Organization (WMO), and a fourth experiment organized by the Taiwan Central Weather Bureau called TATEX (Taiwan Area Typhoon Experiment).

The TCM-90 field experiment was the culmination of a five-year Tropical Cyclone research initiative of the Office of Naval Research Marine Meteorology Program. TCM-90 was specially designed to study tropical cyclone motion. The aims of the experiment were to obtain an enhanced observational data set that could be used to test hypotheses on the mechanisms of tropical cyclone motion. This observational network of the Western North Pacific represented a unique opportunity to quantitatively study individual case and time period tropical cyclone steering flow currents. Special data collection efforts were made, especially during 17 days which were designated as Intensive Observing Periods (IOPs) during which rawinsondes were launched at 6-hourly intervals and other observation platforms increased their data coverage. The rawinsonde observations were taken at regular WMO stations as well as at special sites and weather ships. These special observations, particularly the extra ship rawinsonde observations, provided the best opportunity yet to measure steering flow surrounding individual cyclones. In addition, satellite-derived cloud-drift winds were provided during a number of the IOPs studied. For further details on the TCM-90 experiment, refer to Elsberry *et al.* (1990).

1.3 Summary of Objectives

A major feature of the TCM-90 field experiment was to determine if the rawinsonde augmentation employed together with the special satellite techniques would be able to give significantly improved individual case and time period steering information so as to improve understanding and forecasting of cyclone motion. This study uses the enhanced

data base gathered during the TCM-90 project and examines several aspects of tropical cyclone motion:

1. A data compositing scheme is used to compare a 21-year WNP rawinsonde data base to that gathered during TCM-90. Deep-layer-mean (850-300mb) wind flow vectors found at various radii relative to the tropical cyclone center positions are analyzed. This information is examined to try to determine a representative steering flow for cyclone motion and for any possible forecast clues that might be used operationally.

2. The typical variability of individual rawinsonde data is examined to determine the extent to which individual time period steering currents can be determined. Reasons for individual case variations are discussed.

3. A comparison is made of the environmental wind field differences between Typhoon Flo, a storm that recurved to the northeast, and those storms that maintained a west-northwesterly track throughout their entire life cycles. Critical levels and locations for zonal wind differences are determined and their temporal relationship to storm recurvature is investigated.

Chapter 2

RAWINSONDE COMPOSITING AND DATA ANALYSIS PROCEDURES

2.1 Rawinsonde Compositing Philosophy

Tropical cyclones spend most of their lifetimes over data sparse oceanic areas. Due to the scarcity of oceanic rawinsonde data, representative information on the characteristics of surrounding flow patterns of individual tropical cyclones is usually very deficient. However, by compositing the available rawinsonde soundings from many cyclones with similar motion characteristics over many parts of the ocean, many of the data limitations can be overcome and the basic physical processes and relationships involved with the tropical cyclone motion process better understood.

Compositing procedures smooth out features peculiar to an individual tropical cyclone. The value of composites lies in the large number of observations whose insensible average smooths over small scale natural wind variations and the random instrumental inconsistencies. Large numbers of observations will tend to counteract the inconsistencies of individual soundings. The resulting composite averages should reveal characteristics common to all cyclones in a given stratification and allow for quantitative analysis of these features. A more detailed description of compositing philosophy can be found in Williams and Gray (1973), Frank (1977), Gray (1981), and in other Colorado State University tropical cyclone research reports.

2.2 Rawinsonde Compositing Procedures

This study has used composites based on 21 years (1957-77) of Western North Pacific rawinsonde data and on two months (Aug-Sept, 1990) of TCM-90 rawinsonde data from the same geographic area. The rawinsonde data comprising the 21 year data set are

taken from data tapes of the Asheville, North Carolina US Climatic Center, the National Center for Atmospheric Research (NCAR), and from Japanese and East Asian upper air soundings. The TCM-90 data set draws from all available land based and ship based rawinsonde soundings taken during the experiment. This includes data taken at both regular and special locations and times. Comparisons of the TCM-90 experiment data are made with the extensive additional measurements from previous years. Figure 2.1 shows the rawinsonde data network for the TCM-90 project.

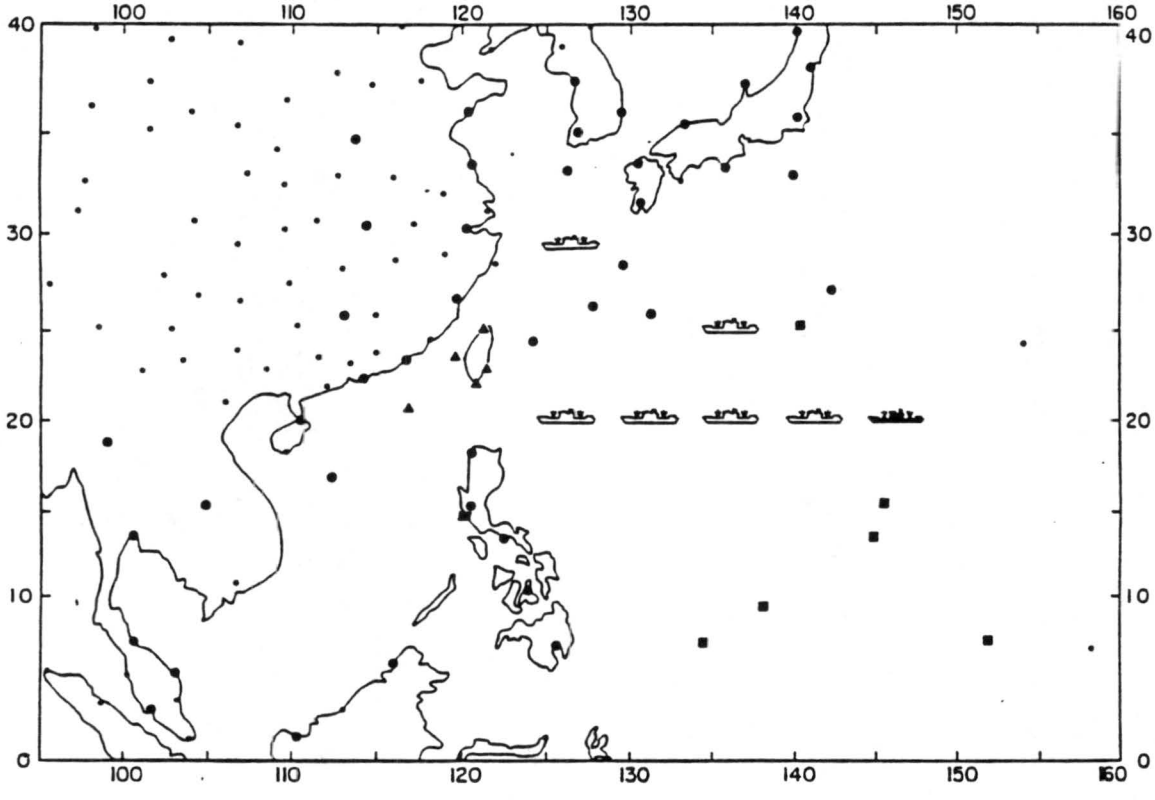

Figure 2.1: Upper-air network for TCM-90 and concurrent experiments. Regular rawinsonde stations with 12-hourly soundings are indicated by small dots. The large dots, squares, and triangles represent the special rawinsonde stations at 06 and 18 UTC for SPECTRUM, U.S. and Taiwan stations, respectively. The ship symbols show the fixed positions of the participating ships. (after Elsberry *et al.*, 1990).

The rawinsonde compositing techniques used with this study display data on a 15° circular radius grid. All rawinsondes were composited into a cylindrical coordinate system centered on the cyclones' best track positions. Soundings taken within 15° latitude radius of a tropical cyclone were used in the compositing grid shown in Fig. 2.2. The grid consists of eight radial bands, extending from 0-1, 1-3, 3-5, 5-7, 7-9, 9-11, 11-13, and 13-15° from the tropical cyclone center. The grid also has eight octants of 45° extent that display data in various azimuthal directions and 23 vertical pressure levels from the surface up to 50 mb.

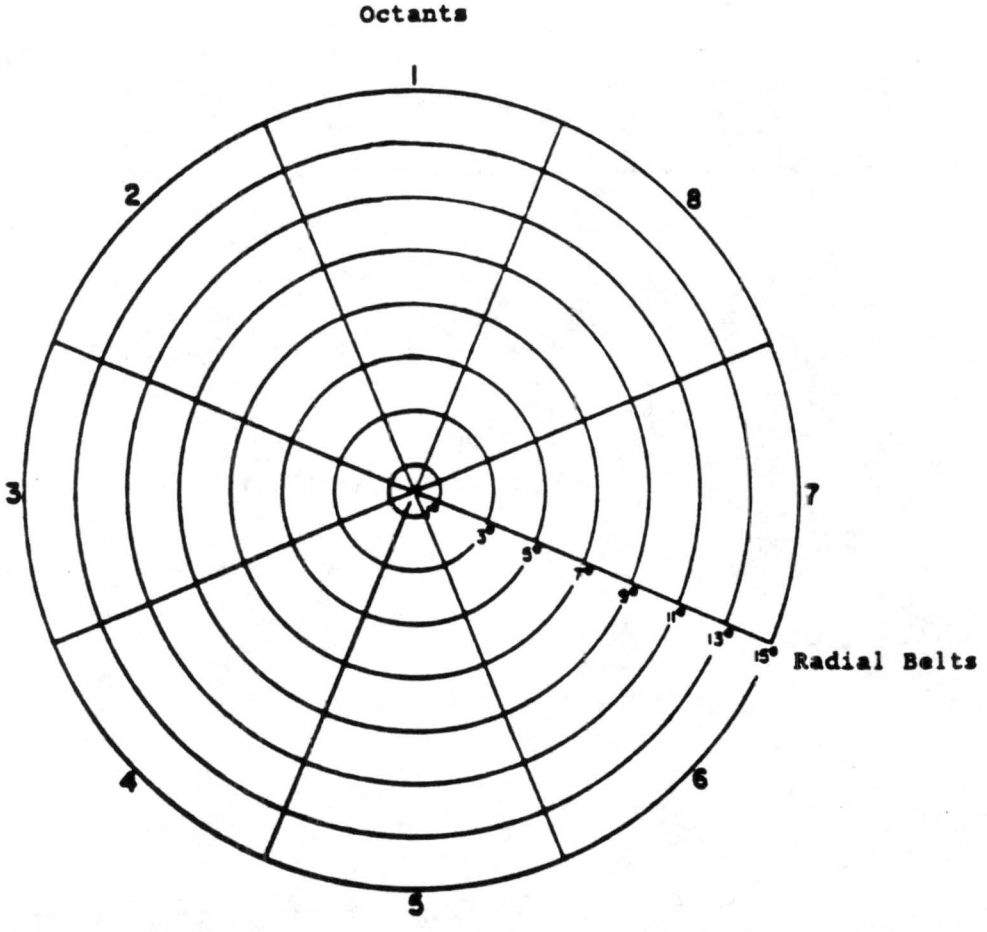

Figure 2.2: Grid used for compositing rawinsonde data. Note the eight azimuthal octants and eight radial belts used in the compositing system. (Chan and Gray, 1982).

Two different reference frames are used. The first is the unchanged Natural or NAT coordinate system. The NAT system composites data relative to the instantaneously fixed

cyclone center in a N-S-E-W or geographical coordinate system. One of the averaged parameters available in this system is the zonal wind component; this will be used extensively in Chapters 4 and 5.

The second reference frame involved is the Rotated or (ROT) coordinate system which composites data both with respect to the instantaneously fixed cyclone center position and with respect to the direction of motion of the storm. Each wind vector observation is resolved into a component parallel to the direction of cyclone movement and a component normal to the direction as shown in Fig. 2.3. These components are used in Chapter 3 to examine the relationship of the environmental winds to the actual cyclone motion.

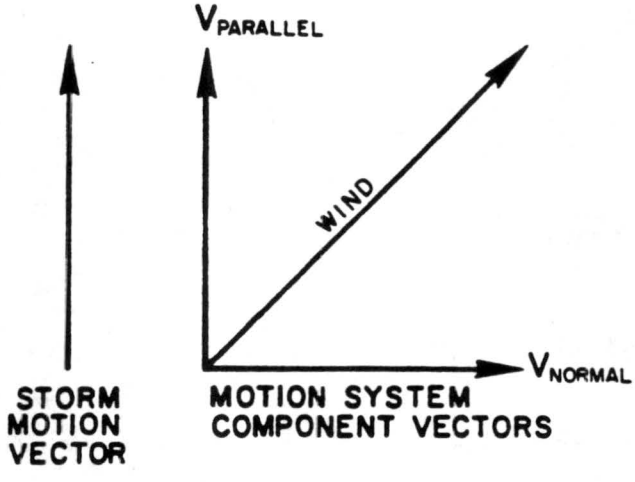

Figure 2.3: Parallel and perpendicular components of a wind vector showing their relation to the storm motion vector. (Chan and Gray, 1982).

2.3 Cyclone Track Stratifications

This motion study analyzes two types of cyclone tracks: recurving cyclones and non-recurving cyclones. Figure 2.4 shows the typical illustrations of these two basic types of cyclone tracks. The Joint Typhoon Warning Center (JTWC, 1988), defines tropical cyclone recurvature as "The turning of a tropical cyclone from an initial path west and poleward to east and poleward". Figure 2.5 illustrates this definition. In the present study, the location where recurving cyclones first begin to turn to the right from their previous west-northwesterly track is of primary importance. This location is taken to be

the point of initial recurvature and has been designated the "R-point" (Hodanish, 1991), and is shown in Fig. 2.6.

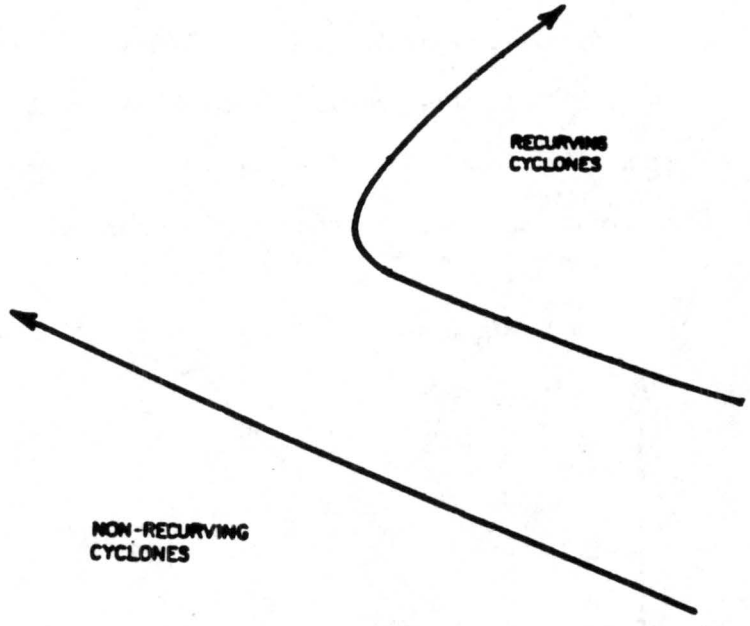

Figure 2.4: Typical tracks of the cyclones analyzed in this study.

Recurving cyclones (R) in this study are defined as those which change direction a minimum of 45° to the right of their previous west-northwest course within 36 hours after passing the R-point. The cyclone must also have undergone recurvature (by JTWC definition) within 48 hours after passing the R-point. In addition, recurving cyclones must move on a course between 260° and 330° for a minimum of 24 hours prior to reaching the R-point. This last restriction allows for the observation of any changes which may occur in the wind fields prior to the beginning of recurvature (Hodanish, 1991).

Non-recurving (NR) cyclones are defined here as cyclones which tracked between 260° and 330° throughout their lifetime. In addition to the recurving and non-recurving cyclones, three additional cyclone stratifications were made according to the general direction of motion, i.e., West, North, and Northeast. These are examined in Chapter 3. Tracks of the 13 TCM-90 cyclones are found in the Appendix.

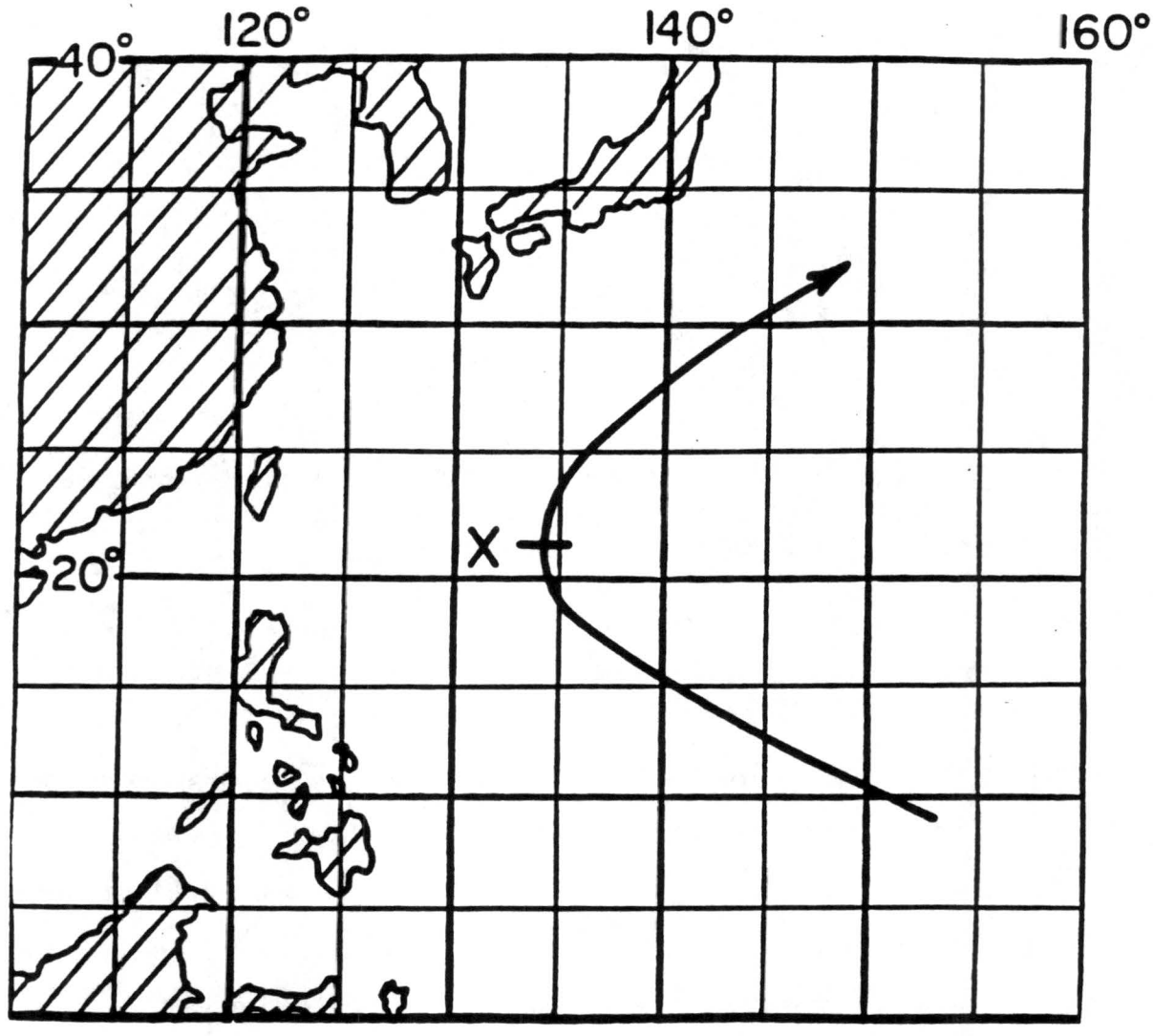

Figure 2.5: A typical recurving cyclone track. According to JTWC (1988), a cyclone undergoes recurvature when the cyclone first takes on an eastward component of motion (shown here by the letter "X"). (JTWC, 1988)

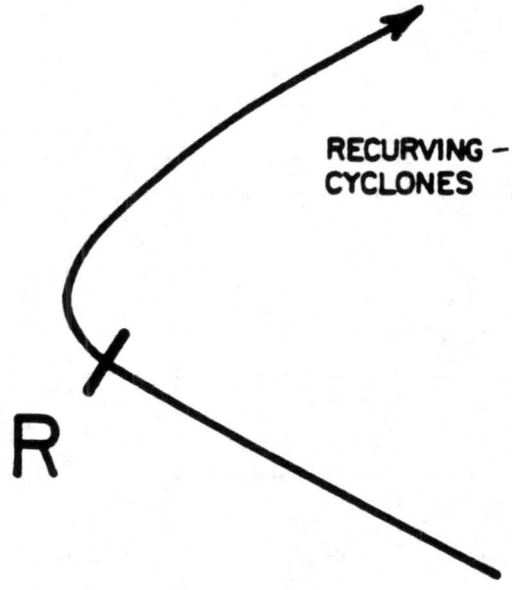

Figure 2.6: Track of recurving cyclone, where the "R" represents the R-point as used in this study. This is the location where the recurving cyclone first begins to turn to the right from their west-northwest track. (Hodanish, 1991)

2.4 Designated Time Periods for the Analysis of Recurvature

Temporal changes of the environmental wind fields surrounding the cyclones are observed by dividing the recurving tracks into five consecutive 24-hour time segments. (See Fig. 2.7). Time is measured with respect to the R-point. This procedure facilitates the examination of how synoptic scale wind fields interacted with the cyclone circulation prior to and after its recurvature. The first three time periods, R0, R1, and R2 occur as the cyclones move on a west-northwest course, prior to reaching the R-point, while the fourth and fifth time periods, R3 and R4, occur after the cyclone has passed the R-point.

Non-recurving cyclone tracks were divided into three equal time periods as no track reference position equivalent to the R-point can be designated. The average length of each NR period was 42 hours for the TCM-90 cyclones. Figure 2.7 shows a typical non-recurving track, divided into the three specified time periods. Figure 2.8 summarizes the mean track speed and direction information for recurving and non-recurving cyclones during TCM-90. Table 2.1 contains a summary of the same information but in a different

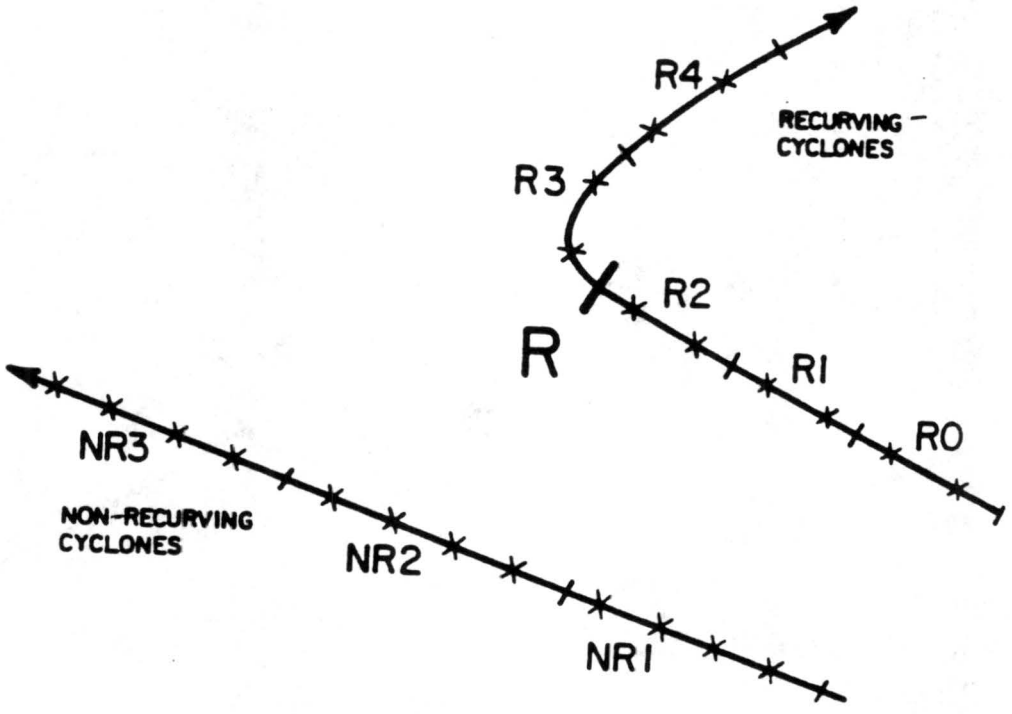

Figure 2.7: The TCM-90 recurving (R0 through R4) and non-recurving (NR1-NR3) cyclone tracks divided up into individual time periods. Table 2.1 and Fig. 2.8 summarize individual characteristics of each time period. The X characters represent 12-hour time steps.

format, and gives specific information on Typhoon Flo, a recurving storm from TCM-90 which is examined more closely in Chapter 4.

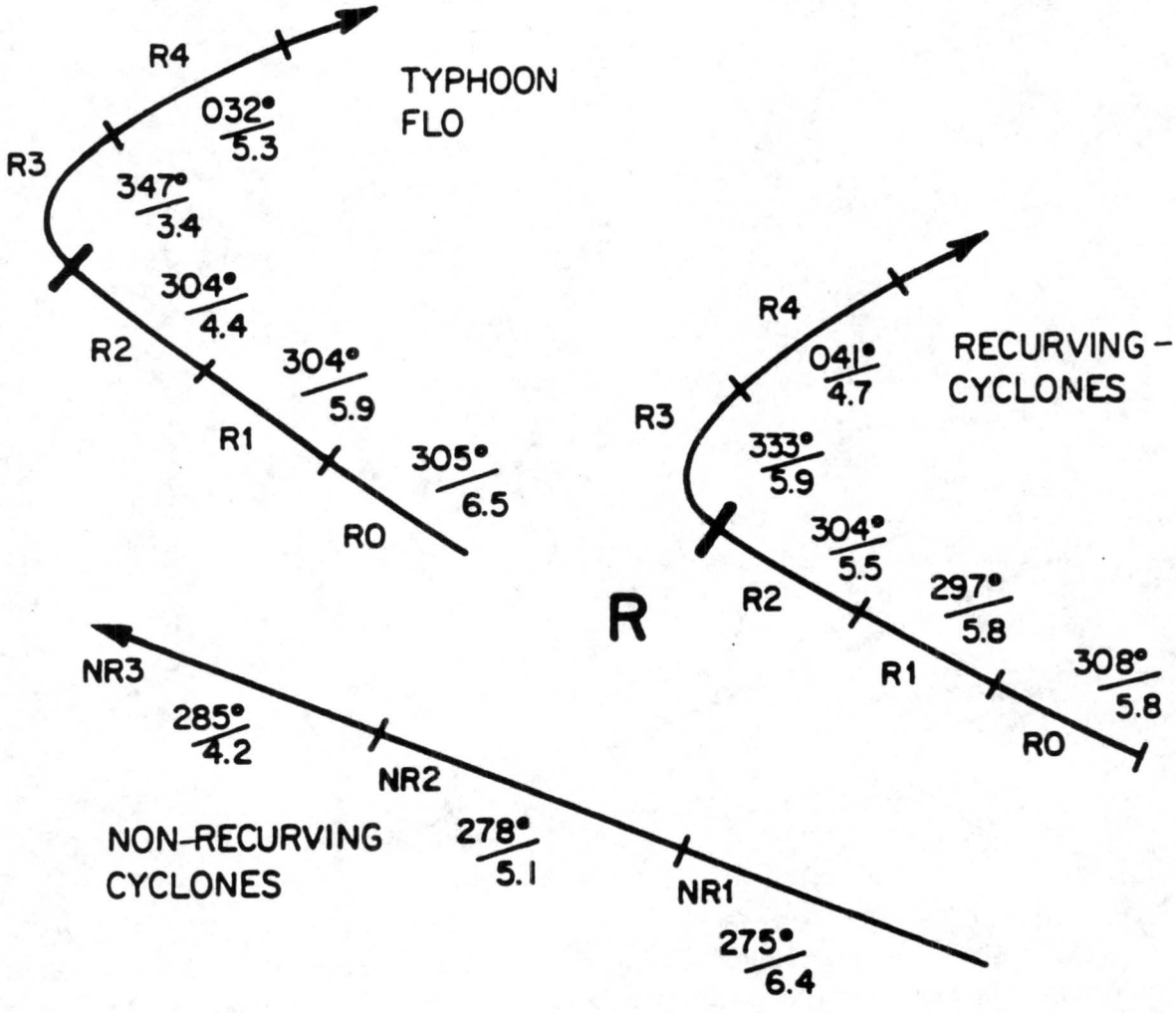

Figure 2.8: Composite average speed and direction for recurving, non-recurving TCM-90 time periods and for Typhoon Flo. Units in m/s.

2.5 TCM-90 Data Set

2.5.1 Rawinsondes

The TCM-90 rawinsonde data set covering the time span August through September, 1990, was composited and analyzed in the same manner as the 21-year Gray research

Table 2.1: Summary data for TCM-90 time periods for non-recurving, recurving cyclones and for Typhoon Flo.

Name	Time Period	Description	Average Direction	Composite Speed (m/s)
Non Recurving Cyclones	NR1	First 1/3 of track	275	6.4
	NR2	Second 1/3 of track	278	5.1
	NR3	Last 1/3 of track	285	4.2
Recurving Cyclones	R0	48-72 h before recurvature	308	5.8
	R1	24-48 h before recurvature	297	5.8
	R2	0-24 h before recurvature	304	5.5
	R3	0-24 h after recurvature	333	5.9
	R4	48-72 h after recurvature	041	9.7
Typhoon Flo	R0	48-72 h before recurvature	305	6.5
	R1	24-48 h before recurvature	304	5.9
	R2	0-24 h before recurvature	304	4.4
	R3	0-24 h after recurvature	347	3.4
	R4	48-72 h after recurvature	032	5.3

project data set. Due to the intensive data gathering effort expended during this project, an unprecedented number of observations, in both geographical and temporal coverage, were available. This provided the opportunity to investigate individual cases of cyclone steering motion. The data sample size and coverage appeared sufficient to explore if meaningful quantitative steering flow for an individual storm could be obtained. Table 2.2 summarizes the numbers of rawinsonde observations which were used. Comparing data amounts, we find that the TCM-90 experiment obtained a volume of data which was approximately 15 percent of the size of the total rawinsonde data available during August-September of the 21-year data sample and was about 7 percent of the size of the data available during the entire 21-year period.

2.5.2 Satellite-Derived Cloud-Drift Winds

In addition to the rawinsonde data used from TCM-90, Japanese GMS satellite-derived cloud drift winds were available for three of the IOP's. Satellite wind data for the time period covering Typhoon Flo received special post-processing at the University

Table 2.2: Number of rawinsonde observations in composites by radial band and stratifications for (A) WNP 1957-77, (B) WNP (Aug-Sept) 1957-77, (C) TCM-90, (D) TCM-90 non-recurving, (E) TCM-90 recurving, (F) Typhoon Flo, (G) Typhoon Flo satellite winds.

A

Western North Pacific 1957-77

Radius	West Mover	North Mover	Northeast Mover
10	5776	5036	2652
8	4667	4436	2355
6	3627	3465	1940
4	2354	2349	1314
2	1012	1104	645

B

Western North Pacific (Aug-Sept) 1957-77

Radius	West Mover	North Mover	Northeast Mover
10	2524	2296	1023
8	2097	2012	902
6	1708	1631	789
4	1135	1141	576
2	491	584	295

C

TCM–90

Radius	West Mover	North Mover	Northeast Mover
10	474	264	219
8	406	229	167
6	293	185	150
4	169	163	104
2	96	72	57

Table 2.2: Continued.

D

TCM-90

Non-Recurving Cyclone Time Periods

	NR3			NR2			NR1		
	Octant								
Radius	3	2	1	3	2	1	3	2	1
10	22	35	43	36	67	47	16	48	22
8	33	32	40	27	63	41	13	40	15
6	20	19	36	23	51	50	6	28	24

E

TCM-90

Recurving Cyclone Time Periods

	R4			R3			R2			R1			R0		
	Octant														
Radius	3	2	1	3	2	1	3	2	1	3	2	1	3	2	1
10	20	18	17	28	21	21	29	14	15	12	10	10	3	5	3
8	16	12	16	18	19	17	15	7	8	13	6	4	2	5	3
6	9	11	16	14	8	10	16	6	3	5	6	5	1	4	0

F

Typhoon Flo

Recurving Cyclone Time Periods

	R4			R3			R2			R1			R0		
	Octant														
Radius	3	2	1	3	2	1	3	2	1	3	2	1	3	2	1
10	7	7	4	9	7	9	15	3	6	2	4	2	1	4	2
8	8	4	6	9	3	7	8	3	3	4	4	0	1	1	2
6	1	3	8	8	0	3	4	1	3	1	3	4	1	1	0

G

Typhoon Flo–200 mb Satellite Cloud-Drift Wind Observations

Recurving Cyclone Time Periods

	R4			R3			R2			R1			R0		
	Octant														
Radius	3	2	1	3	2	1	3	2	1	3	2	1	3	2	1
10	0	2	23	3	1	1	1	0	5	0	1	15	6	3	10
8	0	12	29	8	1	5	9	14	19	0	0	20	1	0	12
6	6	28	23	9	15	13	13	20	14	0	8	15	2	0	9

of Wisconsin Satellite Data Center under the direction of Chris Velden. This wind vector information is considered to be of very high quality due to the careful editing and processing that the Wisconsin group provided. Satellite wind information was available at several levels in the atmosphere, with the majority of the data concentrated in the upper and lower troposphere (i.e., approximately 200 mb and 850 mb levels). A special computer program was developed by the Gray research project to composite this 200 mb satellite wind information in cylindrical coordinates and to compare it with the rawinsonde data in the same coordinates.

Chapter 3

TROPICAL CYCLONE STEERING MOTION

3.1 Steering Flow

Tropical cyclones typically move in directions and with speeds very closely related to the broad-scale environmental flow fields in which they are embedded. This environmental flow is referred to as the "steering current". There are, however, many questions as to how this steering current should be defined and if there are systematic differences between TC motion versus the basic steering flow.

There is uncertainty as to which atmospheric level or layer primarily determines the motion of tropical cyclones (Dong and Neumann, 1986). Some studies have demonstrated a higher correlation of tropical cyclone displacements with the flow at mid-tropospheric levels (e.g., Neumann, 1979; Pike, 1985). Neumann indicates that he attains somewhat better forecast performance using data for a mass-weighted deep-layer mean flow rather than a middle level steering current. Holland (1983) has stated that the asymmetric inflow-outflow jets present in the low level frictional layer and upper level outflow layers of the cyclone can significantly distort evaluations of the basic current. The ONR experiment (Elsberry, 1985) has suggested that these highest and lowest layers were neglected and a mass-weighted 850-300 mb average has been used to define the basic current.

Through much additional observational analysis with different levels and radii, it has been determined that, indeed, the best steering current for tropical cyclones appears to be the deep-layer (850-300 mb) and 5–7° radius mean wind flow. However, significant deviations from the environmental flow are observed in composite studies of motion by George and Gray (1976), Chan and Gray (1982), and Holland (1984) and in composites of operational analyses by Brand *et al.* (1981). In the mean over many storms, cyclones

of the Northern Hemisphere have been observed to deviate to the left from the basic environmental current as defined by azimuthal averages of flow within radial bands around the cyclone (Chan and Gray, 1982; Elsberry, 1985).

3.2 Analysis Objectives

This study analyzes the differences in actual tropical cyclone motion versus the direction of the steering current at various radii. The new TCM-90 data composites and those generated by the Gray research project for all WNP cyclones in the 1957-77 data set are used. Indicators of the key radii for steering flow are obtained from the observational data bases. The goals are to:

1. Verify previous findings obtained from a large 21-year composite of data for August through September and for all months in 21-year data sample.

2. Compare these results with the much smaller though intensive two month August through September, 1990, observational period of the TCM-90 project.

3. Examine the composites of recurving and non-recurving storms observed during the TCM-90 project for possible forecast indicators of turning motion or recurvature.

3.3 Comparison of 1957-77 Composite Data Set Steering Motion to the TCM-90 Composites

Figures 3.1, 3.2, and 3.3 show the layer average (850-300 mb) symmetric wind vectors in various radial bands relative to the mean cyclone motion. The TCM-90 composites (Aug-Sept, 1990) are compared to both the complete 21-year (1957-77) NWP composites compiled by the Gray research project, and to a smaller subset using just the Aug-Sept 1957-77 data. This latter stratification of the data was done so as to eliminate any seasonal bias that may occur and to allow for a more refined comparison. Table 3.1 gives the directional stratifications used for the west, north, and northeast composites.

Only tropical cyclones that had reached tropical storm intensity (17 m/s or greater) and were moving at least 2 m/s were included in the composites. This is done to eliminate very weak and disorganized cyclones and those that lack a definable direction of motion.

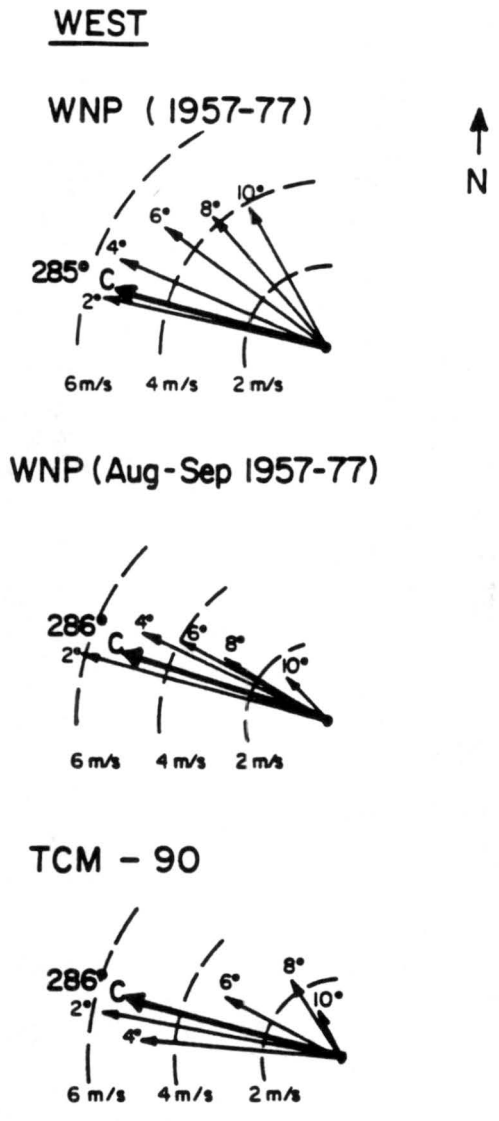

Figure 3.1: The layer average (850-300 mb) symmetric wind vectors relative to the cyclone motion (denoted by a "C") in two degree radial bands extending from 2 to 10° from the center. These diagrams are composites for all west moving cyclones in each of the three different data sets.

Table 3.1: Description of the criteria used to stratify cyclones by direction.

STRATIFICATION	DESCRIPTION
West Moving Cyclones	240° < cyclone direction < 315°
North Moving Cyclones	315° < cyclone direction < 045°
Northeast Moving Cyclones	020° < cyclone direction < 090°

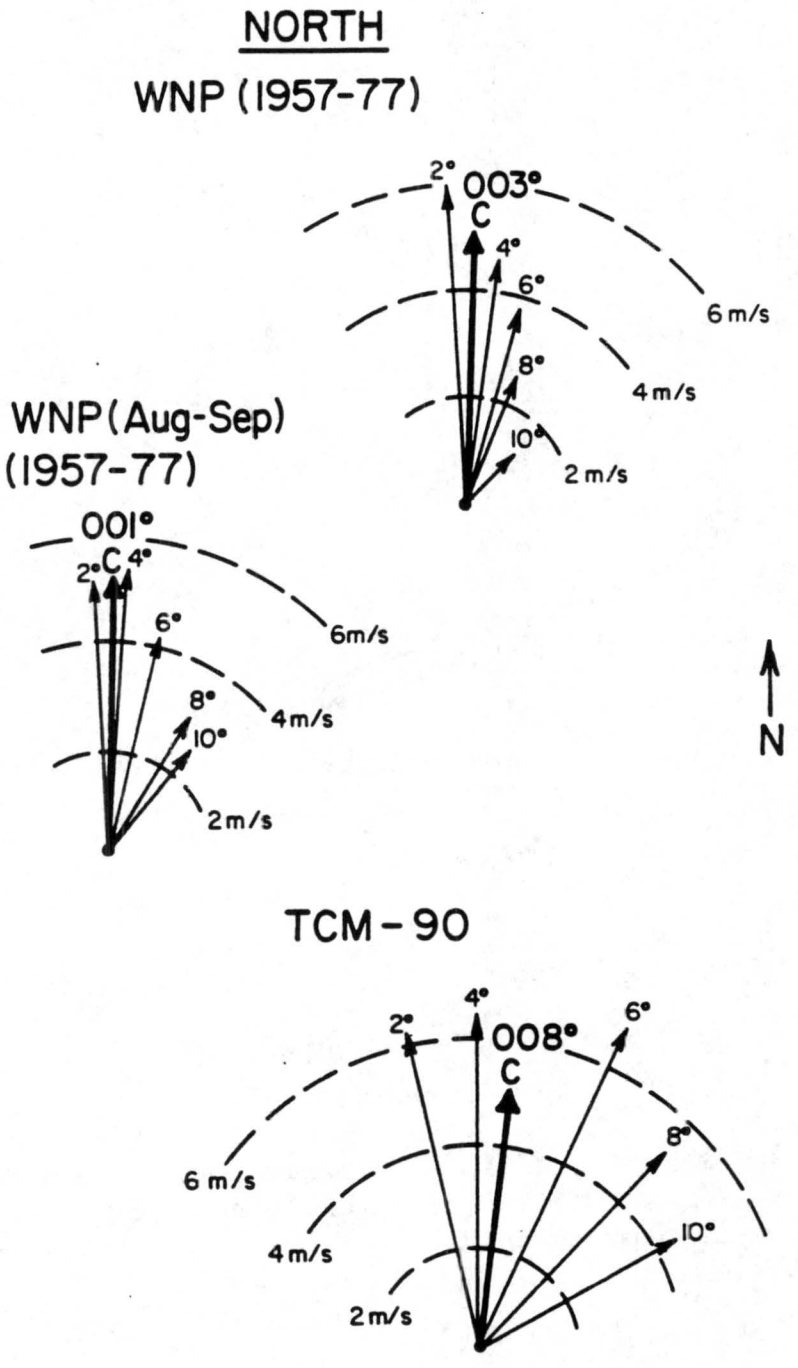

Figure 3.2: The layer average (850-300 mb) symmetric wind vectors relative to the cyclone motion (denoted by a"C") in two degree radial bands extending from 2 to 10° from the center. These diagrams are for all north moving cyclones in each of the three different data sets.

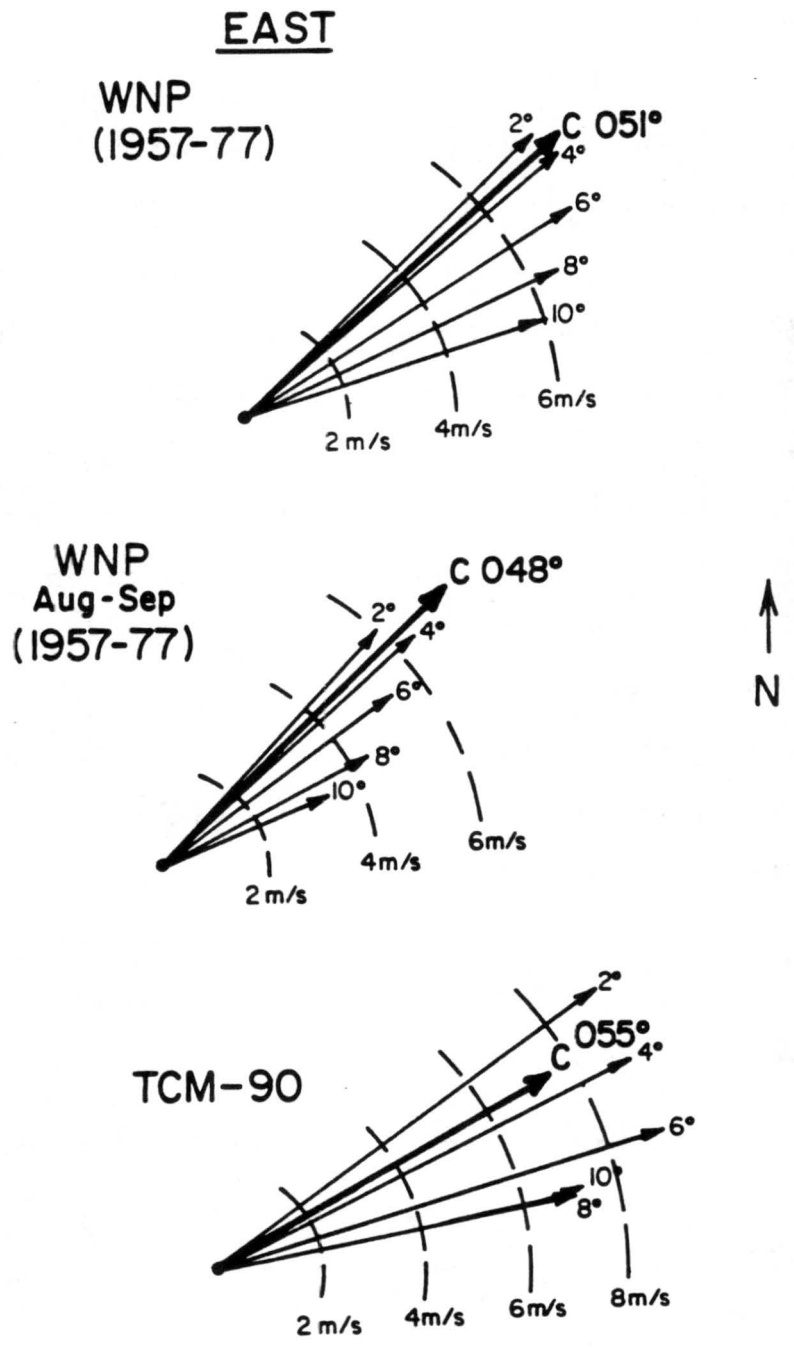

Figure 3.3: The layer average (850-300 mb) symmetric wind vectors relative to the cyclone motion (denoted by a "C") in two degree radial bands extending from 2 to 10° from the center. These diagrams are for all northeast moving cyclones in each of the three different data sets.

In summary, the results from the large data sets indicate that, on average, tropical cyclones move with a direction very close to that of the interior 3° radius tropospheric mean wind currents. However, the TCM-90 data set for a two month period in a single season showed a tropical cyclone motion direction closer to the 5° radius layer average wind for the west and north moving storms. Northeasterly moving cyclones in all data sets consistently showed the 2° (850-300 mb) layer average flow as the best indicator of the actual cyclone motion. The speed of movement from the large composite data set was very close to the 2° radius mean composite wind speed. Although the TCM-90 data had the same composite wind speed as the larger data set, it indicated a motion 1-2 m/s slower than its' surrounding flow for both the north and northeast composites.

The differences encountered between the TCM-90 data set composites versus the much larger 21-year data set composites are likely due to the sizes of the data sample involved. The TCM-90 composites contained at most several hundred observations versus the thousands of observations compiled in the larger data set (see Table 2.2). The transient and hence unique global, synoptic, and mesoscale conditions present during the 13 TCM-90 study likely included wind field anomalies which may have resulted in slightly different relative steering motion than the much larger 21-year composites. There were certainly a wide variety of storm tracks included in the TCM-90 data set (see Appendix A for TCM-90 tracks). It is not unreasonable that in this smaller sample size that composite averages may be relatively distinct from the much larger data samples.

3.4 Comparison of Steering Motion for TCM-90 Non-Recurving and Recurving Storms

Four TCM-90 storms were classified as non-recurving cyclones and three as recurving cyclones. Data for these cyclones were composited into non-recurving time periods NR1 through NR3 and recurving time periods R0 through R4. Figure 3.4 contrasts the differences in steering flow found during recurving cyclone time period R2, just before recurvature versus non-recurving cyclone time period NR2. Figure 3.5 contrasts period R3, during recurvature, with non-recurving period NR3. Figure 3.6 shows the individ-

ual non-recurving periods NR1, NR2, NR3, and the combined composite of these three periods.

We observe in Fig. 3.4 that there is a much more pronounced flow toward the southwest evident at the 3-5° radius during non-recurving period NR2. It is more than twice the speed of the composite vector in period R2. Also, the outer 7-10° wind flow for R2 shows a greater magnitude in the northwesterly direction than that for NR2. However, the inner 3-5° flow on R2 is not dramatically at variance from a westerly course. There is an obvious change in the steering flow in Fig. 3.5. The 3-5° flow maintains itself for NR3 in a predominantly westerly direction. R3 indicates mostly flow toward the north and northwest at this radius. Figure 3.6 illustrates the variance encountered in individual time period composites. However, the overall composite of the three non-recurving time periods results in steering motion comparable to the 21-year data set steering motion for west moving cyclones.

It should be noted that even though NR3 shows flow directed toward the north and northeast at the 8-10° outer radius, the 3-5° flow best fits the actual cyclone motion. This association indicates that recurvature will not take place; a point which is examined further in Chapter 5. It is also interesting to note the large variance between the different time period vectors. The motion vectors for the individual time periods indicate mean flow which can be significantly different from average data sets.

In terms of recurvature forecasting, there does not appear to be clear 850-300 mb steering flow differentiation between non-recurving and recurving cyclones at the critical phases of the storm track motion such as during period R2 or NR2. This lack of a clear difference in steering flow signal would preclude the timely forecasting of recurvature on an operational basis from typical steering flow information alone. The period immediately before recurvature (R2) in TCM-90 is subject to a very large set of wind varying influences that could cause the composite data set to give ambiguous information in a recurving composite sample size of only three cases. For a single storm case, even with enhanced

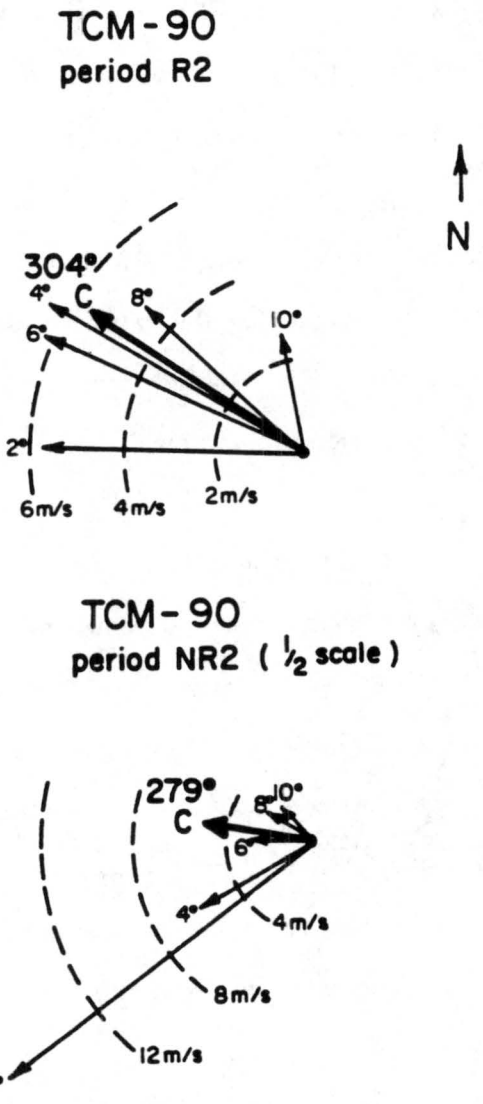

Figure 3.4: The layer average (850-300 mb) symmetric wind vectors relative to the cyclone motion (denoted by a "C") in two degree radial bands extending from 2 to 10° from the center. These diagrams show the composite results for TCM-90 recurving cyclones period R2 and non-recurving cyclones period NR2.

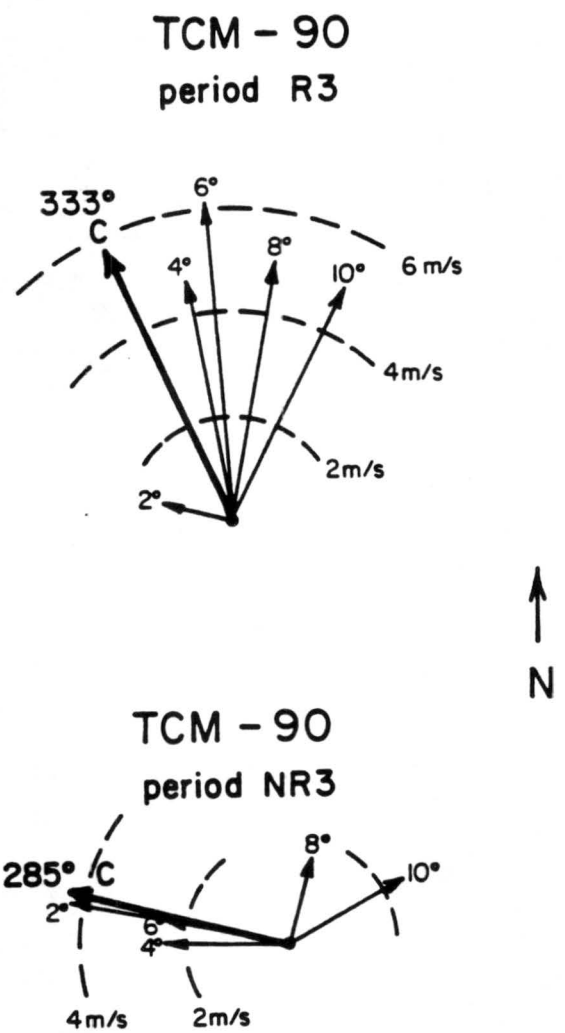

Figure 3.5: The layer average (850-300 mb) symmetric wind vectors relative to the cyclone motion (denoted by a "C") in two degree radial bands extending from 2 to 10° from the center. These diagrams show the composite results for TCM-90 recurving cyclones period R3 and non-recurving cyclones period NR3.

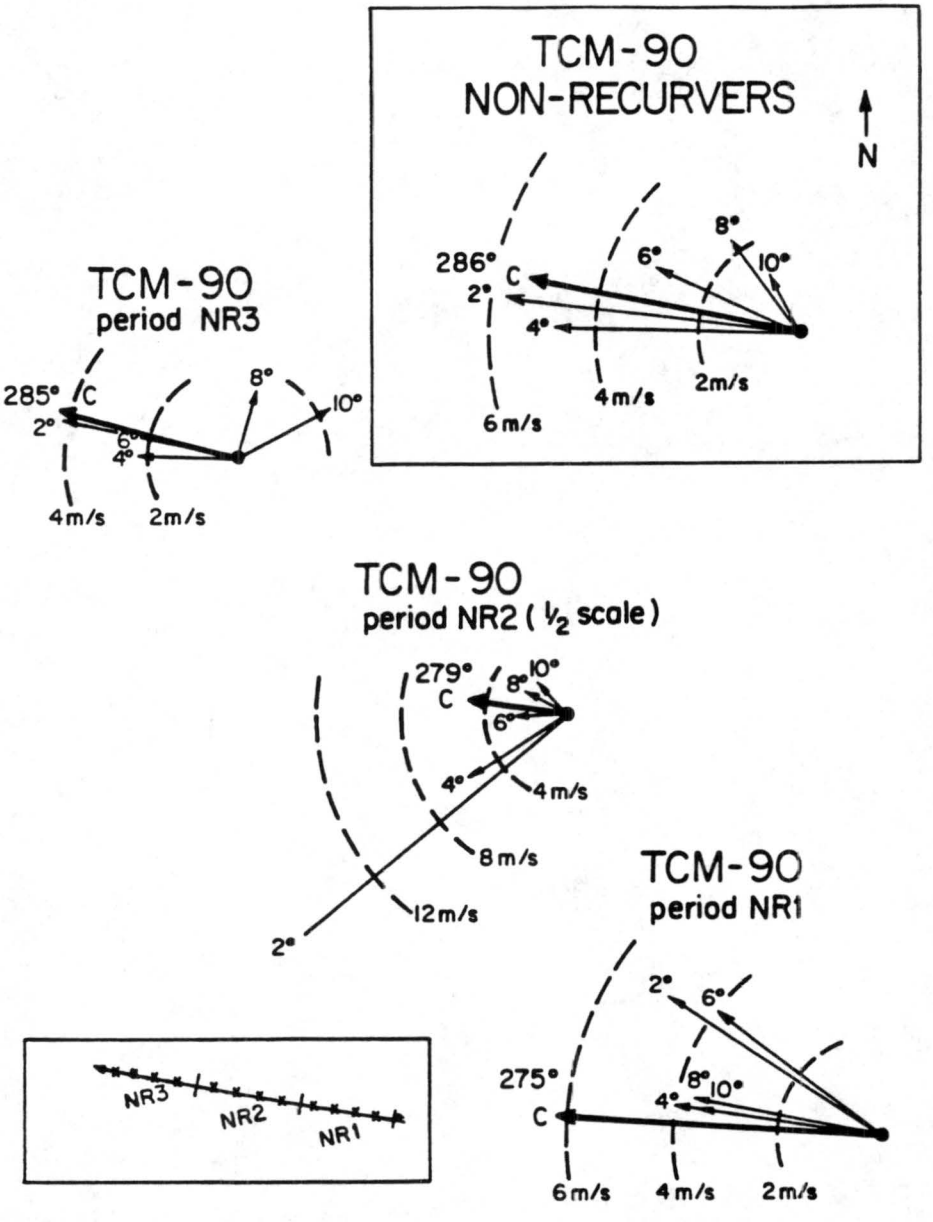

Figure 3.6: The layer average (850-300 mb) symmetric wind vectors relative to the cyclone motion (denoted by a "C") in two degree radial bands extending from 2 to 10° from the center. These diagrams show the composite results for TCM-90 non-recurving periods NR1 through NR3 and the combined composite including all three time periods.

data coverage, it is unlikely that a forecaster would have much confidence in predicting the start of a right turning motion from the steering flow indications alone.

3.5 Comparison of Typhoon Flo (Periods R0 through R4) Composite Steering Flow to TCM-90 Non-Recurving Storms Composite Steering Flow

Figure 3.7 compares a combined composite of periods of R0 through R4 for Typhoon Flo, a recurving TCM-90 cyclone to three composite TCM-90 non-recurving time periods. Both TCM-90 composites show a similar key radius of steering motion at approximately 5°. The 2° radius vector for Typhoon Flo shows a highly anomalous eastward direction. Consequently, in a larger overall TCM-90 composite data sets such as all non-recurvers, or even the complete Typhoon Flo track composite, we see more consistent results as compared to the individual time period composites. The individual composite periods appear not to contain enough observations to be representative of a reliable steering flow current.

3.6 Summary of Steering Flow Observations

Comparison of two independent data sets reveal similar results on the key steering flow radii which determine cyclone motion. The Gray project 21 year data set and the TCM-90 data set show the steering radii to be 5-7°. Given the size differential and temporal coverage between the two data sets, the TCM-90 results verify and compare favorably with the past results. Finally, there is some evidence available in the layer average wind flow information to differentiate between recurving and non-recurving cyclones. However, this difference may not show up in a timely fashion and give clear indications that would aid in specific recurvature or non-recurvature forecasts of initial turning motion.

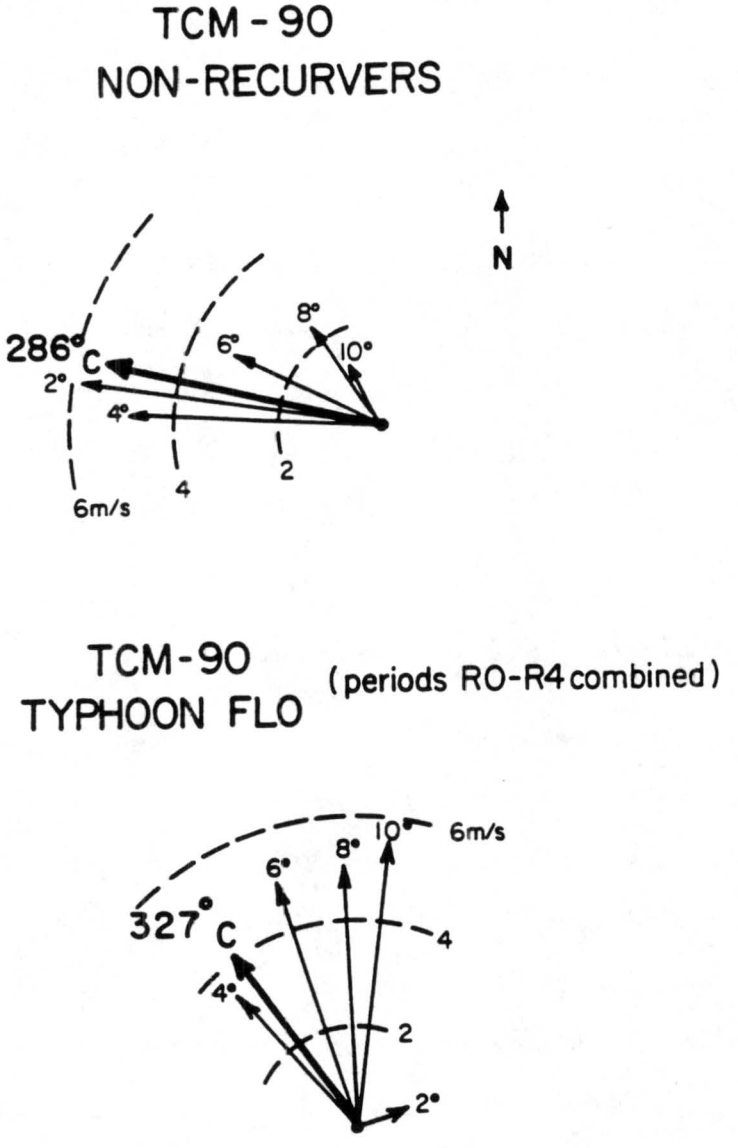

Figure 3.7: The layer average (850-300 mb) symmetric wind vectors relative to the cyclone motion (denoted by a "C") in two degree radial bands extending from 2 to 10° from the center. These diagrams show the composite results for all non-recurving periods combined, and a combined composite of recurving periods R0 through R4 for Typhoon Flo.

Chapter 4

STATISTICAL ANALYSIS OF WIND VARIABILITY

4.1 Sources of Measurement Variations

There are a myriad of unrepresentative measurements (small and large) and instrumental inconsistencies that can occur in the collection of rawinsonde data, especially in data collected near the center of a tropical cyclone. Some of the major data inadequacies are due to the following: (1) Variable cyclone structure and surrounding flow. Every storm is unique and different in its characteristic, intensity, size, and areal coverage of outer winds. This can have a significant impact upon the wind fields surrounding a storm. (2) Natural variability within storms due to convective features, etc. Winds are gusty and unrepresentative when taken near convective-scale features. (3) Measurement conditions. Every instrument has characteristic limitations and error sources. The sensing, transmitting, receiving and processing of atmospheric data can introduce unrepresentative steering flow features. (4) Compositing limitations. Even if the data were 100 percent accurate, some positioning and temporal representativeness are introduced into each composite analysis. A large data set is required to overcome or at least diminish these inherent positioning inconsistencies.

4.2 Data Spread

To assess the degree of reliability and significance of the composited data, several basic statistical analyses were performed on the TCM-90 rawinsonde and satellite wind data composites. These tests were to determine the degree of scatter for individual parameter values about their means. Figure 4.1 shows the typical spread for the 200 mb zonal wind component, by octant, during the TCM-90 composite period NR1 for non-recurvature at

200 mb and 6° radius (i.e., 5-7° radius). The average value for the seven standard deviation values shown in the figure is approximately ± 6 m/s. The individual mean zonal wind values for each octant vary from 0.9 m/s to 9.7 m/s. Figure 4.2 illustrates a similar set of values for the 200 mb wind at 6° during the second, or NR2, period of recurvature. With the exception of octant 4, the spread is somewhat more uniform in comparison with NR1. The larger sample size available for the NR2 composites appears to result in a smoothing of the spread to a more consistent value of approximately 7 m/s for most octants. Figure 4.3 shows the spread in the R2 period composite for Typhoon Flo, just before recurvature. There were no observations for several octants. The mean standard deviation for those octants which did have observations was 4-5 m/s.

A comparison of 200 mb zonal winds at 8° radius for Typhoon Flo (a recurving TCM-90 storm) during period R2 versus NR2 in selected octants is shown in Fig. 4.4. The results in this figure depict the dramatic zonal wind differences observed between periods R2 in octants 1 and 2 of Typhoon Flo and in NR2. The probability (as assessed by a t-test) that Flo R2 zonal wind values at 8° radius in octant 1 are not different from the NR2 observed zonal winds is 3×10^{-7}. A similar t-test for zonal winds in octant 3 found little probability that the two data sets are different. Specifically, for 98% confidence level t-test on Flo data for period R2 in octant 3, a confidence interval of (-10.7,4.4) m/s is observed. For period NR2 in octant 3, we get values of (-9.7, -2.1) m/s. Hence, the probability that the observed Flo period R2 zonal wind value in octants 3, 4, or 6 falls in the NR2 data range is, by contrast with the octant 1 and 2 values, quite high.

These test results indicate the importance of zonal wind differences in areas north and northwest of recurving versus non-recurving cyclones. The observed zonal wind differences in octants 1 and 2 are clearly much larger than the typical spread of zonal winds. Therefore, these differences can be used as a predictor. In other octants, such as 3, 4 and 6, recurvature versus non-recurvature differences are comparatively small, well within the expected range of normal wind variability.

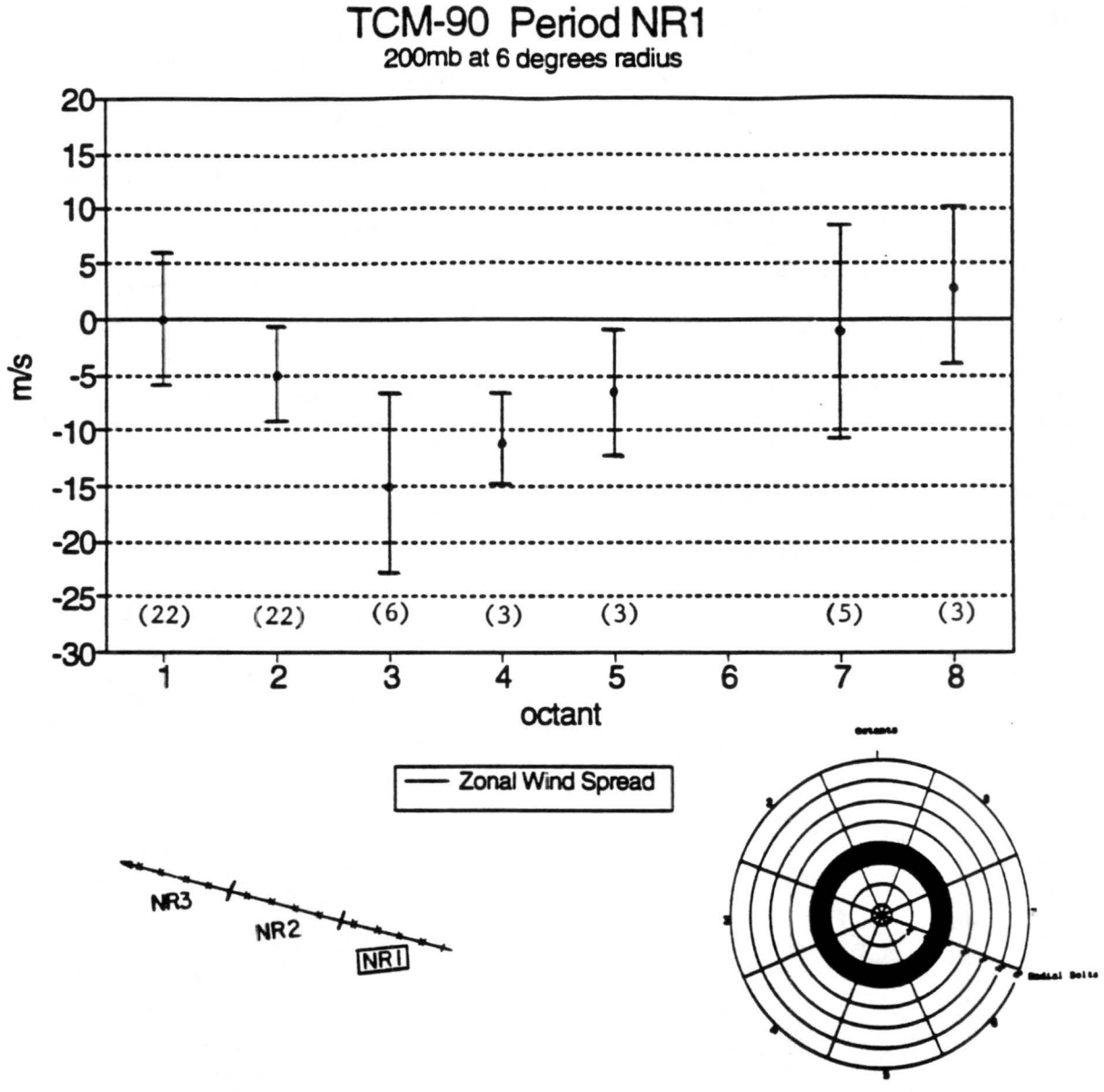

Figure 4.1: Mean and standard deviation of zonal wind values (in m/s) for TCM-90 period NR1 at 200 mb and 6° from the cyclone center. The vertical lines represent ± one standard deviation of the mean values. The numbers in parentheses indicate the number of observations in each octant. The lower panels show the typical NR track and the 6° radial band.

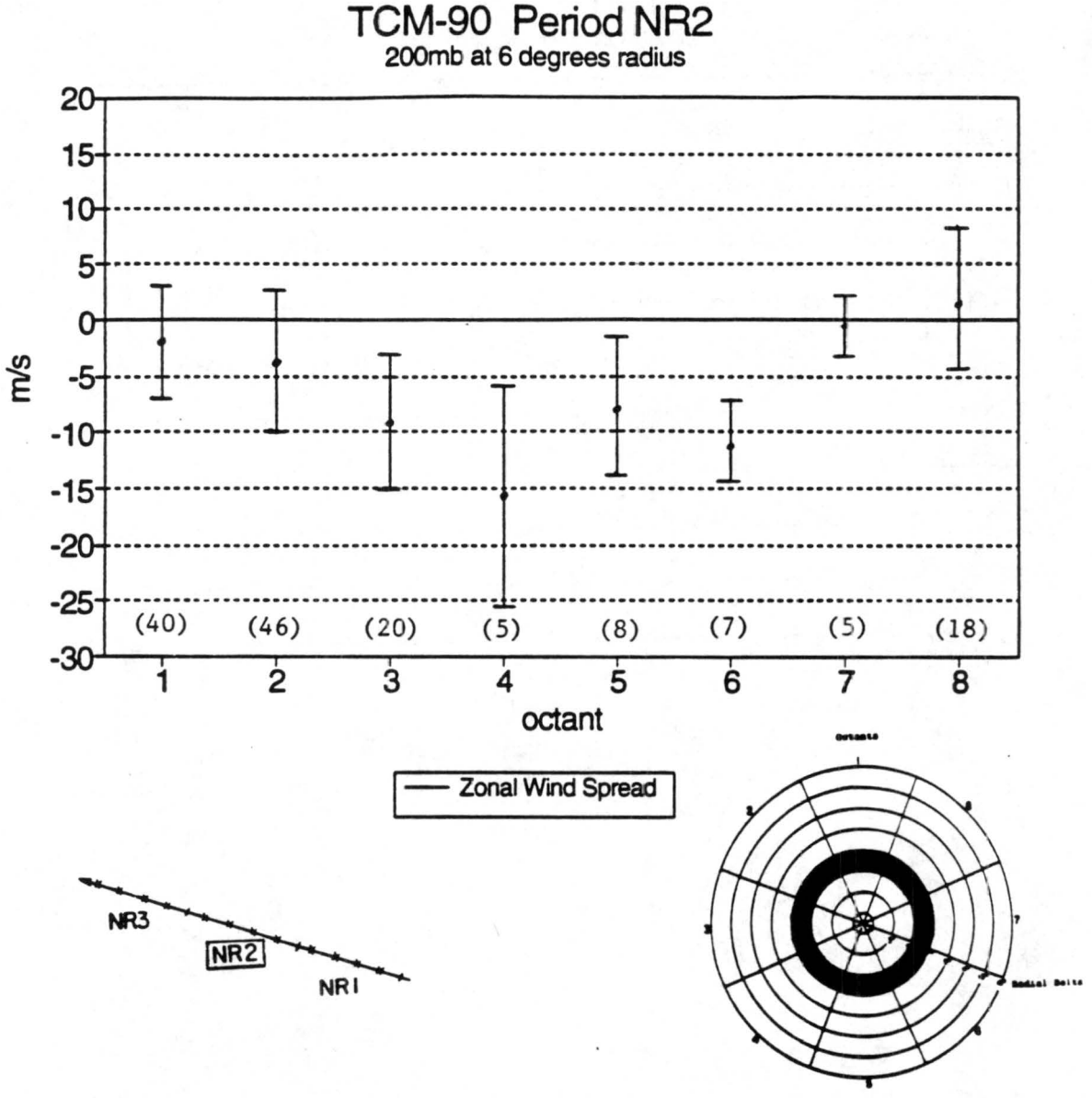

Figure 4.2: Mean and standard deviation of zonal wind values (in m/s) for TCM-90 period NR2 at 200 mb and 6° from the cyclone center. The vertical lines represent ± one standard deviation of the mean values. The numbers in parentheses indicate the number of observations.

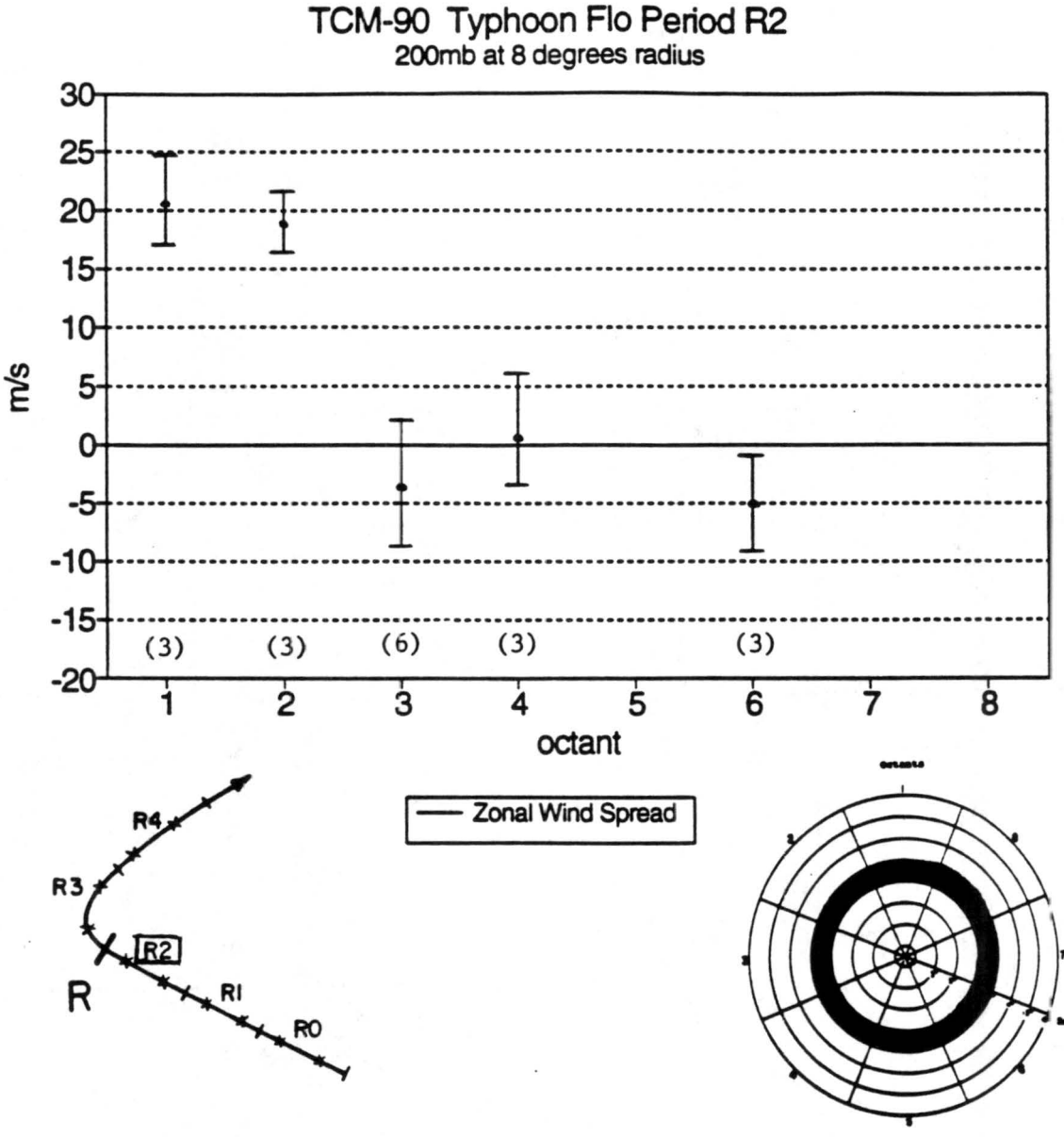

Figure 4.3: Mean and standard deviation of zonal wind values (in m/s) for TCM-90 Typhoon Flo period R2 at 200 mb and 8° from the cyclone center. The vertical lines represent ± one standard deviation of the mean values. The numbers in parentheses indicate the number of observations.

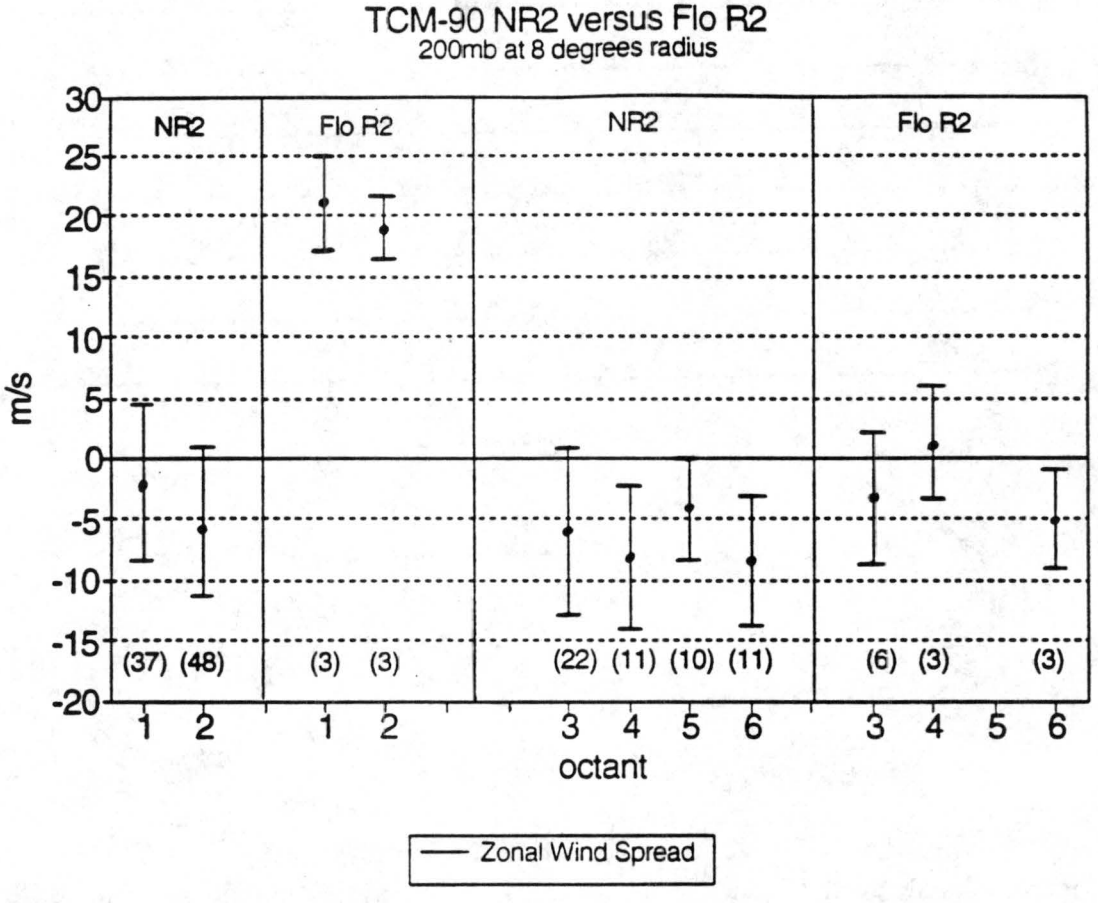

Figure 4.4: Standard deviation of 200 mb 8° zonal wind values (in m/s) for TCM-90 non-recurving cyclones period NR2 compared to Typhoon Flo period R2. The vertical lines bracket the standard deviation of values. The numbers in parentheses indicate the number of observations.

4.3 Standard Deviation of Satellite Cloud-Drift Winds

The satellite winds in this data set were very carefully reprocessed after the field experiment was completed. Table 4.1 shows the standard deviation values for 200 mb satellite cloud-drift winds at 6, 8, and 10° radius from the cyclone center in octant 1 during the five 24-hour time periods for Typhoon Flo. The S.D. of these satellite winds was typically on the order of 6 m/s. Hence, the average S.D. of these satellite winds compares favorably with the S.D. of the rawinsonde data.

Table 4.1: Standard deviations (in m/s) of Typhoon Flo for 200 mb satellite derived cloud-drift zonal winds. Values are for octant 1 and for periods R0 through R4 at three radial belts from the storm center.

Typhoon Flo Satellite Wind Standard Deviations
Octant 1
Period

Radius	R4	R3	R2	R1	R0
10	8.6	3.9	6.8	4.6	16.2
8	6.5	2.9	5.8	5.3	8.8
6	5.3	N/A	4.7	3.5	5.5

4.4 Summary

The standard deviation of individual octant and 2° radial belt wind data in prior Gray research project composites indicated a S.D. of about 8 m/s for zonal and meridional wind components in the upper troposphere (see Table 4.2). These larger composites involved thousands of soundings versus hundreds available for most of the TCM-90 time periods studied here. From both of these studies we can specify an expected range for composite zonal wind values of about 7-8 m/s. The spread at lower levels is somewhat smaller.

Table 4.2: Approximate standard deviation value for wind components of individual octant wind averages for specific levels in m/s for data collected between 1957-1977 (from Gray, 1981).

	900 mb	500 mb	200 mb
Zonal wind (u)	~ 5	~ 5	~ 8
Meridional wind (v)	~ 5	~ 5	~ 8
Tangential wind (V_θ)	~ 5	~ 5	~ 8
Radial wind (V_R)	~ 5	~ 5	~ 8

Chapter 5

ENVIRONMENTAL WIND FIELDS—COMPARISON OF RECURVING AND NON-RECURVING CYCLONES

5.1 Introduction

Previous studies have attempted to identify those features of the wind fields surrounding tropical cyclones which are conducive to recurvature (see Hodanish, (1991) and Chan and Gray (1982)). It is accepted that the turning motion of tropical cyclones is controlled by the large scale surrounding flow (Elsberry, 1988). We now assess those flow feature in the TCM-90 data which distinguish tropical cyclone recurvature from non-recurvature.

Hodanish (1991) examined the environmental wind fields of non-recurving and recurving cyclones prior to the beginning of recurvature. Table 5.1, from Hodanish (1991), emphasizes the importance of the upper tropospheric (100-300 mb) zonal winds in areas north and northwest (octants 1 and 2) of the cyclone's center in specifying differences between recurvature and non-recurvature. The maximum zonal wind differences were observed in octants 1 and 2 whereas negligible differences were observed to the south and east (octants 4 through 7). His results were based on rawinsonde composites from a 21-year (1957-77) data set. In this study, we will use composites from the TCM-90 data set for comparing with Hodanish's results. We shall also attempt to determine if an individual case of recurvature (Typhoon Flo) could be shown to quantitatively resemble the larger data set.

5.2 Zonal Wind Fields for TCM-90 Non-Recurving Cyclones

Figures 5.1 and 5.2 show the 6° and 8° zonal wind profiles, respectively, for the three TCM-90 non-recurving time periods NR1, NR2 and NR3 in octant 1, hence, on

Table 5.1: Zonal wind differences between sharply recurving cyclones prior to recurvature (period R2) and the non-recurving cyclones (Hodanish, 1991). Units in ms^{-1}

Sharply Recurving Cyclones (Period R2) Minus Non-recurving Cyclones								
Zonal Wind Differences–8 Degrees from Cyclone's Center								
P (mb)	Oct 1	Oct 2	Oct 3	Oct 4	Oct 5	Oct 6	Oct 7	Oct 8
100	14.5	16.6	7.8	1.8	4.3	3.5	2.9	9.3
200	15.4	16.3	8.7	3.7	3.0	0.4	1.9	4.8
300	9.7	17.6	10.0	2.4	1.4	1.3	0.6	3.7
400	8.5	13.8	8.6	-0.4	-0.1	4.2	-0.7	3.7
500	6.6	11.6	5.9	-0.1	-1.2	-0.5	-0.2	3.7
600	3.8	6.8	2.4	-1.3	-2.5	-0.5	1.4	4.0
700	3.0	4.3	-0.7	-1.8	-2.1	1.7	0.7	2.8
800	3.1	2.2	-0.7	-2.1	-3.3	2.5	-0.5	2.7
Layer Ave.	8.1	11.2	5.3	0.3	-0.1	1.6	0.8	4.3

the north side of the cyclone. Figures 5.3 and 5.4 present similar profiles for octant 2 to the northwest of the cyclone. The 6° zonal wind profiles show that zonal winds in both octants for all three non-recurving time periods are from an easterly direction throughout the troposphere, except in octant 1 where weak zonal winds in the upper troposphere are from a westerly direction. The 8° profiles show zonal winds in octant 1 during periods NR1 and NR2 which are (easterly) are negative during period NR3, but become positive and penetrate into the mid and upper troposphere.

TCM-90 cyclones which moved west throughout their lifetimes were observed to be imbedded in a deep easterly flow at nearly all levels in the troposphere at 6° radius. The zonal wind fields at 8° were also from an easterly direction throughout most of the levels of the troposphere except during the last time period, NR3. During the latter period, positive zonal winds penetrated into the mid and upper troposphere to the north and northwest of the cyclone. Hodanish (1991) states that these positive zonal winds during this last time period are most likely associated with the mid latitude westerly wind regime which occur near eastern Asia. Tropical cyclones which track in this direction (westward) will eventually move to higher latitudes and approach the southern limits of the mid-latitude

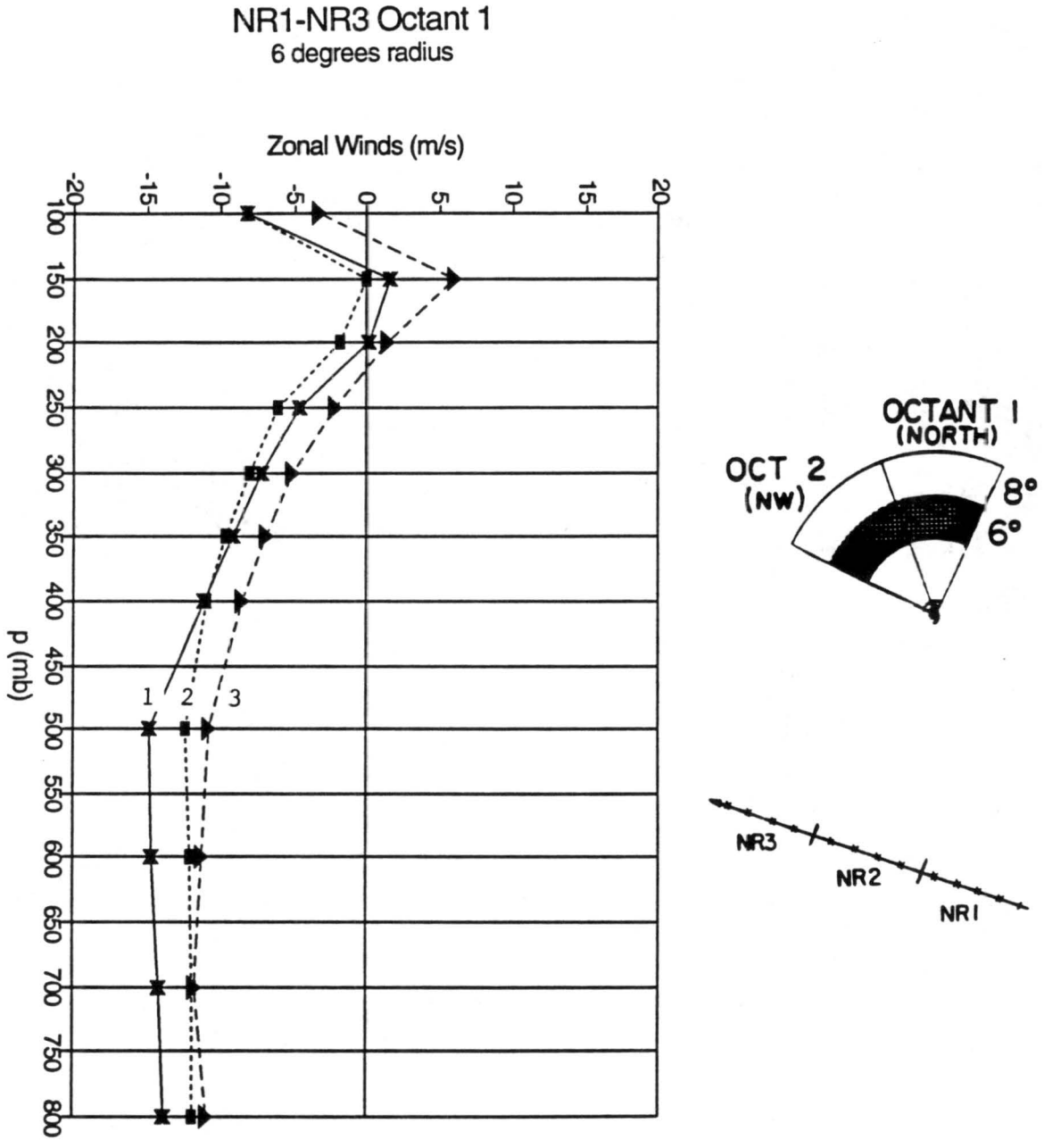

Figure 5.1: Zonal wind vertical profile for periods NR1 through NR3 in octant 1 at 6° radius from the cyclone center.

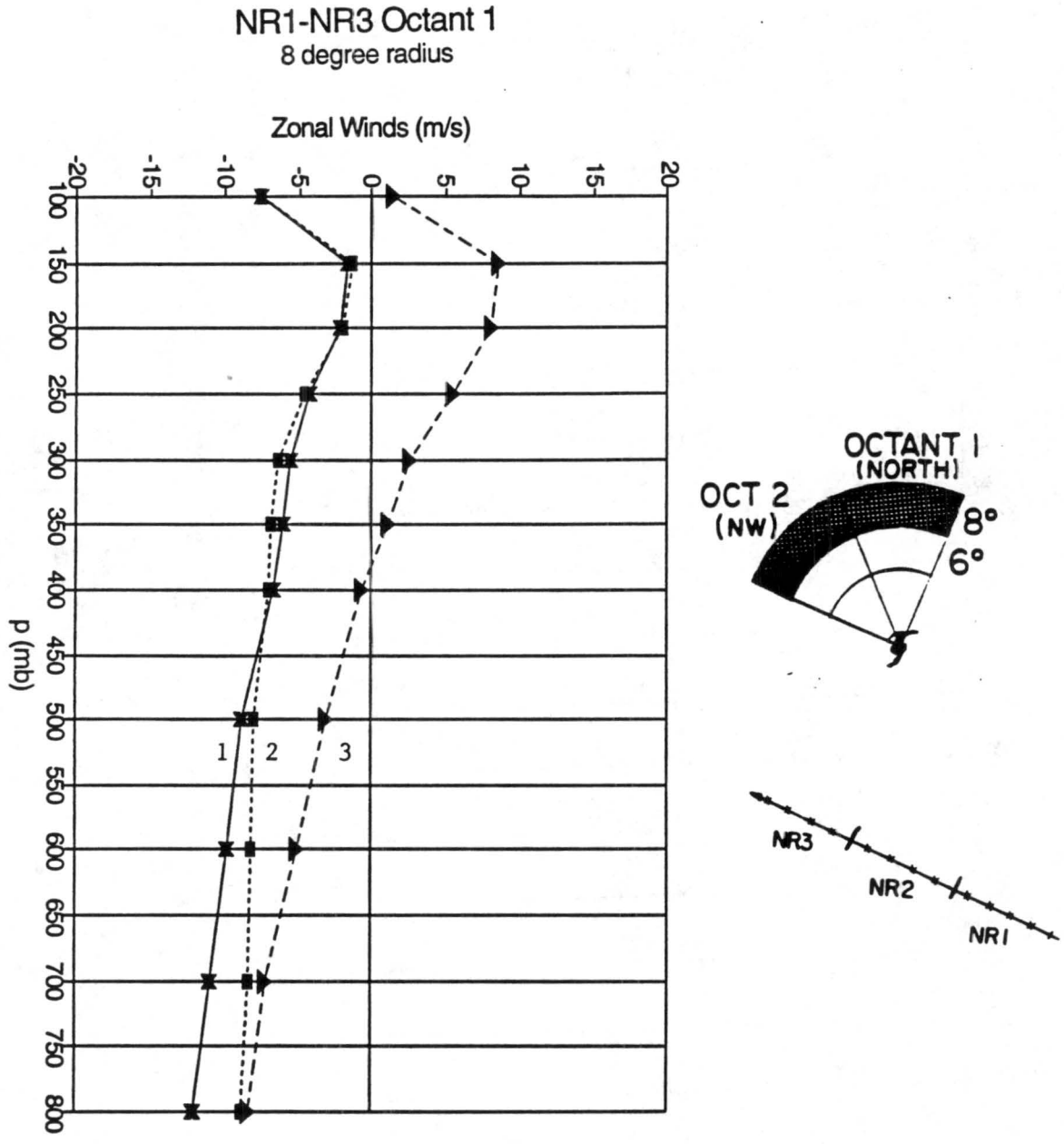

Figure 5.2: Zonal wind vertical profile for periods NR1 through NR3 in octant 1 at 8° radius from the cyclone center.

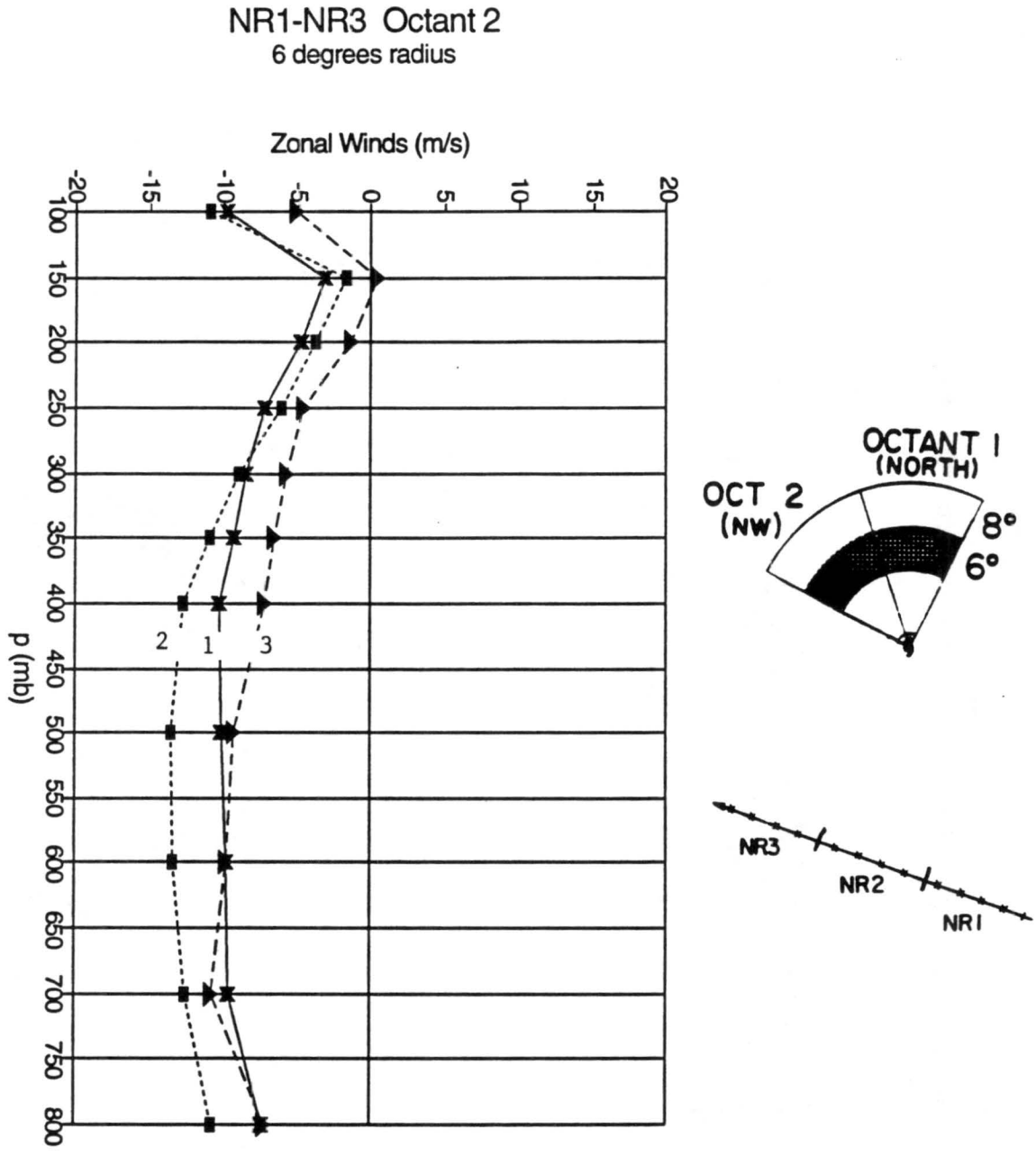

Figure 5.3: Zonal wind vertical profile for periods NR1 through NR3 in octant 2 at 6° radius from the cyclone center.

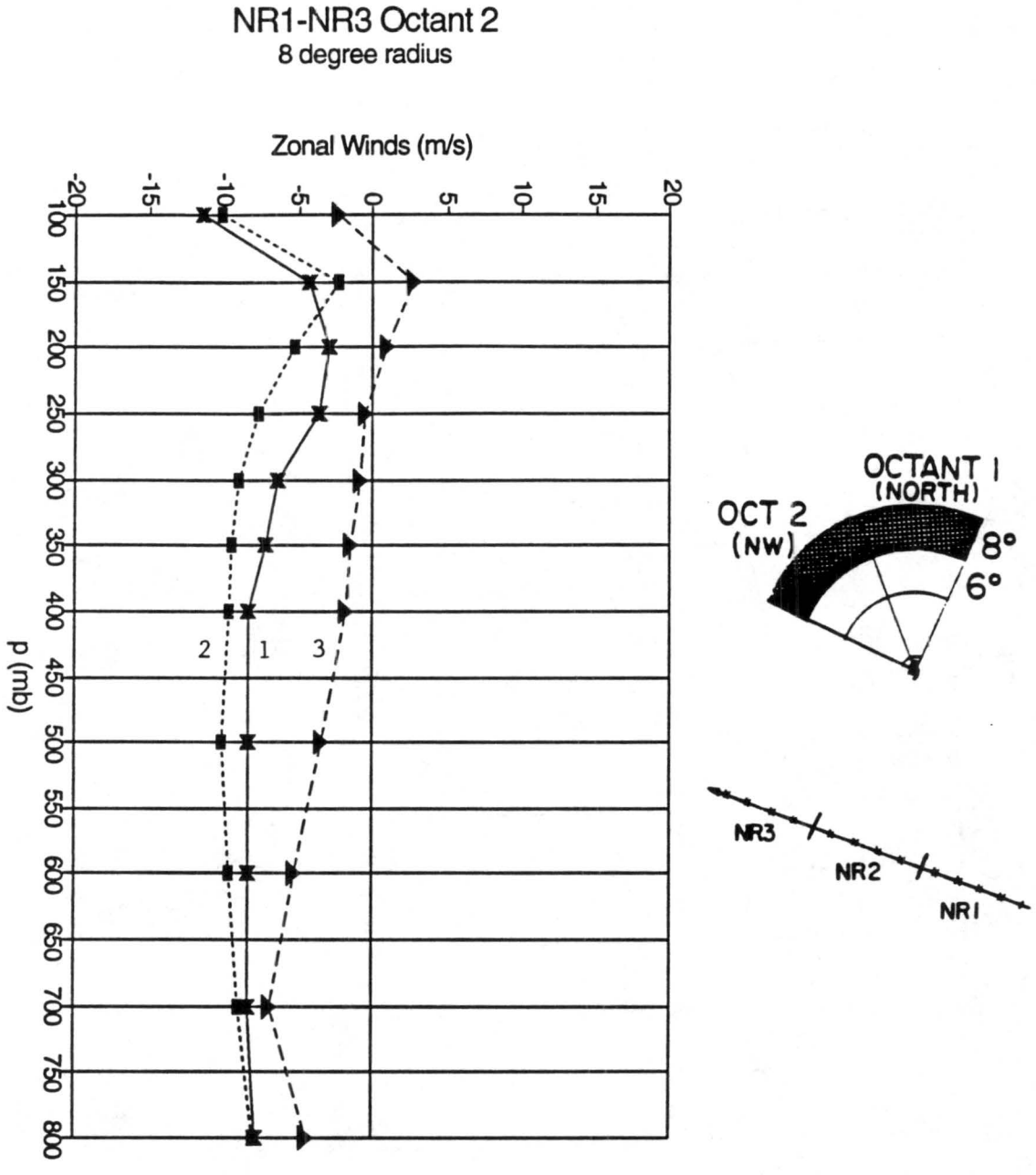

Figure 5.4: Zonal wind vertical profile for periods NR1 through NR3 in octant 2 at 8° radius from the cyclone center.

westerly wind regime. The feature of note for TCM-90 cyclones is that the westerlies penetrated the mid and upper troposphere 8° to the north and northwest of the westward moving cyclones and yet had no effect on their motion.

5.3 Typhoon Flo

Figure 5.5 presents the best track for Typhoon Flo (JTWC, 1991). Flo maintained west-northwesterly movement at approximately 12 knots for nearly eight days until encountering a trough on the northwest side which eventually acted to recurve it to the northeast. An unusually large number of rawinsonde and satellite wind observations were made in the area surrounding Flo. Hence, it was chosen for analysis because of its relatively abundant data and because it provided a classical example of cyclone recurvature.

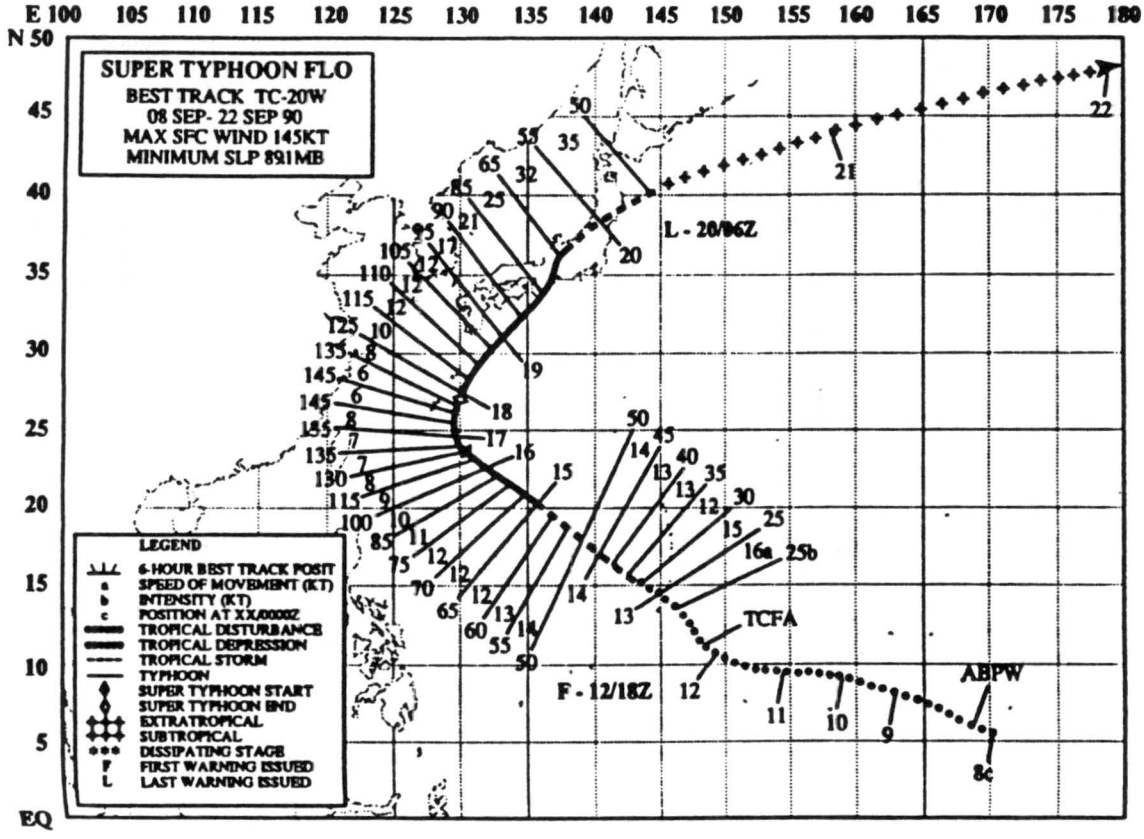

Figure 5.5: Best track for Typhoon Flo. (JTWC, 1991)

5.3.1 Results of Rawinsonde Composite

Figures 5.6 and 5.7 show the zonal wind profiles at 6° radius for Flo during the five recurving time periods R0 through R4 in octants 1 and 2, respectively. Figures 5.8 and 5.9 give the profiles at 8° radius for the same time periods and octants. The 6° profiles show negative zonal winds for periods R0 through R2 in octant 2 at all levels of the troposphere. In octant 1 the zonal winds are easterly for all but the 150-200 mb levels wherein they are weak and from the west. By periods R3 and R4 there is very strong westerly flow in both octants throughout most of the depth of the troposphere. Zonal wind profiles at 8° in octant 1 and octant 2 indicate strong upper tropospheric westerly flow during period R2. Periods R0 and R1 show mostly negative zonal winds. For periods R3 and R4 there is substantial westerly flow through the entire vertical extent of the troposphere.

Figures 5.6 and 5.7 show that Flo did not begin to recurve until positive zonal winds in octant 2 had penetrated to within 6° of the center. This is consistent with the findings of Hodanish (1991). It is likely that these upper tropospheric zonal winds northwest of the cyclone at 6° radius are a crucial factor determining wherein the cyclone actually begins recurving or remains on a west-northwest course. Zonal wind profiles at 8° showed that significant changes in the environmental wind fields can occur with no immediate effect on the motion of the cyclone. Such changes may signify that the storm is likely to begin recurving within the next 24 hours. But the key to the recurvature is as Hodanish (1991) found; positive zonal winds must reach to within 6° radius before the cyclone actually begins its initial right turn movement.

5.4 Satellite Cloud-Drift Wind Results

Figures 5.10 and 5.11 provide satellite derived cloud-track zonal winds for octants 1 and 2 respectively at 200 mb and 6° from the center of Typhoon Flo. Figures 5.12 and 5.13 show the same information at 8° and 10° radius for octant 1 and Fig. 5.14 provides an overall look at octant 1 zonal winds at 10°, 8°, and 6° from the cyclone center. The cloud track winds at the 200 mb level for Typhoon Flo provide results which are similar to

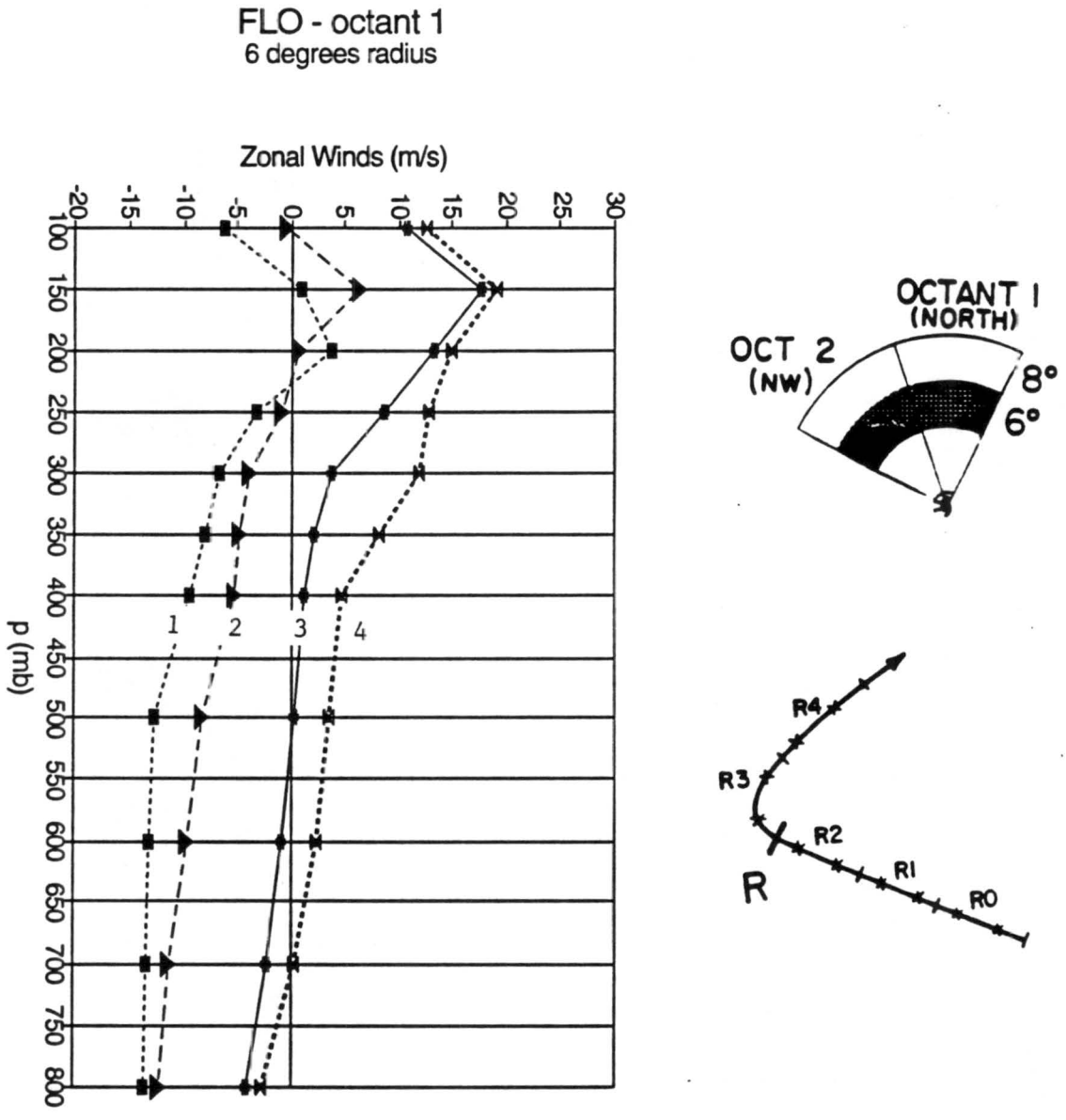

Figure 5.6: Zonal wind vertical profile for Typhoon Flo for periods of R1 through R4 in octant 1 at 6° radius from the cyclone center.

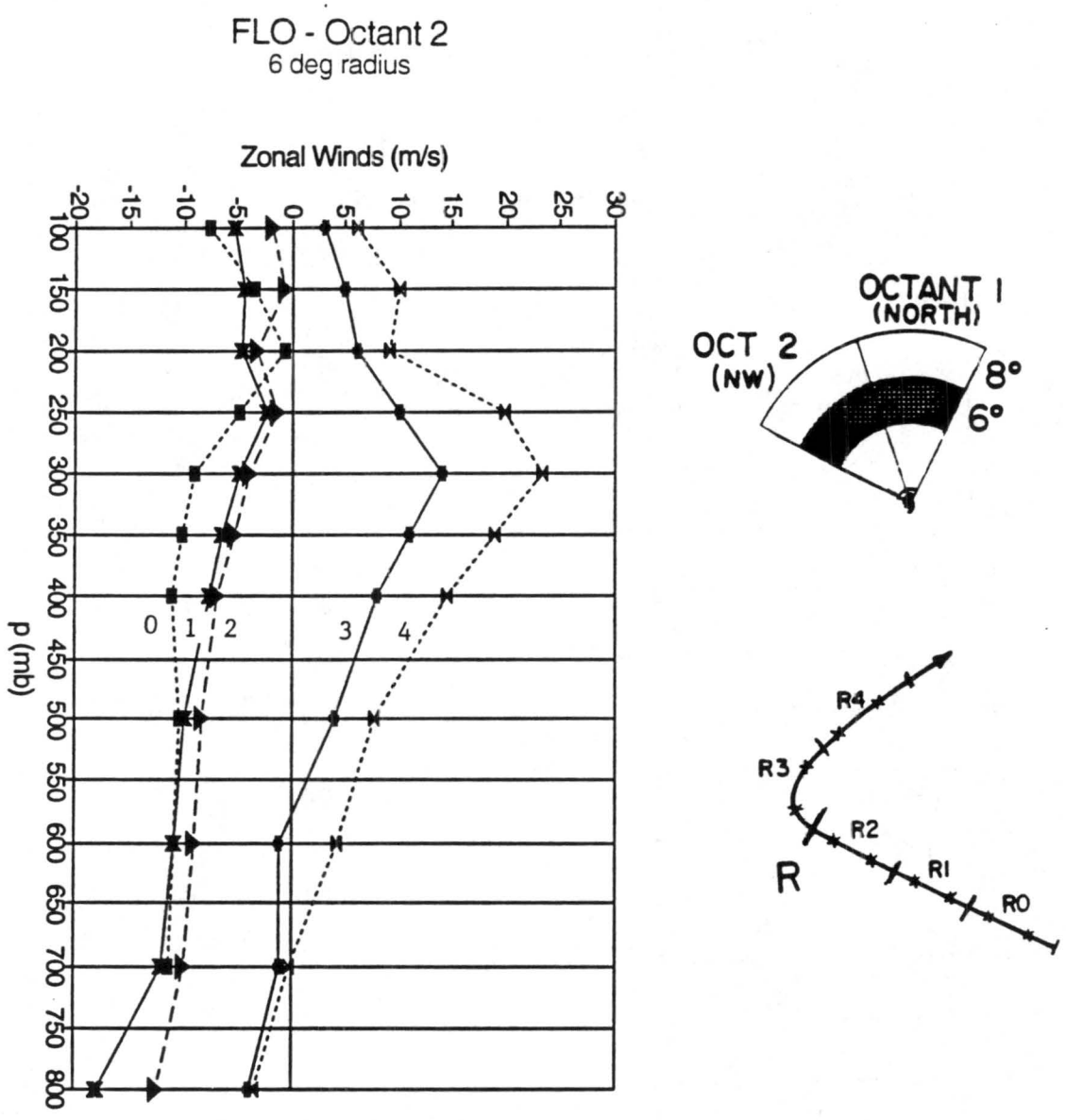

Figure 5.7: Zonal wind vertical profile for recurving Typhoon Flo for periods of R0 through R4 in octant 2 at 6° radius from the cyclone center.

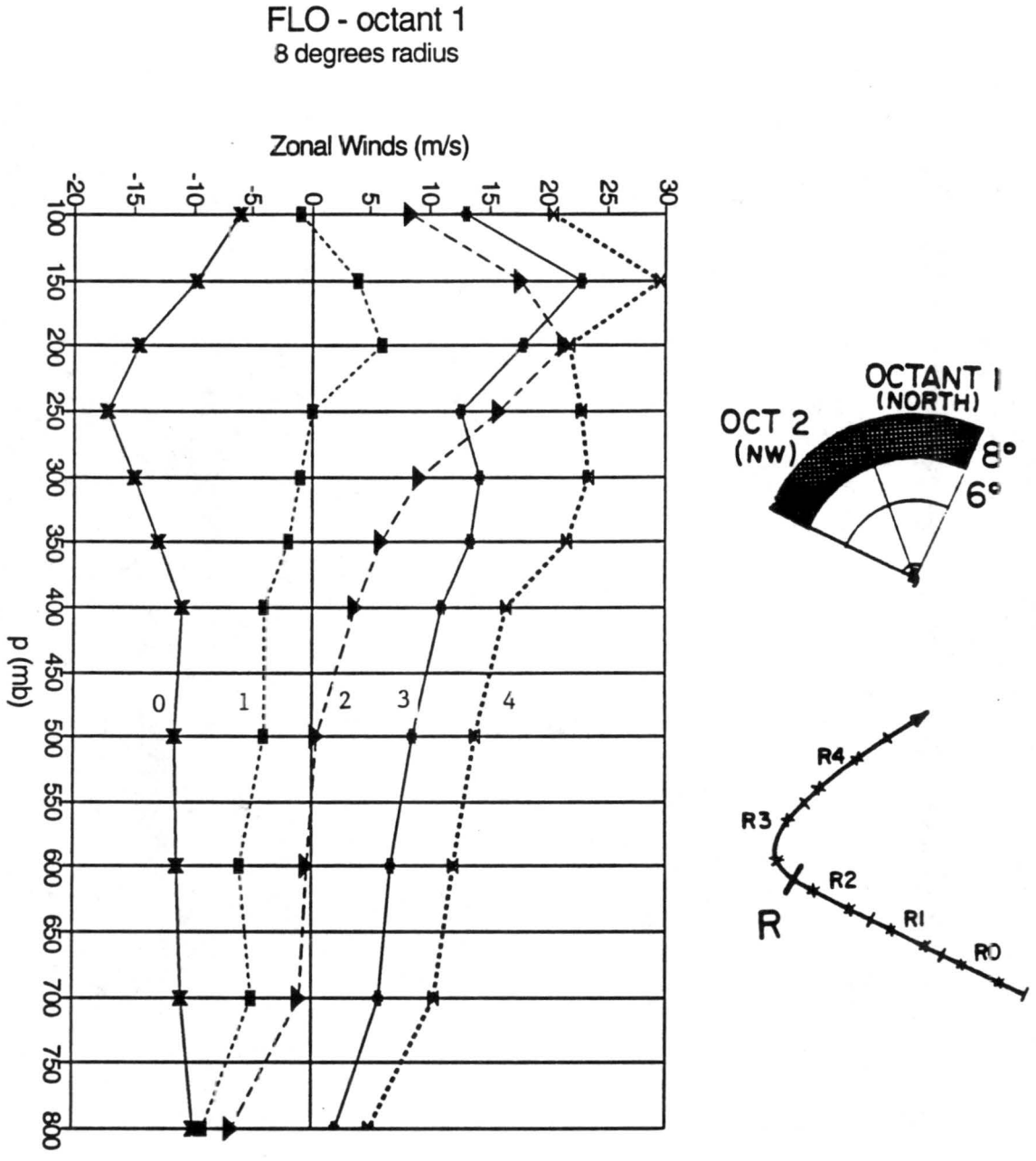

Figure 5.8: Zonal wind vertical profile for recurving Typhoon Flo for periods of R0 through R4 in octant 1 at 8° radius from the cyclone center.

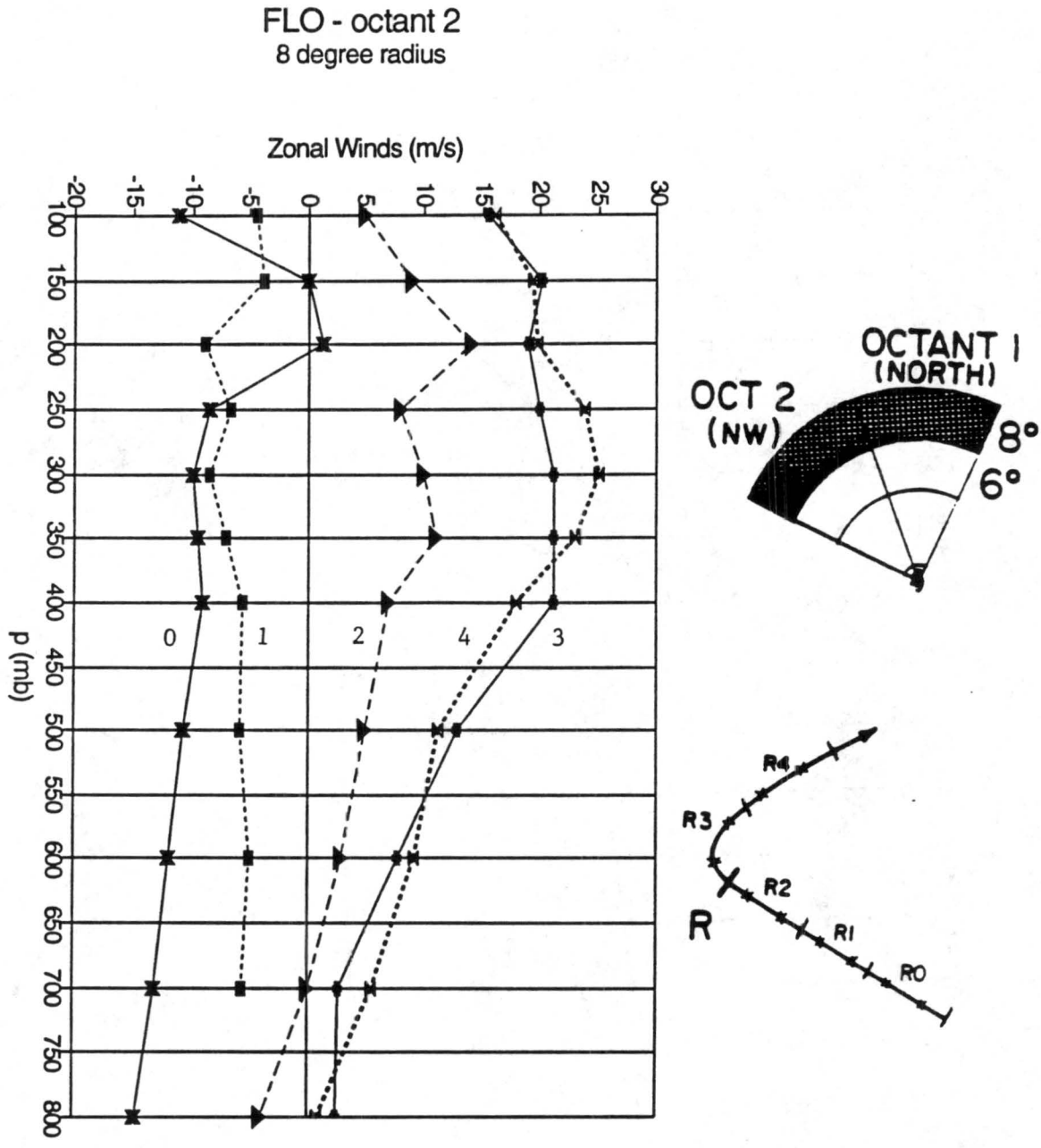

Figure 5.9: Zonal wind vertical profile for Typhoon Flo for periods of R0 through R4 in octant 2 at 8° radius from the cyclone center.

those found in the rawinsonde composites. When the zonal winds at 6° radius in octant 2 became westerly during period R3, the cyclone was already in its recurvature process. The octant 2, 6° radius winds during period R2 were weak and from the east. Octant 1 showed increasing westerly flow from period R2 onward. At 8° and 10° radius in octant 1, there were positive zonal winds observed during period R1. In summary, the satellite winds agree well with the rawinsonde zonal winds for Flo in Figs. 5.6 to 5.9 and support the findings of Hodanish (1991).

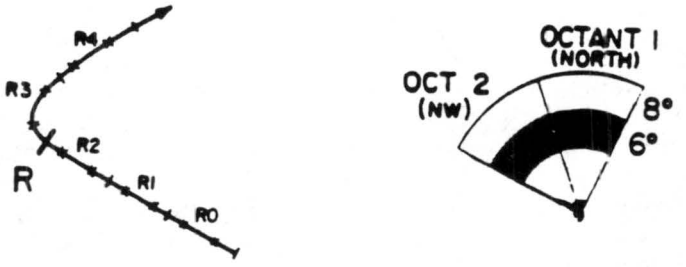

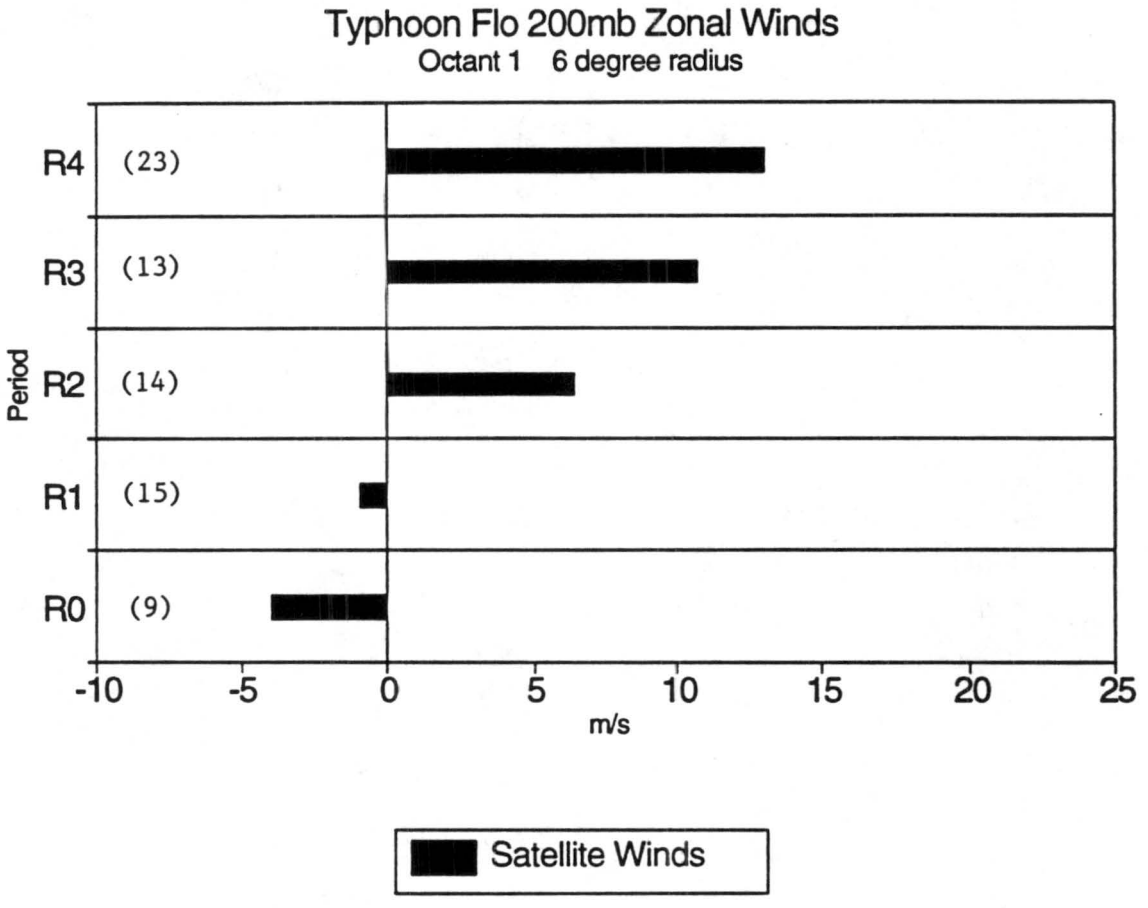

Figure 5.10: Satellite-derived 200 mb zonal winds for Typhoon Flo for periods of R0 through R4 in octant 1 at 6° radius from the cyclone center. The numbers in parentheses indicate the number of observations.

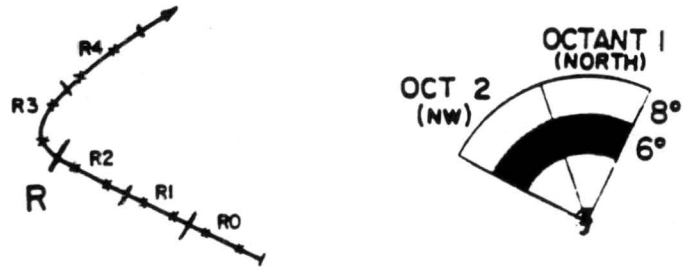

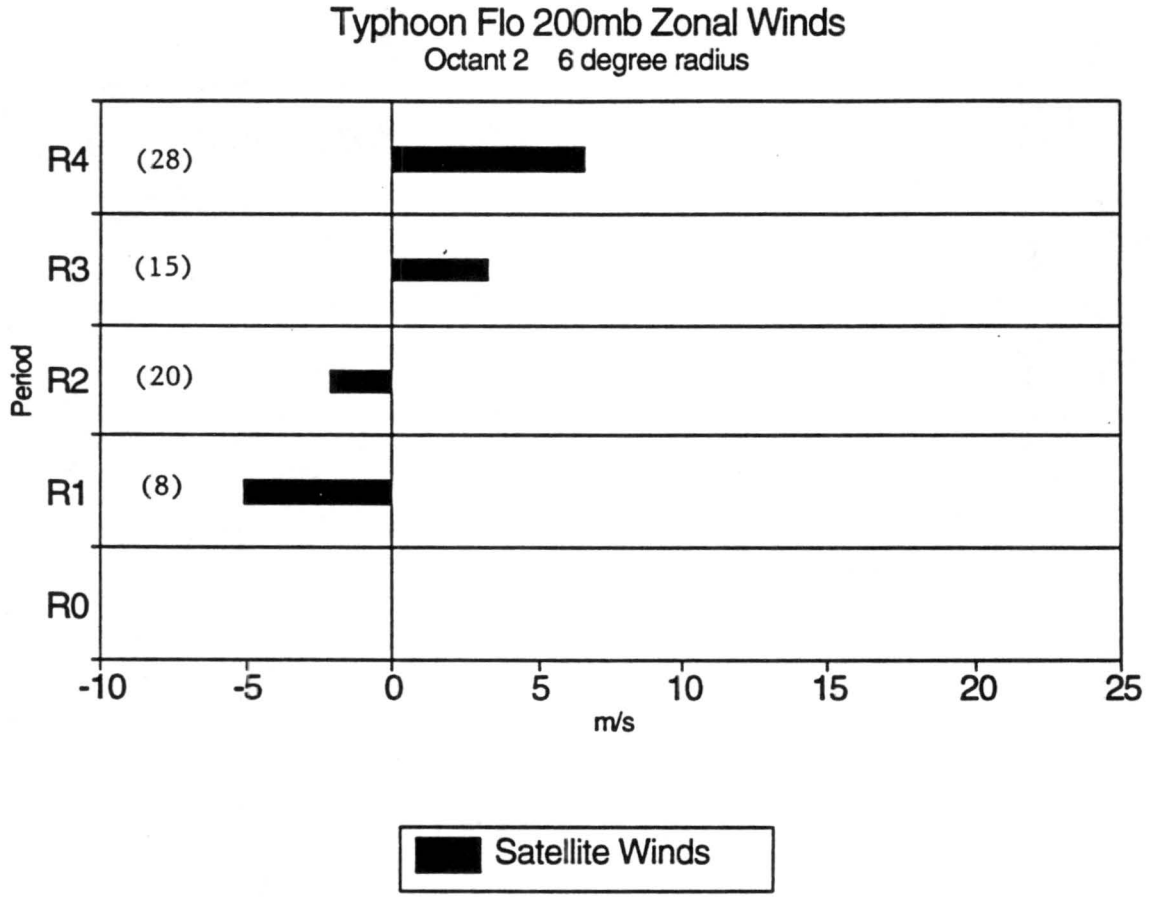

Figure 5.11: Satellite-derived 200 mb zonal winds for Typhoon Flo for periods of R1 through R4 in octant 2 at 6° radius from the center. The numbers in parentheses indicate the number of observations.

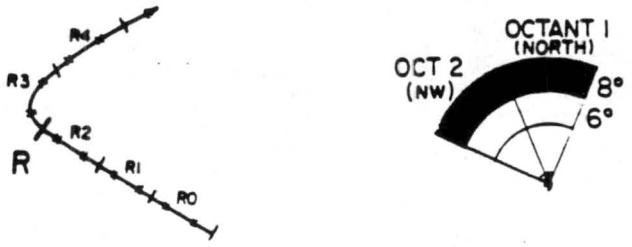

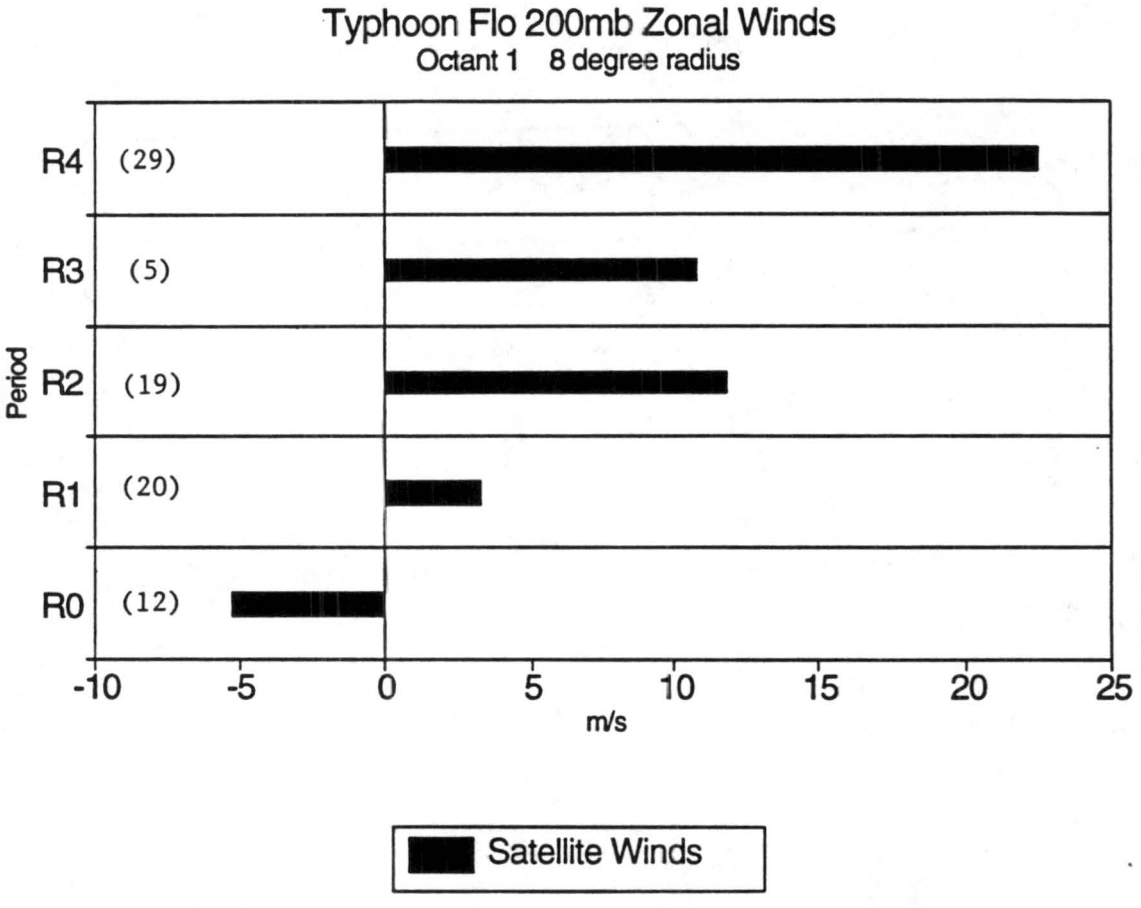

Figure 5.12: Satellite-derived 200 mb zonal winds for Typhoon Flo for periods of R0 through R4 in octant 1 at 8° radius from the cyclone center. The numbers in parentheses indicate the number of observations.

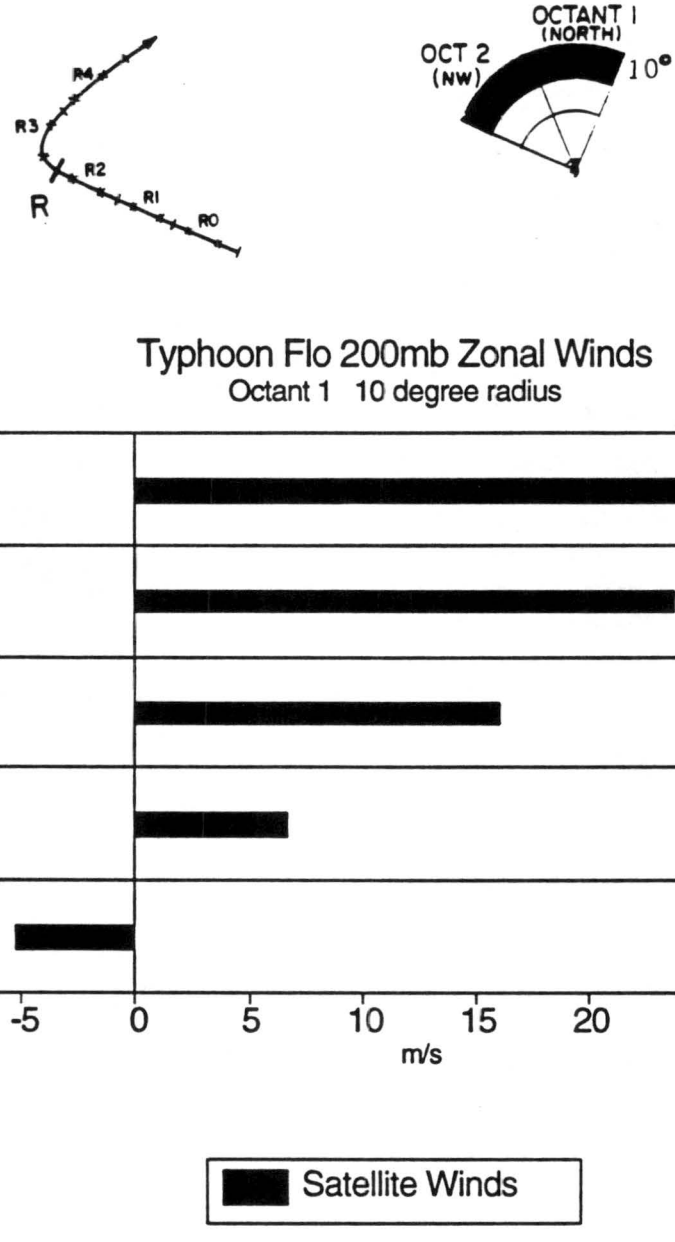

Figure 5.13: Satellite-derived 200 mb zonal winds for Typhoon Flo for periods of R0 through R4 in octant 1 at 10° radius from the cyclone center. The numbers in parentheses indicate the number of observations.

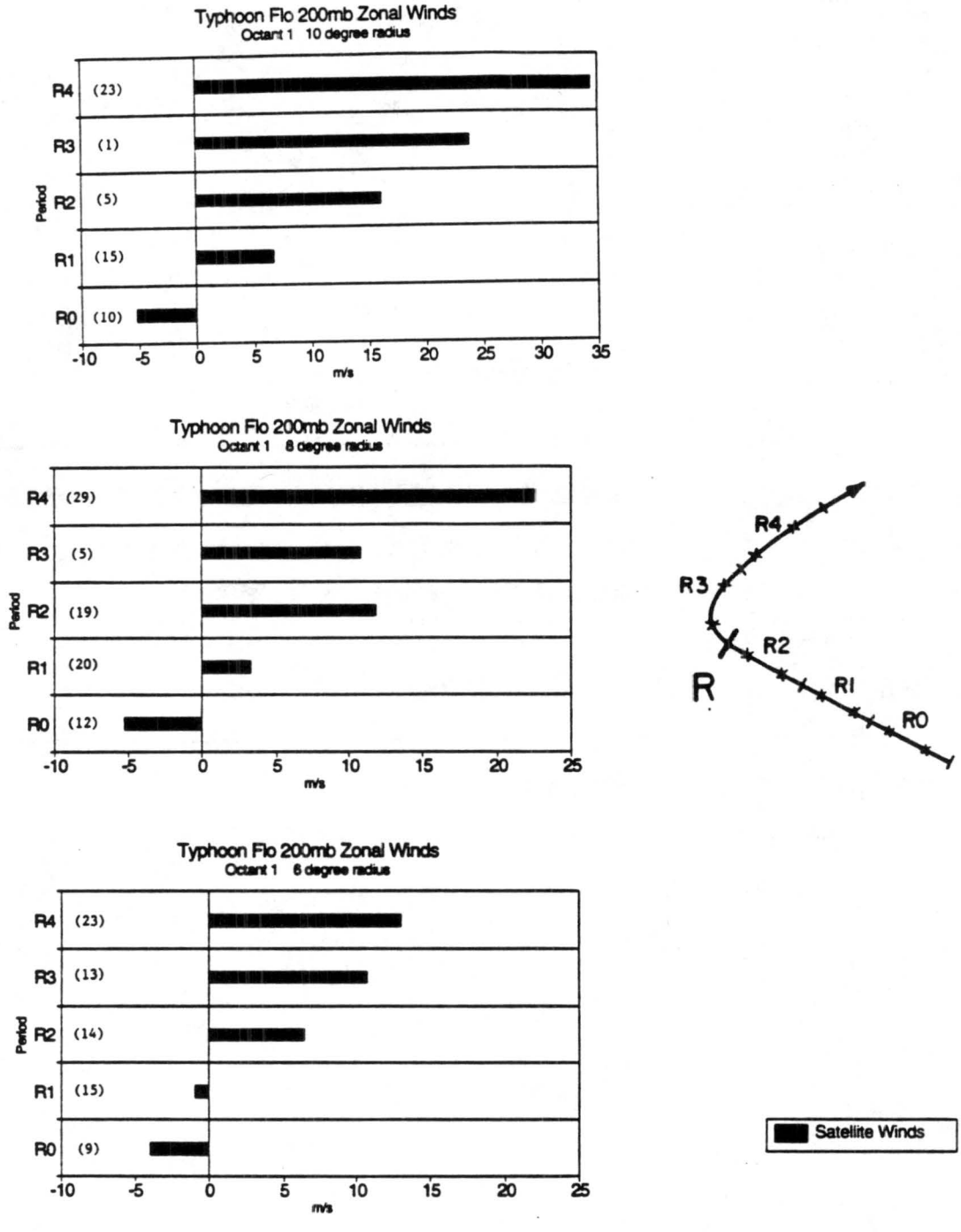

Figure 5.14: Satellite-derived 200 mb zonal winds for Typhoon Flo for periods of R0 through R4 in octant 1 at 10°, 8°, and 6° radius from the cyclone center. The numbers in parentheses indicate the number of observations.

Chapter 6

SUMMARY DISCUSSION

The TCM-90 experiment was specially designed to study tropical cyclone motion. An important feature of this field experiment was to determine if an augmented rawinsonde network was accomplished in the TCM-90 experiment would give improved information for individual case and time period steering flow such that track forecast improvements would result. These special observations, particularly the extra ship rawinsonde observations, provided the best opportunity yet to try to measure individual case cyclone steering flow over the open ocean where large atmospheric data inadequacies are always present.

This analysis of TCM-90 found that:

1. Despite the substantial augmentation in the rawinsonde data network which the TCM-90 experiment and the auxillary international programs effected, the number of rawinsonde observations almost always fell short of providing quantitative information sufficient to specify a reliable individual case cyclone steering current. This was also true of the composite analyses of five to ten cases.

2. When all TCM-90 westward moving cyclones were composited together however, quite similar cyclone motion and outer radius steering flow results were obtained. These composites compared favorably with the much larger 21-year westerly motion composites for the West Pacific and the West Atlantic as discussed by Gray (1991). TCM-90 composites for northward and northeastward moving cases compared reasonably well for direction but not for speed. TCM-90 northward and northeast motion composite cases showed consistently slower cyclone motion than did the more extensive 21-year composite data analysis of Gray (1991, 1992).

We have not been able to determine why the speed of northward and northeastward moving cyclones in TCM-90 were slower than for the more extensive rawinsonde composite measurements. It is difficult to ascribe this speed difference to the smaller data sample. It should be noted that individual case analyses for the NOAA-HRD synoptic-flow experiments (see Franklin, 1990; Kaplan and Franklin, 1991; and Marks *et al.*, 1991) have indicated a generally faster motion for the cyclone center as compared to the average surrounding steering flow; this is in agreement with the earlier 21-year composite analyses.

3. There is a sizable amount of natural variability in the tropical cyclone's surrounding steering flow winds for different cyclones moving with the same approximate direction and speed. It is this natural variability of the surrounding flow together with some interior grid positioning variations which makes accurate determination of the steering flow in the individual motion cases so difficult. Despite the typical presence of an extra 3-5 rawinsonde reports within 6-8° of a cyclone in the TCM-90 cases (and this is quite an enhancement), a reliable steering current could not be determined. It is for this reason that cyclone extrapolation procedures are usually considered a more reliable way to gage a cyclone's steering current than the surrounding wind data.

The results of this study emphasize the difficulty in the measurement of tropical cyclone steering flow over the oceans. Even with the extra observations of a much enhanced special data network such as TCM-90 and the companion programs (TATEX, SPECTRUM), surrounding flow measurements were usually inadequate for a realistic specification of individual case and time period steering. It remains to be seen how much track forecast improvement will be made by the numerical prediction tests with this enhanced data set.

Recurvature. Of all the operational problems involved with tropical cyclones, track forecasting is considered to be of the greatest importance. And of the different track forecasting problems, recurvature is the most important. This research and that of Hodanish

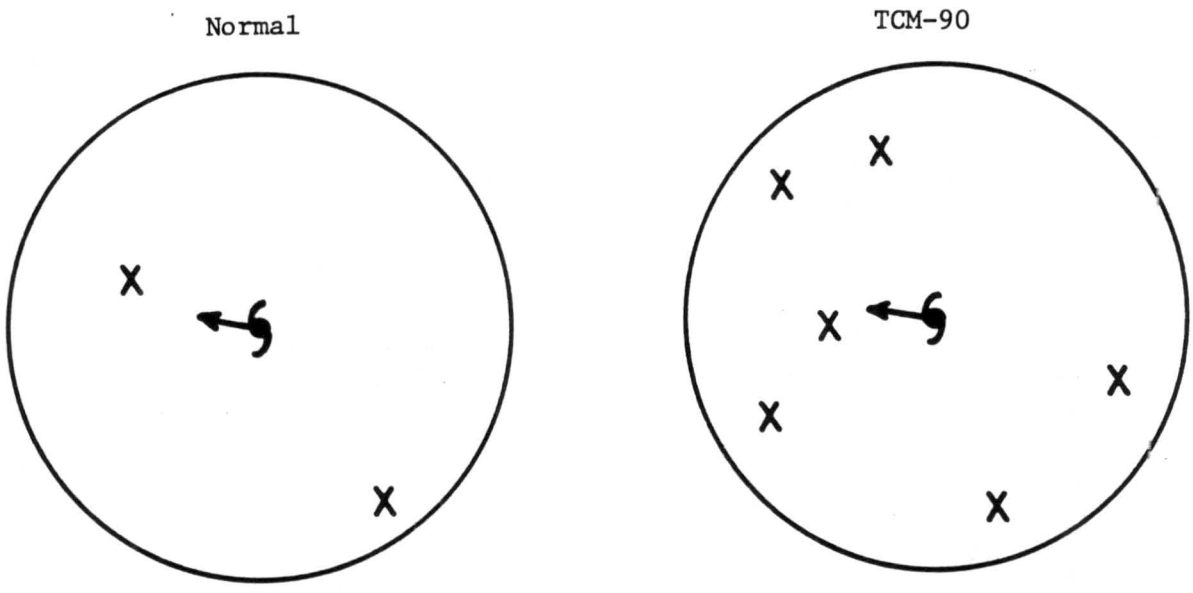

Figure 6.1: Comparison of the typical rawinsonde observational density within 15° radius of a tropical cyclone to that available during the TCM-90 field experiment.

(1991) shows that, with regard to cyclone recurvature, there is a level and area 6 to 8° radius north and northwest of the cyclone which offers a special opportunity for forecasting of individual case recurvature up to 24 hours before it begins (see Fig. 6.2). Here the observed wind differences between recurvature and non-recurvature cases are very large whereas, at other azimuths, radial belts, and levels, wind measurement differences between recurving and non-recurving cases are much smaller and typically within the noise range due to natural turbulent and measurement inconsistencies.

For tropical cyclone recurvature, as with the case of Typhoon Flo, individual case zonal wind values in the upper troposphere ($\sim$ 200 mb) to the north and northwest of the cyclone were observed to be very different ($\sim$ 20 m/s) from the similarly located zonal wind patterns of the non-recurving cases. These large wind differences were much greater than the typical natural and instrumental variability (S.D. $\sim$ 7-8 m/s) inherent in the individual case information at these levels. This special area to the cyclone's north and northwest might be designated as the "forecast window of opportunity".

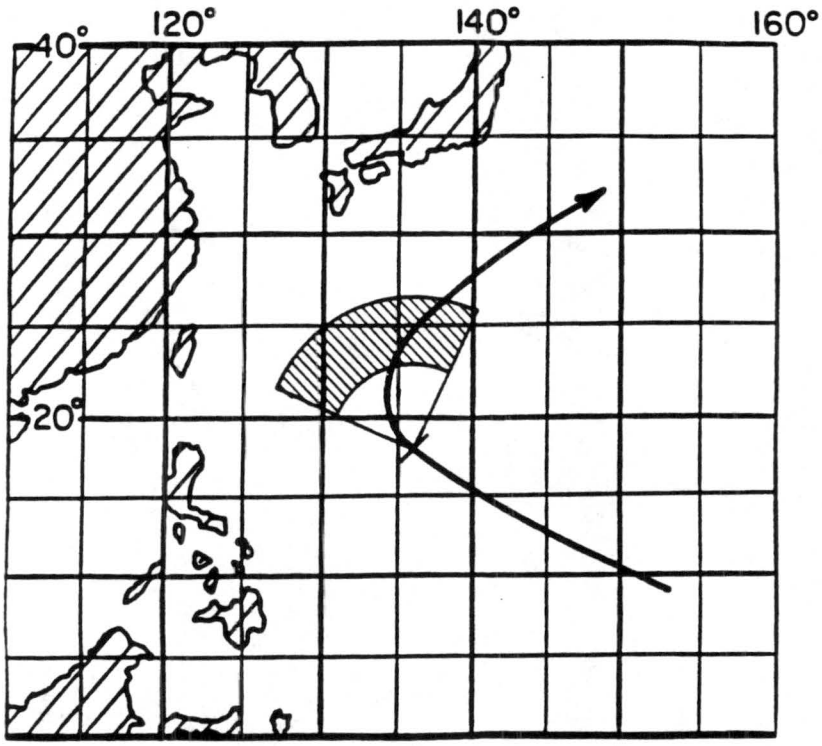

Figure 6.2: Depiction of the critical "window of forecast opportunity" in the upper troposphere where key zonal wind component differences are observed between recurving and non-recurving tropical cyclones.

When strong westerly winds penetrated to within 8° radius on the north or northwest side of the tropical cyclone, the beginning of cyclone recurvature is expected to take place in the next 24 hours (Hodanish, 1991). When westerly winds reach to within 6° radius, then beginning recurvature has just commenced.

An improvement of JTWC 48 and 72-hour forecast skill reported by Shoemaker *et al.* (1990) due to aircraft reconnaissance flights near the 400 mb level and 6-8° north and northwest of the Northwest Pacific tropical cyclone (see Fig. 6.3), gives further observational support (see Table 6.1) of the importance of wind data in this "forecast window of opportunity" region. These JTWC forecast improvements resulted primarily from improvements in the handling of the recurvature situation.

In terms of forecasting future tropical cyclone motion and particularly recurvature, we find that data on the south and east sides of the cyclone contribute little or no improvement, even if this data should be needed to initiate numerical models. It is the data for north and northwest sides which is usually the crucial factor in future cyclone turn-

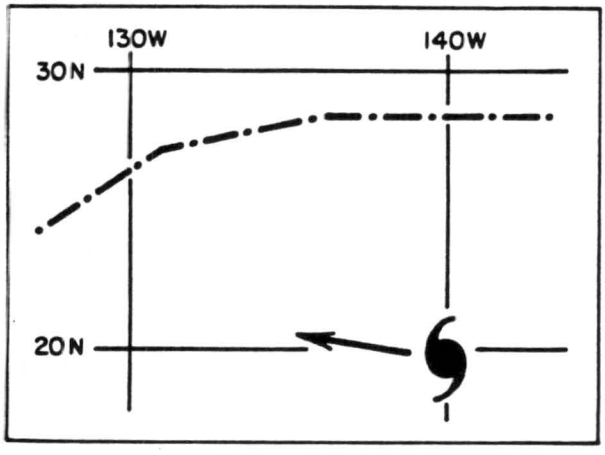

Figure 6.3: Illustration of typical reconnaissance mission (dot-dash line) in relation to current storm position (spiral arms) in the western North pacific. Flights were at 400 mb and observations were made every 111 km. (From Shoemaker *et al.*, 1991).

Table 6.1: Comparison of JTWC TC forecast track errors during 1983-86 for forecasts made in the 6-, 12-, 18-, and 24-h periods following synoptic reconnaissance vs similar forecasts that were made when synoptic reconnaissance data were not available. The number of cases in parentheses. Errors are given in km. (From Shoemaker *et al.*, 1991).

	Forecast period	
Stratification	48 h	72 h
With synoptic tracks	387 (229)	589 (196)
Without synoptic tracks	468 (1291)	732 (924)
Average percentage greater forecast error without synoptic reconnaissance	21%	24%

ing motion determination. Because tropical cyclones are infrequent, it appears that the type of information needed for improved forecasting is not necessarily a denser rawinsonde network which would regularly provide enhanced information. Rather, the capability to selectively sample the occasional tropical cyclone at middle and upper tropospheric level on its' poleward side appears to be most desirable. If routine rawinsonde and satellite information cannot provide the desired information, then it would be very beneficial, in an important forecast situation, that reconnaissance aircraft be deployed to gather such information.

The findings of this paper as to the inability of the TCM-90 data to adequately measure individual steering flow at individual time periods should not be interpreted as proof that additional upper level atmospheric information provided by aircraft or satellite is not highly beneficial. The aircraft appears to be the most useful tool for such selective and high quality data enhancements.

An important step in this direction appears to have been taken by the synoptic flow experiments by the Hurricane Research Division (HRD) of NOAA which have been directed towards providing denser and more spatially uniform wind fields in individual tropical cyclone cases by deploying Omega dropwindsondes from a flight level of about 400 mb. Lord and Franklin (1987) have described the three-dimensional, nested analysis of these wind fields. Franklin *et al.* (1991) and Franklin and DeMaria (1992) have discussed the impact of these Omega dropwindsondes on the hurricane track forecasts using the barotropic VICBAR model. Depending upon how the evaluation was made and the frame of reference, it was found that in 12 cases of ODW analysis the 24 to 36 hour track forecasts were estimated to have been improved by about 10-25 percent.

Thus, the general success of the special Pacific reconnaissance missions for track improvement as discussed by Shoemaker *et al.* (1990) and the ODW program in the Atlantic rests with the ability to dictate the most profitable location where supplementary wind information should be collected. This flexibility offers advantages over the enhanced but fixed rawinsonde data network of TCM-90. The fixed network frequently cannot

supply wind information surrounding the cyclone for areas where it gives the best forecast advantage.

When aircraft or large-scale conventional analyses at 500 to 200 mb levels and within 5-9° radius to the north and northwest of the tropical cyclone center are not available or are considered to be of poor quality, then it may be possible to augment the information of this region through use of upper tropospheric synchronous-satellite cloud-drift winds. It may also be possible, with testing and extra calibration, that practical use can be made of new satellite sounder systems in this crucial northwest region. It may also prove beneficial to try to use satellite-derived water vapor imagery at levels of 300-400 mb to deduce wind conditions in the important "forecast window of opportunity" region. Dvorak (1984) indicates some success with this approach.

ACKNOWLEDGEMENTS

The author is deeply grateful for the enthusiastic guidance and support provided by his thesis advisor Professor William M. Gray. This paper would not have been possible without the extensive computer assistance received from William Thorson. Appreciation is extended to Barbara Brumit and Laneigh Walters for their professional help in manuscript preparation, and Judy to Sorbie-Dunn for drafting the figures.

This research has been partly supported by an ONR Grant. The author thanks Patrick Haar and Russell Elsberry of NPG, Monterey for providing the TCM-90 data tapes needed to perform this study.

I would also like to thank the U.S. Air Force and the Air Force Institute of Technology for their sponsorship of my Master's program at Colorado State. For their many valuable suggestions, I extend my gratitude to the members of the Gray research project.

The author is appreciative of the opportunities he has had to learn of tropical cyclones first hand through aircraft reconnaissance experience on Guam and from duty as a reconnaissance flight coordinator at the National Hurricane Center in Miami.

And, special thanks are extended to Connie for her love and understanding during this long process.

REFERENCES

Anthes, R. A., 1982: Tropical cyclones: Their evolution, structure and effects. *Amer. Meteor. Soc.*, 208 pp.

Brand, S., C. A. Beunafe and H. D. Hamilton, 1981: Comparison of tropical cyclone motion and environmental steering. *Mon. Wea. Rev.*, 109, 908-909.

Chan, J. C. L., W. M. Gray and S. Q. Kidder, 1980: Forecasting tropical cyclone turning motion from surrounding wind and temperature fields. *Mon. Wea. Rev.*, 108, 778-792.

Chan, J. C. L. and W. M. Gray, 1982: On the physical processes responsible for tropical cyclone motion. Atmos. Sci. Research Paper No. 358, Colo. State Univ., Fort Collins, Co, 200 pp.

Chan, J. C. L. and W. M. Gray, 1982: Tropical cyclone movement and surrounding flow relationships. *Mon. Wea. Rev.*, 110, 1354-1374.

Chan, J. C. L., 1984: An observational study of the physical processes responsible for tropical cyclone motion. *J. Atmos. Sci.*, 41, 1036-1048.

Dvorak, V. F., 1984: Satellite observed upper level moisture patterns associated with tropical cyclone movement. *Postprints, 15th Conf. on Hurricanes and Tropical Meteorology*, AMS, Miami, FL, 163-168.

Elsberry, R. L., 1985: A global view of tropical cyclones, Chapter 4. International Workshop on Tropical Cyclones, WMO, Bangkok, Thailand, 25 November to 7 December, 1985.

Elsberry, R. L., 1990: International experiments to study tropical cyclones in the western North Pacific. *Bull. Amer. Meteor. Soc.*, 71, 1305-1316.

Elsberry, R. L., W. M. Frank, G. J. Holland, J. D. Jarrell and R. L. Southern, 1988: *A global view of tropical cyclones.* Office of Naval Research, Marine Meteorology Program, 185 pp.

Elsberry, R. L., B. C. Diehl, J. C. L. Chan, P. A. Harr, G. J. Holland, M. Lander, T. Neta, and D. Thom, 1990: ONR Tropical cyclone motion research initiative: Field experiment summary. Technical Report NPS-MR-91-001, Naval Postgraduate School, Monterey, CA, 93943, 106 pp.

Elsberry, R. L. and R. F. Abbey, Jr., 1991: Overview of the tropical cyclone motion (TCM-90) field experiment. *Preprints of 19th Conf. Hurricanes and Tropical Meteorology*, AMS, Boston, MA, 02108, 1-6.

Fett, R. W. and S. Brand, 1975: Tropical cyclone movement forecasts based on observations from satellites. *J. Appl. Meteor.*, 14, 452-456.

Frank, W. M., 1977: The structure and energetics of the tropical cyclone, I: Storm structure. *Mon. Wea. Rev.*, 105, 1119-1135.

Franklin, J. L., 1990: Dropwindsonde observations of the environmental flow of Hurricane Josephine (1984): Relationships to vortex motion. *Mon. Wea. Rev.*, 118, 2732-2744.

Franklin, J. L. and M. DrMaria, 1992: The impact of Omega dropwindsonde observations on barotropic hurricane track forecasts. *Mon. Wea. Rev.*, 120, 381-391.

Franklin, J. L., M. DeMaria and C. S. Veldon, 1991: The impact of Omega dropwindsonde and satellite data on hurricane track forecasts using the VICBAR model. *Proc., 19th Conf. Hurricanes and Tropical Meteorology*, Miami, AMS, 87-92.

George, J. E. and W. M. Gray, 1976a: Tropical cyclone motion and surrounding flow parameter relationships. *J. Appl. Meteor.*, 15, 1252-1264.

George, J. E. and W. M. Gray, 1976b: Recurvature and non- recurvature as related to surrounding wind/height fields. *J. Appl. Meteor.*, 16, 43-42.

Gray, W. M. 1981: Recent advances in tropical cyclone research from rawinsonde composite analysis. WMO Programme on Research in Tropical Meteorology, World Meteorological Organization, Geneva, Switzerland, 404 pp.

Gray, W. M. 1987: Recent Colorado State University tropical cyclone research of interest to forecasters. NEPRF Research Paper No. CR 87-10, Monterey, CA.

Gray, W. M., 1991: Tropical cyclone propagation. *Preprints of 19th Conf. Hurricanes and Tropical Meteorology*, AMS, Boston, MA, 02108, 385-390.

Gray, W. M., 1992: Physical factors influencing tropical cyclone propagation. New ONR report in preparation.

Gray, W. M., C. Neumann, T. Tsui, 1991: Assessment of the role of aircraft reconnaissance on tropical cyclone analysis and forecasting. *Bull. Amer. Meteor. Soc.*, Vol. 72, 12, 1867–1883.

Guard, C. P., 1977: Operational application of a tropical cyclone recurvature/non-recurvature study based on 200 mb wind fields. FLEWEACEN Technical Note No. 77-1, U.S. Fleet Weather Central, Guam.

Hodanish, S. J. and W. M. Gray, 1991: An observational analysis of tropical cyclone recurvature. Atmos. Sci. Research Paper No. 480, Colo. State Univ., Fort Collins, CO, 124 pp.

Holland, J. G., 1984: Tropical cyclone motion: A comparison of theory and observation. *J. Atmos. Sci.*, 41, 68-75.

Joint Typhoon Warning Center, 1981-91: Annual Tropical Cyclone Reports 1980-90. U.S. Naval Oceanography Command Center/Joint Typhoon Warning Center, COMNAVMARIANAS Box 17, FPO San Francisco, 96630.

Kaplan, J. and J. L. Franklin, 1991: The relationship between the motion of tropical storm Florence (1988) and its environmental flow. *Preprints of 19th Conf. Hurricanes and Tropical Meteorology*, AMS, Boston, MA, 02108, 93-97.

Lajoie, F. A., 1976: On the direction of movement of tropical cyclones. *Aust. Meteor. Mag.*, 24, 95-104.

Lord, S. J. and J. L. Franklin, 1987: The environment of Hurricane Debby (1982). Part I: Winds. *Mon. Wea. Rev.*, 115, 2760-2780.

Marks, F. D., Jr., R. A. Houze, Jr. and J. F. Gamache, 1991: Dual-aircraft investigation of the inner core of Hurricane Norbert. Part I: Kinematic structure. Submitted to *J. Atmos. Sci.*.

Merrill R. T., 1988: Characteristics of the upper tropospheric environmental flow around hurricanes. *J. Atmos. Sci.*, 45, 1665- 1677.

Neumann, C. J. and J. M. Pelissier, 1981: Models for the prediction of tropical cyclone motion over the north Atlantic: An operational evaluation. *Mon. Wea. Rev.*, 109, 522-538.

Pike, A. C., 1985: Geopotential heights and thickness as predictors of Atlantic tropical cyclone motion and intensity. *Mon. Wea. Rev.*, 113, 931-939.

Sandgathe, S. A., 1987: Opportunities for tropical cyclone motion research in the northwest Pacific region. Technical Report NPS-63- 87-006, Naval Postgraduate School, Monterey, CA, 36 pp.

Sheets, R. C., 1990: The national hurricane center - past, present, and future. *Weather and Forecasting*, 5, 185-232.

Shoemaker, D. N., W. M. Gray, and J. D. Sheaffer, 1990: Influence of synoptic track aircraft reconnaissance on JTWC tropical cyclone track forecast errors. *Weather and Forecasting*, Vol. 5, 3, 503–507.

Weatherford, C. L. and W. M. Gray, 1988: Typhoon structure as revealed by aircraft reconnaissance. Part I. Data analysis and climatology. *Mon. Wea. Rev.*, 116, 1032-1043.

WMO, 1986: Proceedings of the WMO International Workshop on Tropical Cyclones (IWTC), Bangkok, Thailand, 25 November-5 December, 1985. Tropical Meteorology Programme Report Series, Report No. 21, WMO/TD-No. 83, WMO, Geneva, Switzerland, 152 pp.

Williams, K. T. and W. M. Gray, 1973: Statistical analysis of satellite observed trade wind cloud clusters in the western north Pacific. *Tellus*, 25, 313-336.

Xu, J. and W. M. Gray, 1982: Environmental circulations associated with tropical cyclones experiencing fast, slow and looping motion. Atmos. Sci. Research Paper No. 346, Colo. State Univ., Fort Collins, CO, 111 pp.

Appendix A

TCM–90 CYCLONE TRACKS

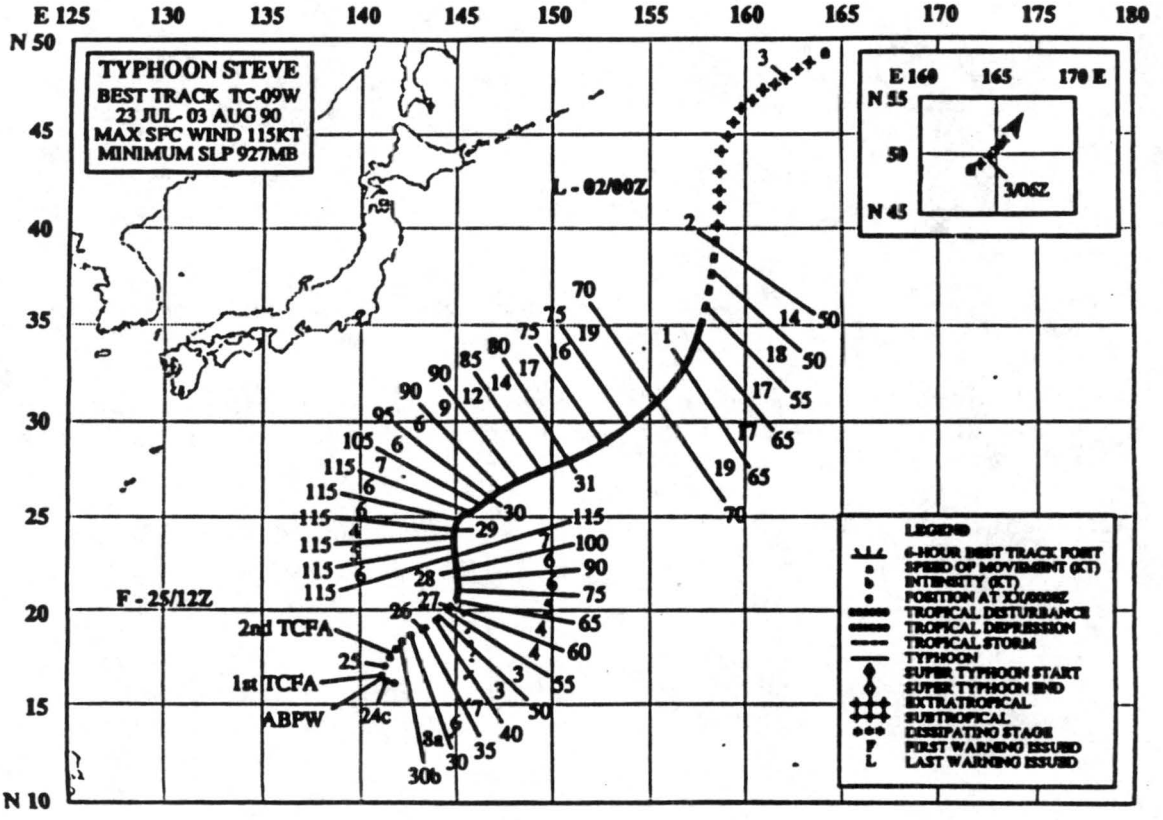

Figure A.1: The best track for Typhoon Steve, one of thirteen tropical cyclones included in this motion study.

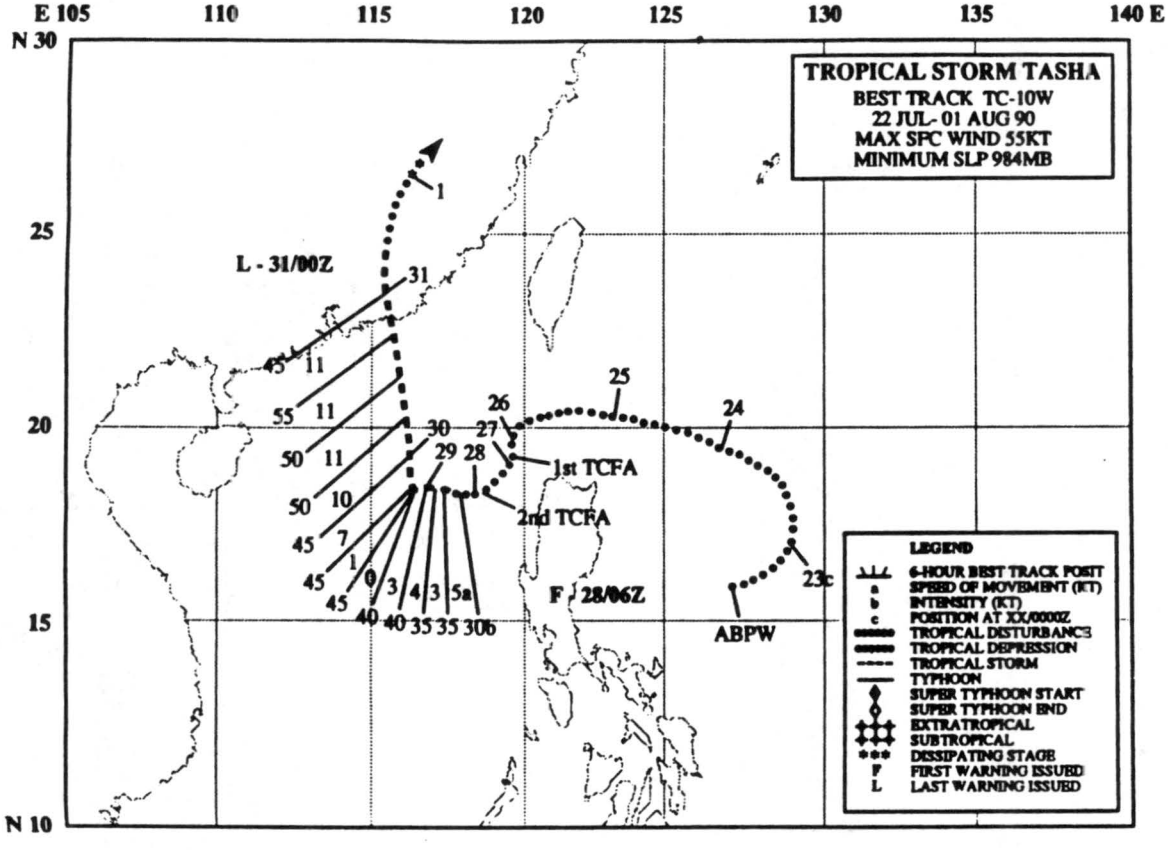

Figure A.2: Same as Fig. A.1 but for Tropical Storm Tasha.

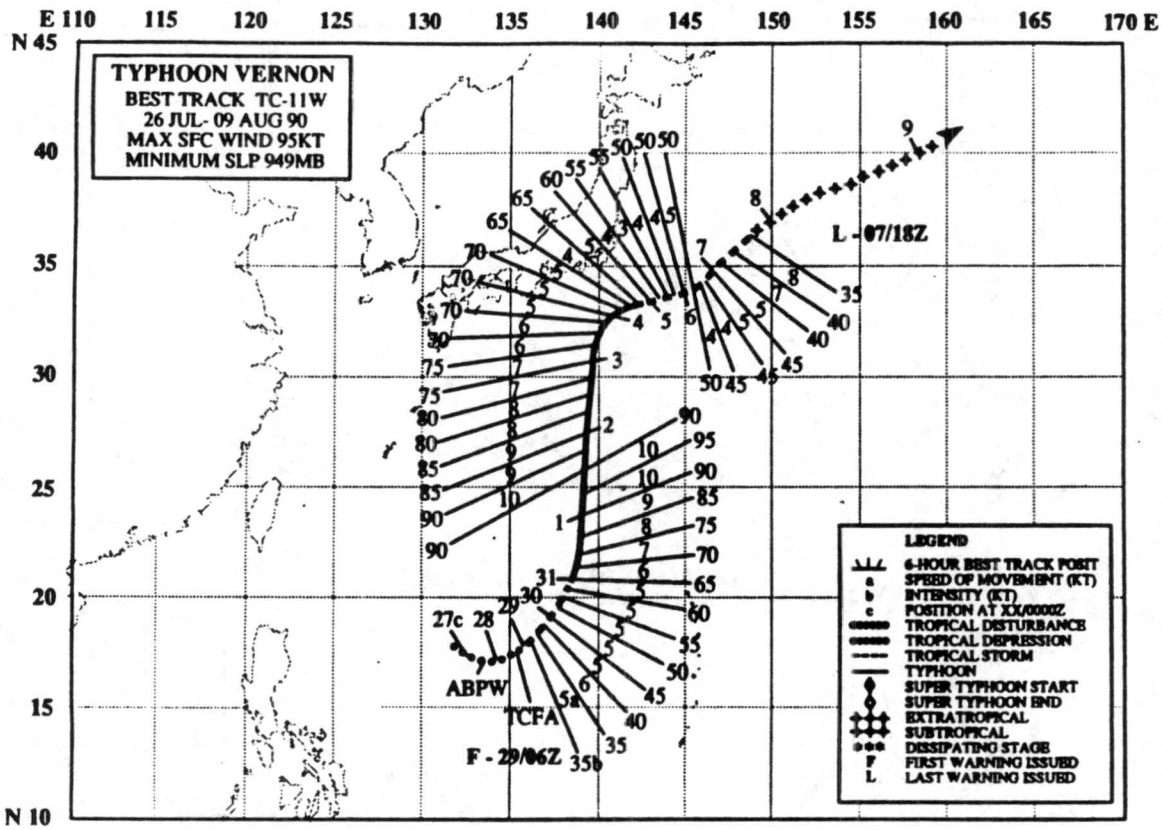

Figure A.3: Same as Fig. A.1 but for Typhoon Vernon.

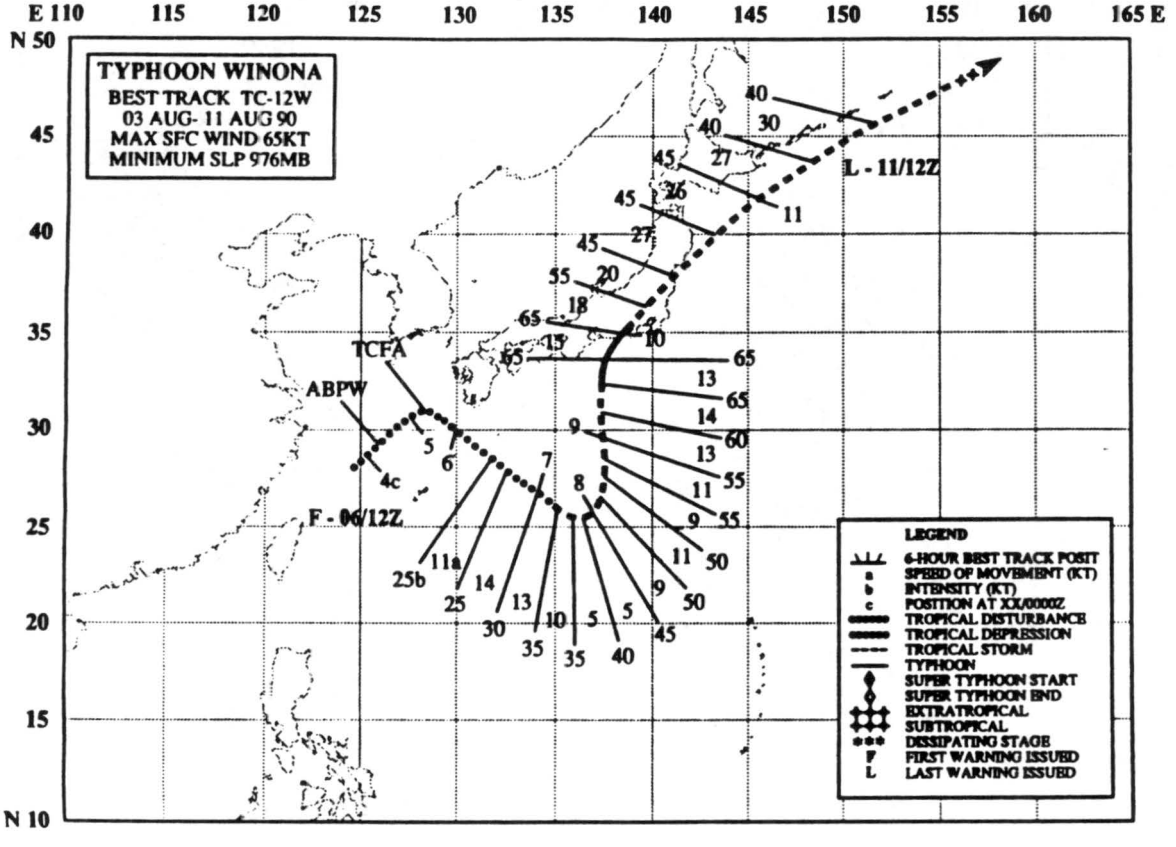

Figure A.4: Same as Fig. A.1 but for Thphoon Winona.

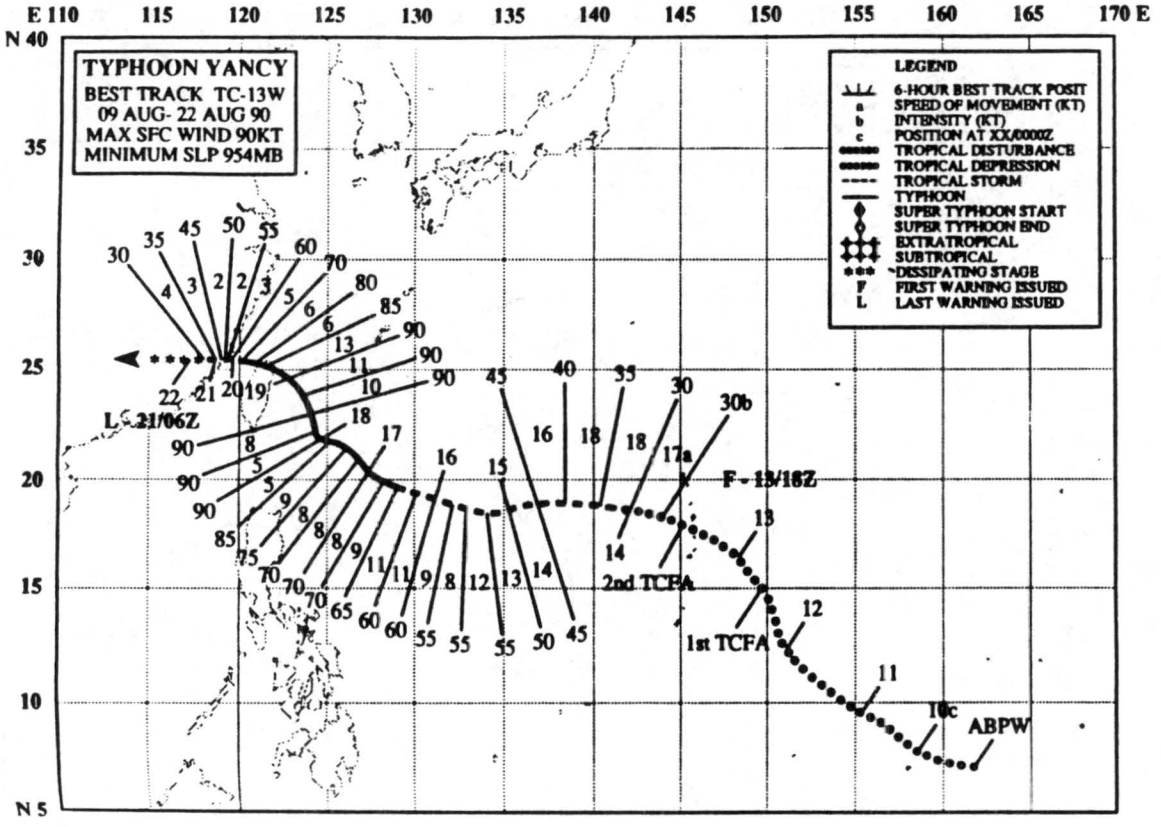

Figure A.5: Same as Fig. A.1 but for Typhoon Yancy.

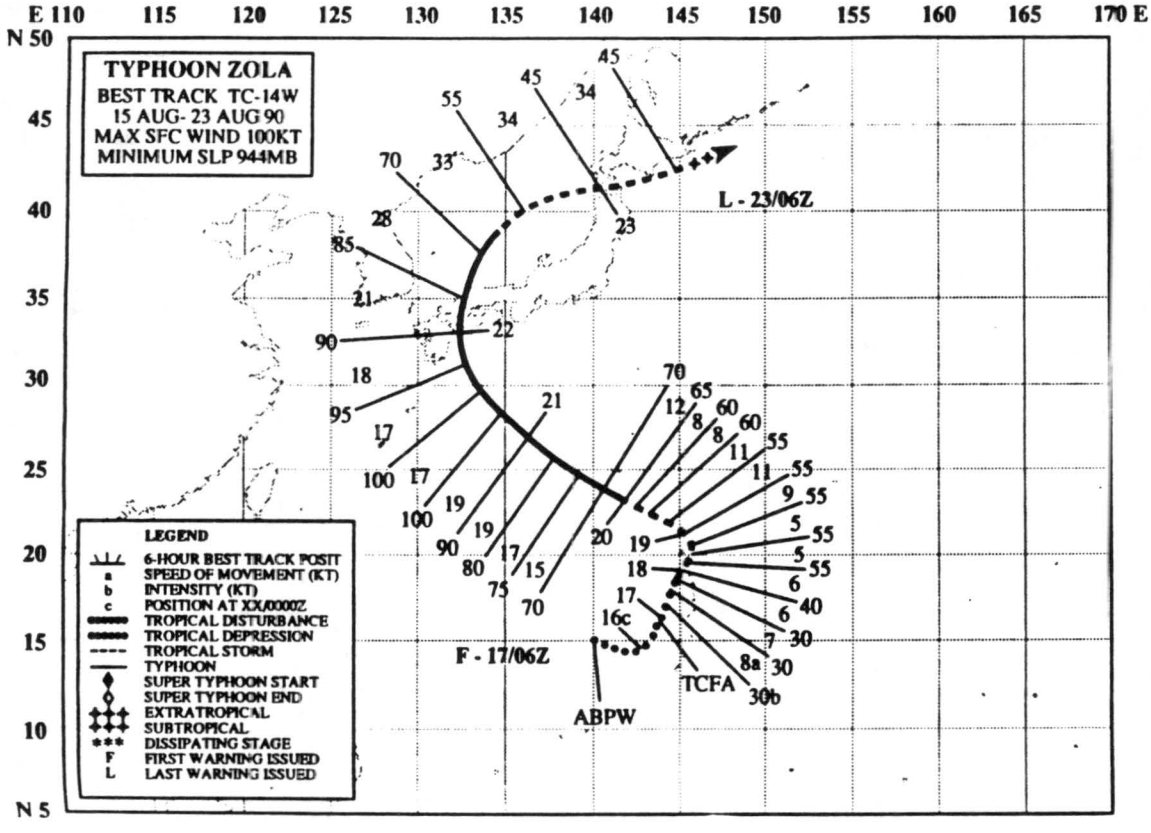

Figure A.6: Same as Fig. A.1 but for Typhoon Zola.

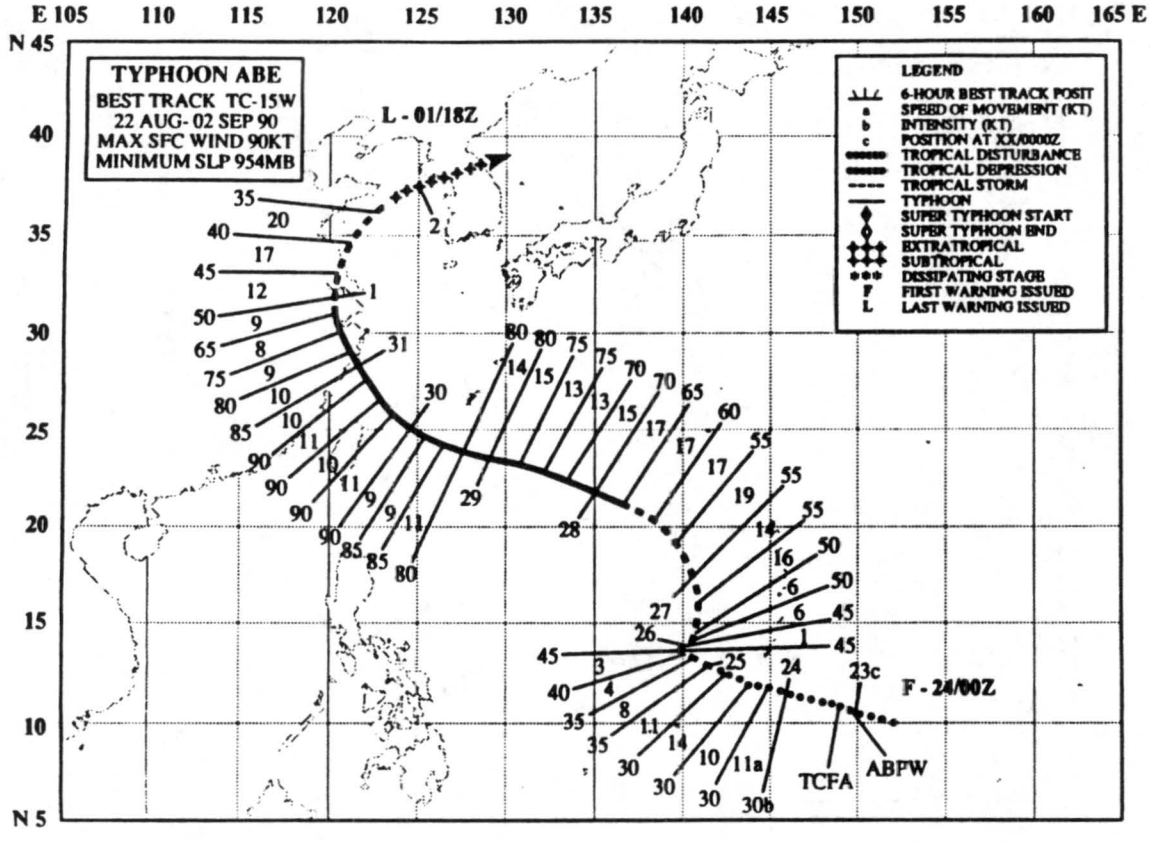

Figure A.7: Same as Fig. A.1 but for Typhoon Abe.

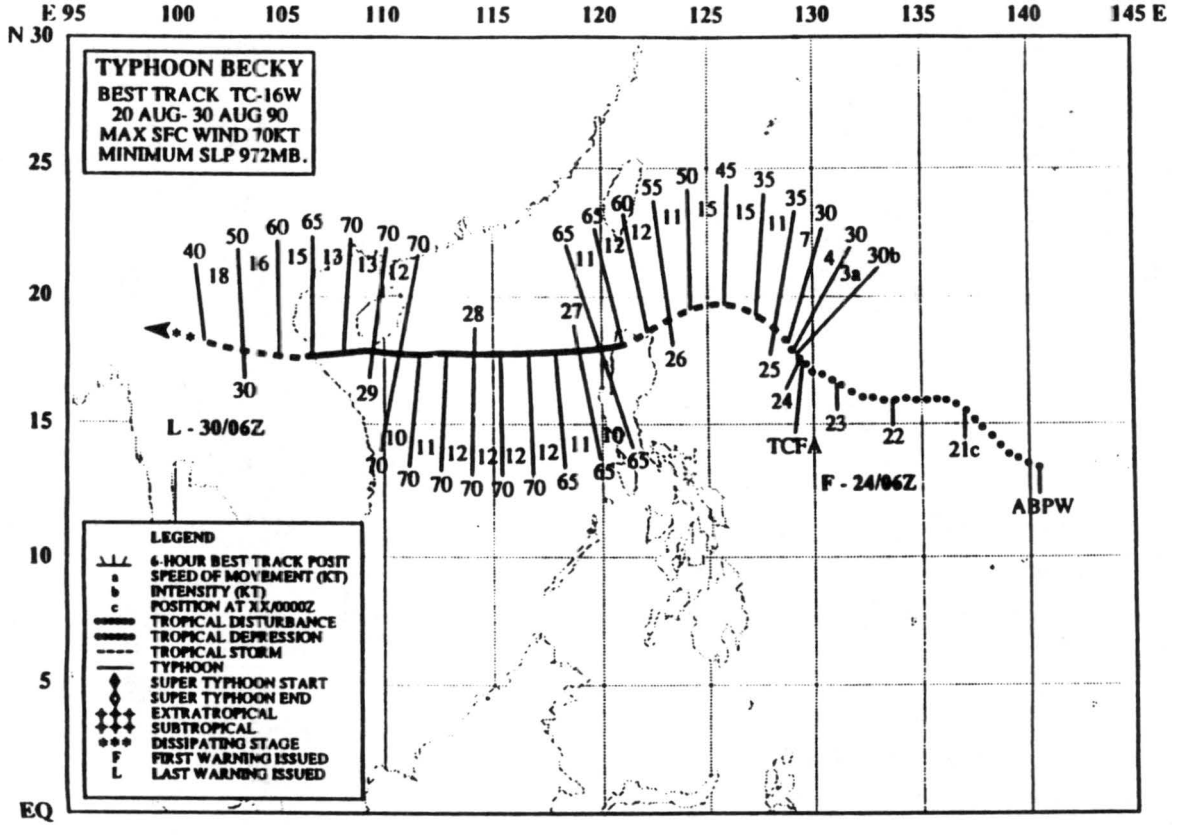

Figure A.8: Same as Fig. A.1 but for Typhoon Becky.

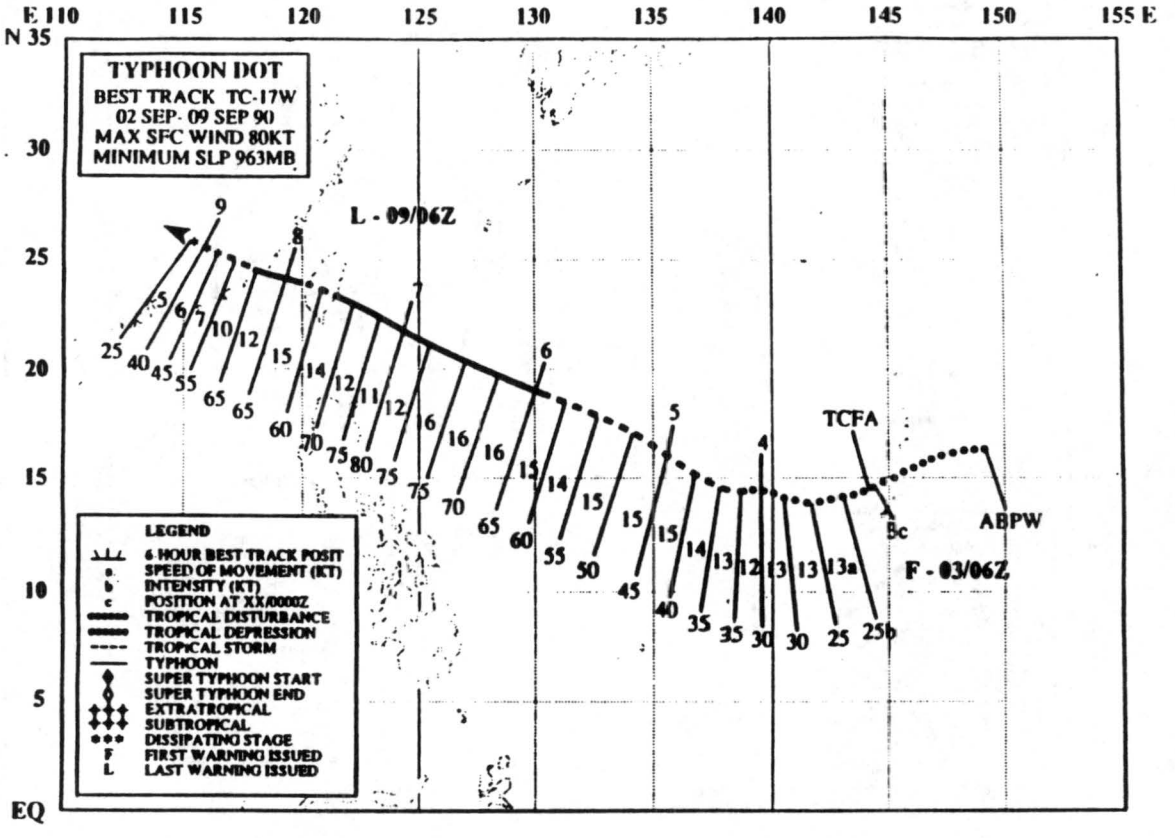

Figure A.9: Same as Fig. A.1 but for Typhoon Dot.

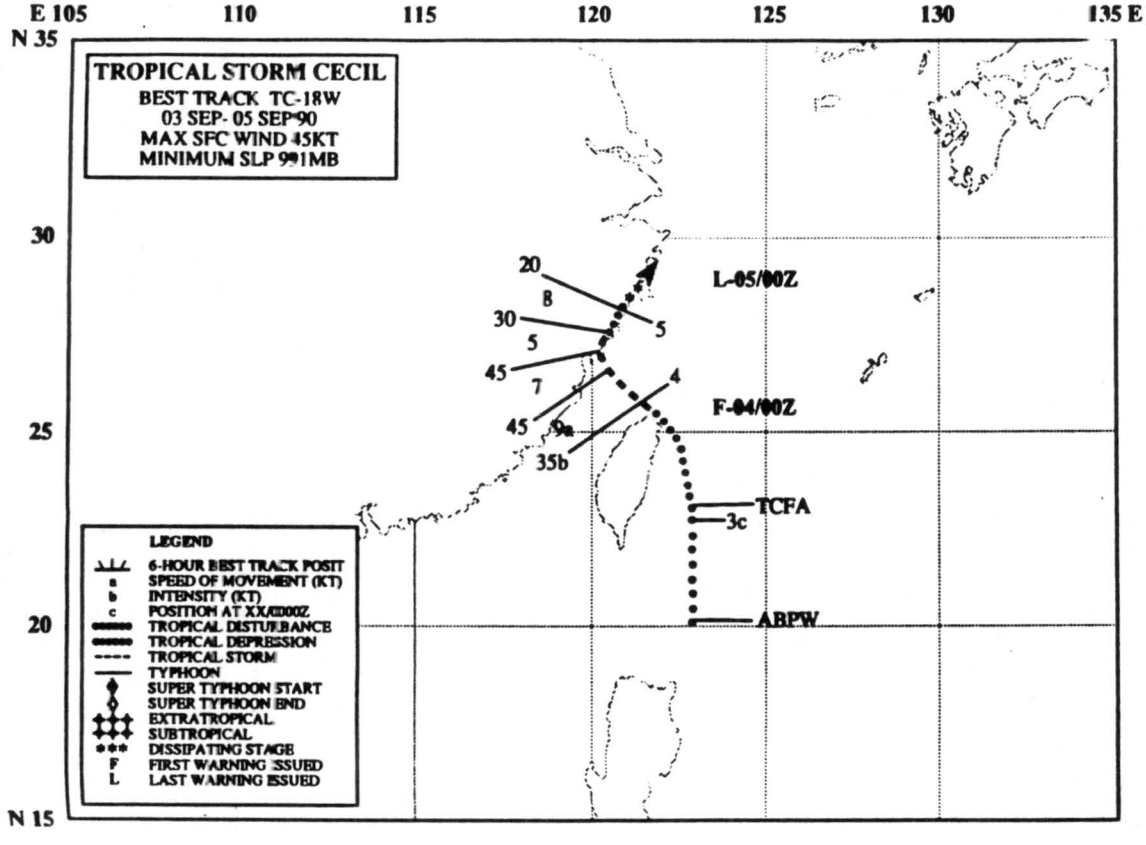

Figure A.10: Same as Fig. A.1 but for Tropical Storm Cecil.

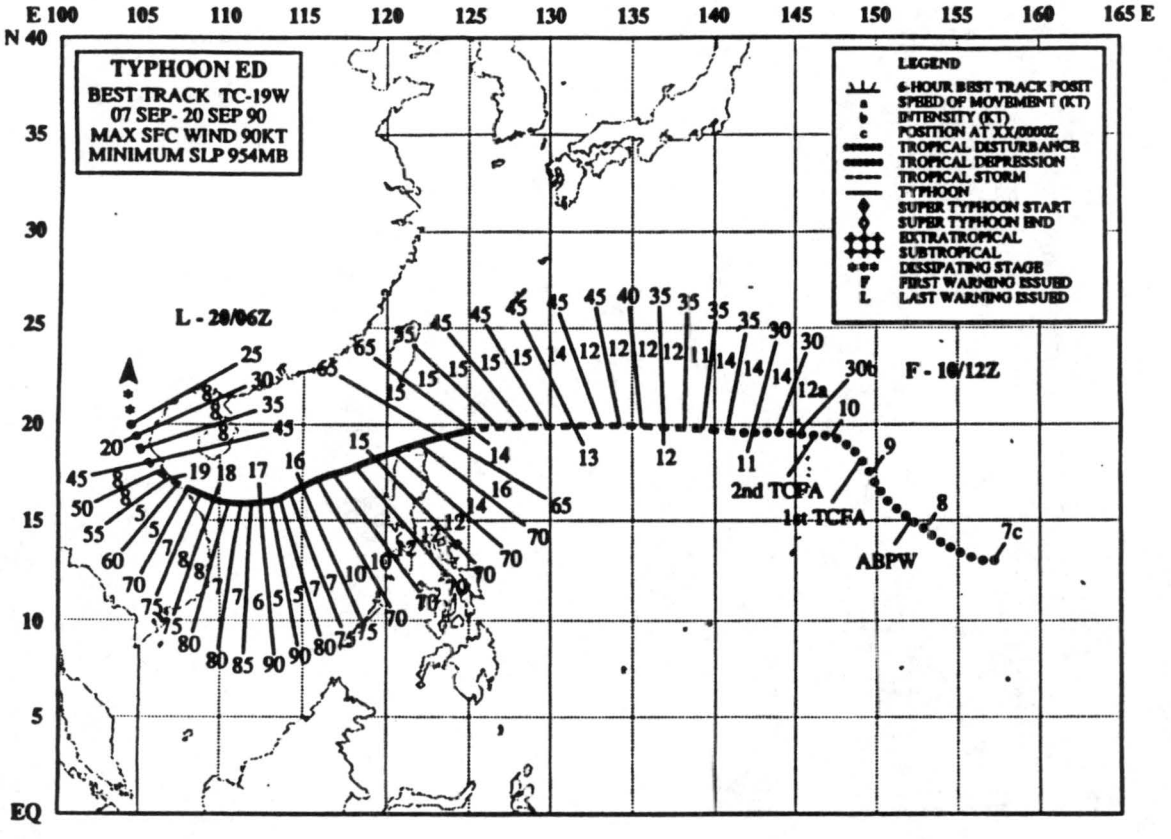

Figure A.11: Same as Fig. A.1 but for Typhoon Ed.

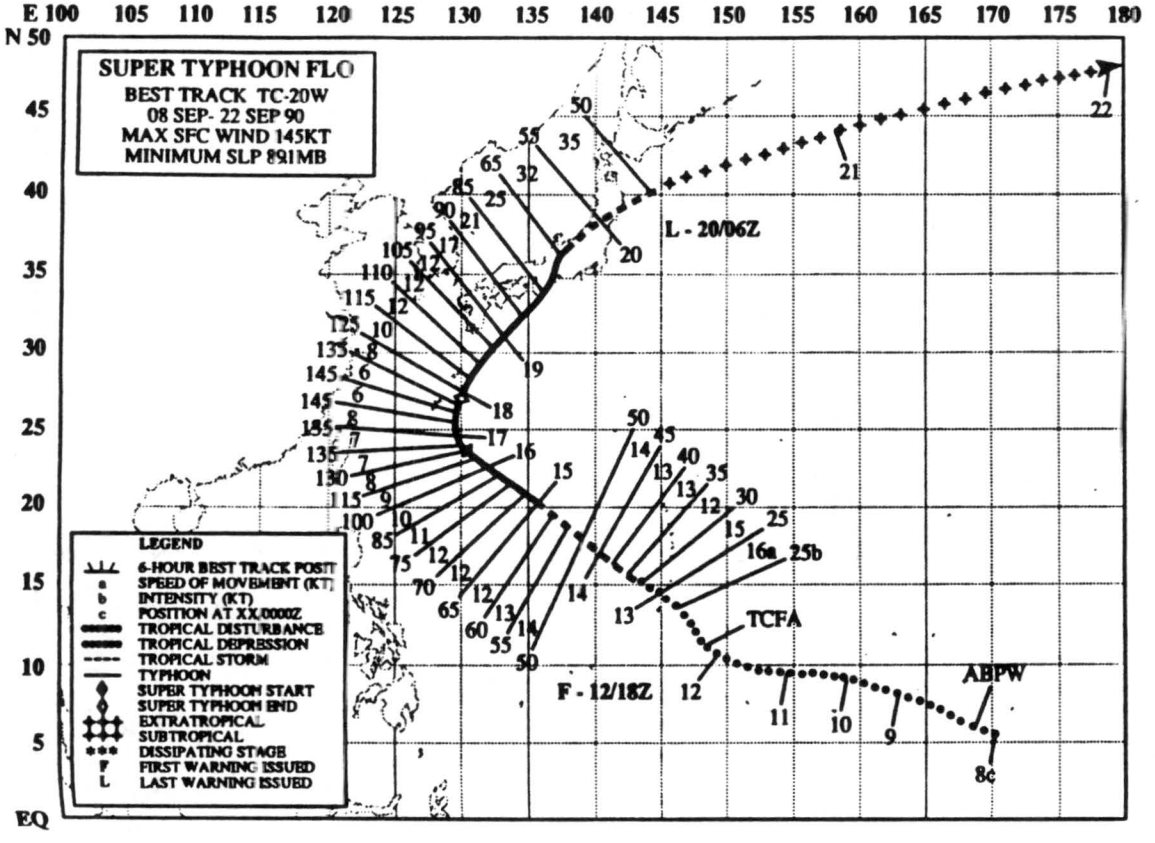

Figure A.12: Same as Fig. A.1 but for Supertyphoon Flo.

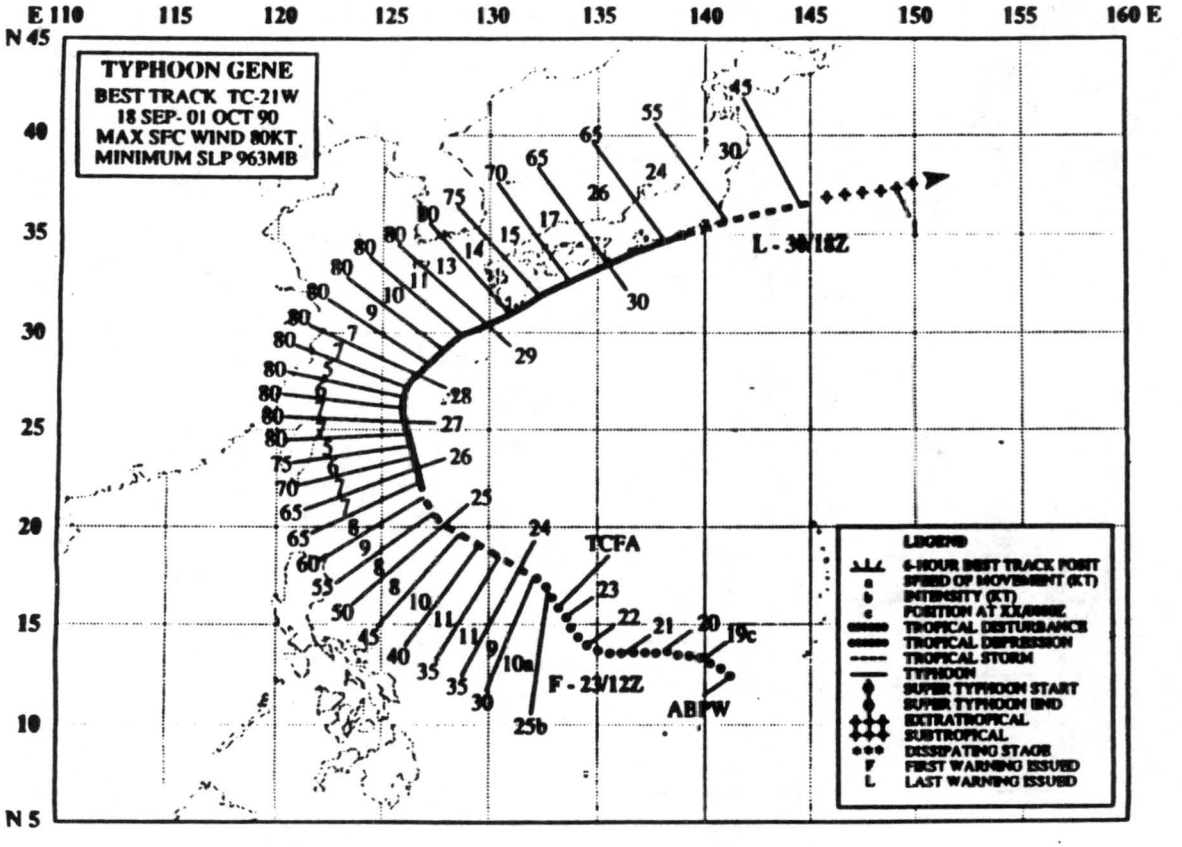

Figure A.13: Same as Fig. A.1 but for Typhoon Gene.